Johanna Krainer, BSc

Arylsilanes

-

First steps towards novel battery materials

Master Thesis

Thesis Submitted to the Faculty of Chemistry, Chemical- and Process
Engineering in Partial Fulfillment of Requirements for the Degree of

Master of Science

in Chemistry at the University of Technology Graz

Supervisor:
Univ.-Prof.Dipl.-Chem.Dr.rer.nat.Frank Uhlig
Institute for Inorganic Chemistry
Graz University of Technology

Graz, February 2014

Danksagung

An dieser Stelle will ich die Chance nutzen, um all jenen zu danken, die mich in dieser Zeit unterstützt und zum erfolgreichen Abschluss dieser Arbeit maßgeblich beigetragen haben.

Mein primärer Dank gilt meinem Betreuer Prof. Frank Uhlig, der es mir ermöglichte diese Masterarbeit in seiner Arbeitsgruppe zu verfassen und mir stets optimistisch mit fachlichen Ratschlägen zur Seite stand.

Ebenso geht mein Dank an alle Mitglieder der AG Uhlig, die durch Wissensaustausch und Hilfsbereitschaft zum erfolgreichen Heranwachsen dieser Arbeit beigetragen haben.

Einen ganz besonderen Dank möchte ich meinen Bürokollegen Cathrin Zeppek, Kristina Schrempf und Johann Pichler und ebenso Ana Torvisco zukommen lassen, die mich stets motiviert und unterstützt haben und die letzten Monate zu einer tollen Erfahrung für mich machten.

Mein größter Dank gilt meinen Eltern, die es mir ermöglichten dieses Studium zu absolvieren und mich stets nicht nur finanziell sondern auch persönlich unterstützten. Natürlich bedanke ich mich auch bei meinen Geschwistern und meinem Freund für die liebevolle und aufbauende Unterstützung in meiner gesamten Studienzeit.

Ich möchte auch meinen Studienkollegen für den regen Wissensaustausch und die kollegiale und freundschaftliche Zusammenarbeit danken, wodurch die erfolgreiche Absolvierung dieses Studiums gefördert und beschleunigt wurde. Die im Studium geschlossenen Freundschaften machten diese Zeit zu einem unvergesslichen Abschnitt meines Lebens.

Kurzfassung

Diese Arbeit befasst sich mit ersten Versuchen zur Synthese neuer Aryl substituierter Silizium-Ringsysteme. Einige unterschiedliche Diaryldichlorsilane Ar_2SiCl_2 (Ar = naphthyl, *o*-tolyl) wurden als Startmaterialien in Anlehnung an bekannte Literatur synthetisiert und mittels sogenannter Wurtz-Kupplungsreaktion mit diversen Alkali- und Erdalkalimetallen umgesetzt (siehe Schema).

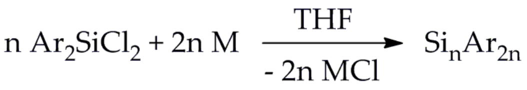

$$n\ Ar_2SiCl_2 + 2n\ M \xrightarrow[-\ 2n\ MCl]{THF} Si_nAr_{2n}$$

Aufgrund der Migrationstendenz der Arylsubstituenten scheiterten bis dato alle Versuche cyclische Produkte zu isolieren, jedoch konnte eine Menge an Daten über mögliche Reaktionsbedingungen gesammelt werden und einige neue Vermutungen zu den Reaktionen angestellt werden.

Erste Versuche neue Graphit/Silan-Hybridmaterialien herzustellen werden ebenso diskutiert.

Abstract

This work deals with first attempts towards the synthesis and characterization of novel aryl-substituted silicon ring systems. A variation of different diaryldichlorosilanes Ar_2SiCl_2 (Ar = naphthyl, *o*-tolyl) were synthesized by known procedures as starting materials for Wurtz-coupling reactions with different alkali and alkaline earth metals (see scheme).

$$\mathrm{n\ Ar_2SiCl_2 + 2n\ M} \xrightarrow[\mathrm{-\ 2n\ MCl}]{\mathrm{THF}} \mathrm{Si_nAr_{2n}}$$

Due to the migration tendency of the aryl substituents, attempts to isolate cyclic products failed so far. Anyhow, a large amount of data concerning possible reaction conditions and some presumptions about the reactions and their products could be gathered.

First attempts towards the preparation of novel graphite/silane hybrid materials will also be discussed.

Contents

1 Introduction

Earth consists of 15% silicon, especially the earth's mantle contains a huge amount of siliceous molten rock whereby silicon is the second most common element on earth after oxygen. Since 1500 BC silicon dioxide SiO_2 plays an important role in the production of glass jars, pearls and other jewelry. In the ancient times of Egypt glass was as precious as gold and gemstones. In 1824 silicon was first mentioned as an element by Jöns Jakob Berzelius and in 1854 the french chemist Henri Etienne Sainte-Claire Deville succeeded in producing pure and crystalline silicon for the first time, breaking ground in the field of silicon chemistry.

Currently silicon and its innumerable derivatives have many important and valuable applications in technology and everyday life products.

A highly specialized group of silicon derivatives, cyclosilanes, containing at least one Si-Si bond, are currently under investigation for industrial applications. Thus a better understanding of this field of silicon chemistry could open new prospects. One possibility for the use of such derivatives comes with the ever growing hunger for novel energy-related materials. Especially novel materials for energy storage are a highly interesting topic for the near future.

The primary aim of this work was the synthesis and characterization of cyclic arylsilanes for the implementation in Li-ion battery materials. The cyclic arylsilanes should be used in such materials directly and after decomposition. This attempt was already pursued at our institute by Judith Binder in her master thesis with the perphenylated 4- and 5-membered Si-rings. The carbon content after thermal decomposition was too high, so that the idea of the synthesis of naphthyl-substituted cyclosilanes came up. The loss of carbon upon heating is suggested to be more likely if the silicon rings exhibit naphthyl moieties. This assumption is due to the high stability of naphthalene as a leaving group during thermolysis. Thus the resulting product should exhibit the preferred low carbon content. Additionally it was tried to synthesize hexanaphthyl disilane with the purpose to use it in the same way as the ring products.

2 Literature

2.1 Silicon – Sources, Production & Applications

Until now elemental silicon can be obtained in about 20 localities in Cuba, Russia, China and other countries. As already mentioned, the earth's crust contains a large amount of silicon in form of silicon oxides.

Therefore, the more common way to gain elemental silicon is the industrially used reduction of SiO_2 with carbon at elevated temperatures of about 1800 °C (Figure 2.1).

$$SiO_2 + 2\,C \longrightarrow Si + 2\,CO$$

Figure 2.1: Industrial synthesis of silicon

Organochlorosilanes are consequently generated *via* a Müller-Rochow synthesis.

$$2\,CH_3Cl + Si \longrightarrow (CH_3)_2SiCl_2$$

Figure 2.2: Müller-Rochow synthesis

In case of arylchlorosilanes only phenyl-substituted derivatives are available on industrial scale. Other arylchlorosilanes are approachable on laboratory scale. For example (2,6-dimethylphenyl)dichlorosilane was synthesized by Gilman *et al.*,[1] (di-*p*-methylphenyl)dichlorosilane afforded by Pink and Kipping[2] in 1923 and dianthryldichlorosilane made by Yamaguchi *et al.*[3] in 1998. Also dinaphthyldichlorosilane was synthesized according to literature.[4]

2.2 Organo Substituted Cyclosilanes

2.2.1 General Aspects & Properties

In general, the properties and reaction behavior of cyclosilanes are completely different from their carbon analogs but apart from that they show electron delocalization effects as aromatic organic rings. Cyclosilanes can either act as electron donors or acceptors due to delocalized, filled orbitals at relatively high energy as well as unfilled orbitals at relatively low energy, like aromatics. This properties are based on the fact of σ-delocalization along the Si-Si bonds.[5] Other unusual properties include the formation of electronically delocalized anion and cation radicals and charge transfer complexes. These delocalization effects preferably occur in four-, five- and six-membered rings, whereas in compounds of larger ring size the effect decreases. This behavior has been known since 1965 and takes place in the reduction with alkali metals.[6] Considerations of hyperfine coupling constants (^{13}C and ^{29}Si) in EPR spectra led to the conclusion that the single occupied molecular orbital (SOMO) is a linear combination of Si-C σ^* and symmetry-adapted Si-Si σ^* hybrid orbitals. The unpaired electron is fully delocalized over the ring.[7]

West *et al.* determined oxidation potentials of a series of cyclosilanes by cyclic voltammetry, which showed that all compounds have at least two anodic peaks separated by 0.2-0.4 V. However even at high scan rates no corresponding cathodic peak could be found. The results suggest that after initial oxidation a cyclosilane cation radical is formed and subsequently rapid Si-Si bond cleavage takes place. This is followed by hydrogen or halogen abstraction to give secondary species which undergo further oxidation. The initial oxidation potentials of cyclosilanes depend as well on ring size (increase from three- to four- and higher-membered rings) and on the bulkiness and nature of substituents.[8, 9]

In general, large substituents favor the formation of small rings and small substituents favor the formation of larger ones. The largest cyclopolysilane of 35 $SiMe_2$ units was isolated by Brough *et al.*,[10] which was synthesized by dropwise addition Me_2SiCl_2 to an Na/K alloy.

A few studies have shown that the bulkiness of substituents has an influence on ring strain, size and stability. Cartledge[11] defined a set of parameters $E_S(Si)$ for alkyl groups which are used for interpretation of steric effects in reactions at Si. This steric parameters allow to assess the preferred ring size as a function of the substituents.

2.2.2 Perarylated Homocyclic Silanes

Cyclotrisilanes

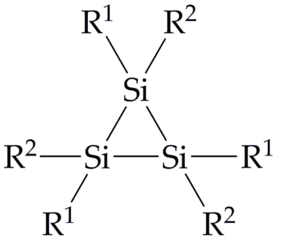

$R^1 = R^2 = -2,6-Me_2C_6H_3$
$R^1 = R^2 = -2,4,6-Me_2C_6H_2$
$R^1 = R^2 = -2,6-Et_2C_6H_3$
$R^1 = -2,6-Et_2C_6H_3$, $R^2 = -2,4,6-Me_2C_6H_2$

The first cyclotrisilane $(2,6-Me_2C_6H_3)_6Si_3$ was prepared in 1982 by Masamune *et al.*[12] *via* a reductive elimination of chlorine using lithium naphthalenide. In 1984 Masamune *et al.*[13] synthesized another cyclotrisilane $(2,6-Et_2C_6H_3)_6Si_3$ (see Figure 2.3).

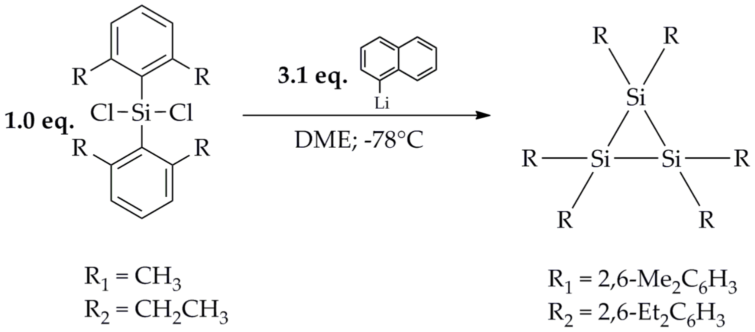

Figure 2.3: Formation of hexaarylcyclotrisilanes

In some cases also alkali or alkaline earth metals were used instead of lithium naphthalenide for the reductive dechlorination. For example in 1991, Probst *et al.*[14] synthesized a nitrogen-containing cyclotrisilane $[2-(Me_2NCH_2)C_6H_4]_6Si_3$ in good yields by using Mg as reducing agent. The presence of an alkyl group in *ortho*-position on the aromatic ring stabilizes the ring system. Because of the endocyclic small angles of about 60° three-membered rings show a high strain, but the larger exocyclic angles between the bulky substituents reduce their unmeant interactions. The interest in cyclotrisilanes does not only lie on the derivatives themselves but also in further reactivity. Their photolytic fragmentation reactions[12] (Figure 2.4) lead to stable and marginally stable disilenes.

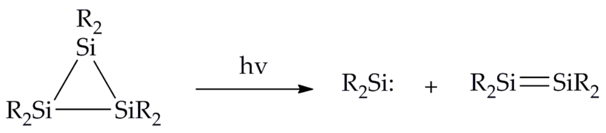

Figure 2.4: Photolytic fragmentation reaction of cyclotrisilanes

In general, three different reaction types can be distinguished in regard to the number of cleaved bonds. The cleavage of one of the three-membered ring bonds leads to open-chain trisilanes and ring-extending products, if a suitable reaction partner is present. Under photolytic conditions or the use of palladium as catalyst two of the three ring bonds can be cleaved forming silylens and disilenes. The third reaction type, the cleavage of all three bonds, would formally lead to three silylenes which has not been observed yet. For more detailed information of further chemistry with cyclotrisilanes as starting materials a review by M. Weidenbruch[15] can be recommended.

Cyclotetrasilanes

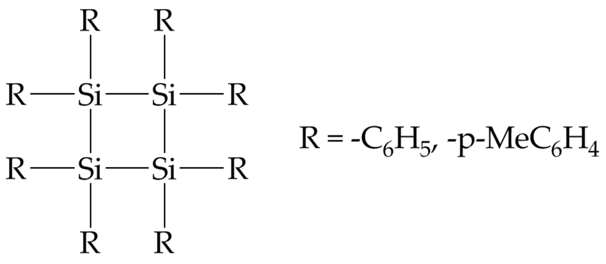

$R = -C_6H_5, -p\text{-}MeC_6H_4$

The synthetic route towards cyclotetrasilanes is the reductive elimination of dichlorodiarylsilanes (Ar_2SiCl_2) by alkali and earth alkaline metals (Wurtz-coupling reaction) (Figure 2.5).

The yield strongly depends on reaction conditions and the alkali metal and solvent used. The preferred metal is lithium and THF as solvent. Metals such as sodium[16] and magnesium[17] have also been used.

$$n\ Ar_2SiCl_2 + 2n\ M \xrightarrow[-\ 2n\ MCl]{THF} Si_nAr_{2n}$$

Figure 2.5: Wurtz-coupling reaction

In comparison to five- and six-membered rings, the four-membered ring shows a high ring strain. Investigations on the formation of the strained four-membered ring pointed out, that the thermodynamic stability of the small rings increases with the bulk of the substituents, as already mentioned. Therefore, methyl substituents favor the formation of a six-membered ring, ethyl groups lead to five-membered products and the four-membered cyclosilane is low in energy exhibiting phenyl groups. The oldest compound known is the phenylated silicon ring, Si_4Ph_8, which was first synthesized by Kipping[18] in 1921. The first synthetic route involves heating up Na and Ph_2SiCl_2 (ratio 2:1) neat. In later investigations the dichloride was diluted in toluene or xylene (Figure 2.6).

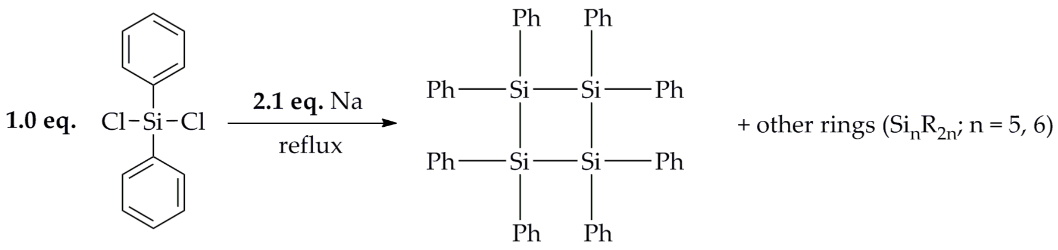

Figure 2.6: Synthesis of octaphenylcyclotetrasilane

This reaction afforded three well-defined crystalline and halogen-free silicon compounds (which were named as compounds A, B C). First, it was suggested that two of the three compounds were Si_4Ph_8, one compound with all silicon atoms in one plane (called ”unsaturated” or compound A), while the other having a tetrahedral configuration (called ”saturated” or compound

B). Later, in 1960 Gilman *et al.*[19] established that the "unsaturated" compound A did not contain any trivalent silicon atoms, refuting Kipping's assumption of containing "two tervalent silicon atoms". The high reactivity or "unsaturation" characteristics were attributed to be the cyclic structure of octaphenylcyclotetrasilane (Si_4Ph_8). In 1929, Steel and Kipping[20] synthesized another aryl-substituted silicon ring, octa-*p*-tolylcyclotetrasilane Si_4pTol_8. The reaction was carried out according to the synthesis of phenyl-substituted derivatives, as mentioned above. As suggested for two of the phenylated silicon compounds, one compound was thought to be an open-chain compound containing two tervalent silicon atoms (as compound A above) and the other a cyclic four-membered product (as compound B above). Another solid was found in a very small amount, which was assumed to have the composition $[Si\textit{p}\text{-}Tol_2]_n$.

An alternative route to synthesize aryl-substituted silicon ring products was achieved by the reductive elimination of halides as an electrochemical reaction. In 1981 Hengge *et al.*[21] showed that diphenyldichlorosilane reacts at the cathode and forms octaphenylcyclotetrasilane in addition to polymeric material. Larger ring sizes ($Si_{n\,=\,5,\,6,\ldots}$) were not obtained.

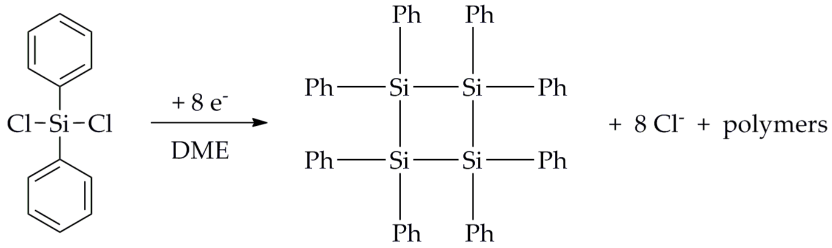

Figure 2.7: Formation of cyclotetrasilane via an electrochemical reaction

Another synthetic route towards cyclotetrasilanes are ring extension reactions reported by Weidenbruch,[15] starting from a three-membered ring. The chemical reactivity of perphenylated silicon rings offered an entry point to other silicon chemistry: Octaphenylcyclotetrasilane treated with X_2 (X = Cl, Br, I) afforded the α,ω-dihalooctaphenyltetrasilane. Ring-opening reactions of octaphenylcyclotetrasilane[22] were possible upon treatment with halogens (X = Cl, Br, I) or PX_5 (X = Cl, Br) in presence of HX/AlX_3 giving perhalogenated tetrasilanes

Si_4X_{10} (X = Cl, Br, I). Another interesting reaction of ring cleavage was found by Becker *et al.*[23] in 1989. This work was based on the ring cleavage of octaphenylcyclotetrasilane by lithium in THF which led to dilithio-octaphenyltetrasilane (crystallized in THF molecules). The isolation of dilithio-octaphenyltetrasilane offered a way to form heterocycles and other important derivatives.

Cyclopentasilanes

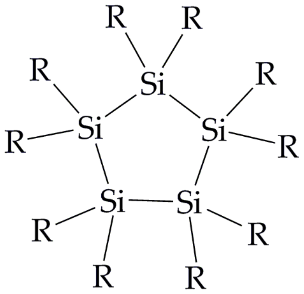

$R = -C_6H_5, -p\text{-}MeC_6H_4$

The oldest known derivative is the perphenylated five-membered silicon ring, discovered by Kipping[18] in 1921 (Figure 2.8), which at that time was thought to be the corresponding cyclotetrasilane, called compound B. In 1960 Gilman *et al.*[24] found out that compound B was dodecaphenylcyclohexasilane, and in 1964 confirmed as decaphenylcyclopentasilane.[25]

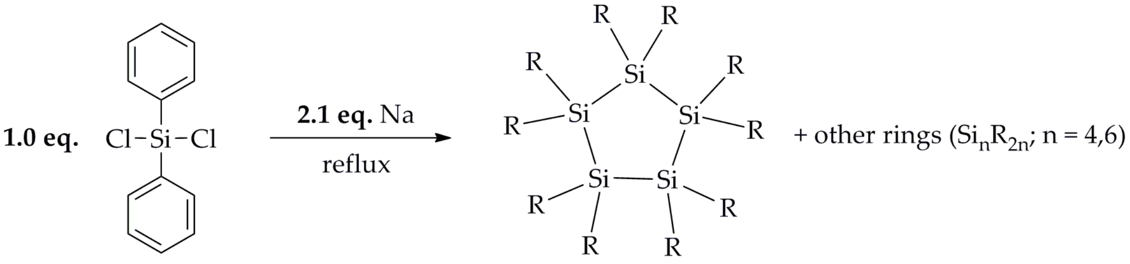

Figure 2.8: Synthesis of decaphenylcyclopentasilane

Lemanski *et al.*[26] prepared a 1,4-dilithiooctaphenyltetrasilane of octaphenylcyclotetrasilane and subjected the lithio-terminated species with diphenyldichlorosilane to obtain decaphenylcyclopentasilane (Figure 2.9).

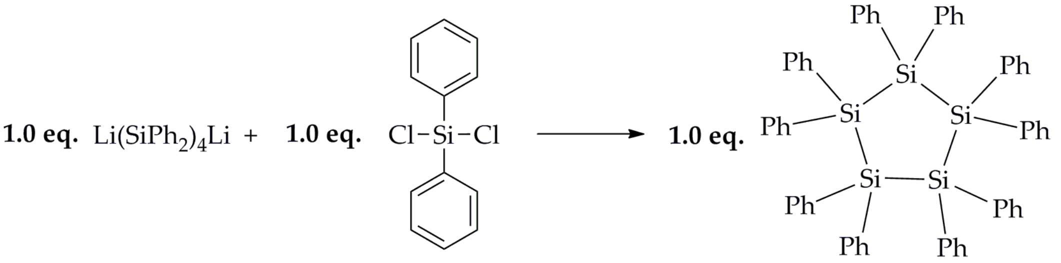

Figure 2.9: Alternative route to synthesize decaphenylcyclopentasilane

In 1929 Steel *et al.*[20] had the same situation of different and unsure product identifications with the *p*-tolyl derivative deca-*p*-tolylcyclopentasilane. The decaphenylcyclopentasilane was very stable in relation to the four-membered ring and melted at about 464 °C without decomposition. The higher stability (in respect of the cyclotetrasilane derivative) was caused by the lower ring strain.

In 1978 Parkanyi *et al.*[27] reported the solid state structure of Si_5Ph_{10} obtained from recrystallization from benzene/ethanol.

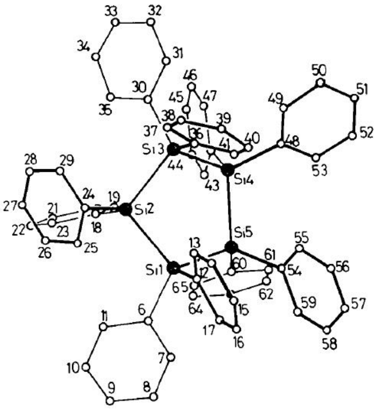

Figure 2.10: Crystall structure of Si_5Ph_{10}

As already mentioned above for perphenylated cyclotetrasilanes, the cyclopentasilane can be cleaved with iodine and dephenylation can be achieved with HI/AlI_3.[22]

The alternative cleavage reaction of cyclopentasilane[28] with PCl_5 formed 1,5-dichlorodecaphenylpentasilane, which was also a starting material for many reactions such as the synthesis of heterocyclic rings with oxygen or 1,5-diaminopentasilane. The ring cleavage was also achieved by using lithium affording 1,5-dilithio-pentasilane.[29] The reaction is strongly dependent on the conditions and also smaller dilithio compounds were found. Chain elongation was performed by the reaction of the 1,5-dilithio-pentasilane with chlorosilanes (e.g. Ph_2SiCl_2) and following hydrolysis, leading to the perphenylated 1,7-dihydroxy-heptasilane (Figure 2.11).

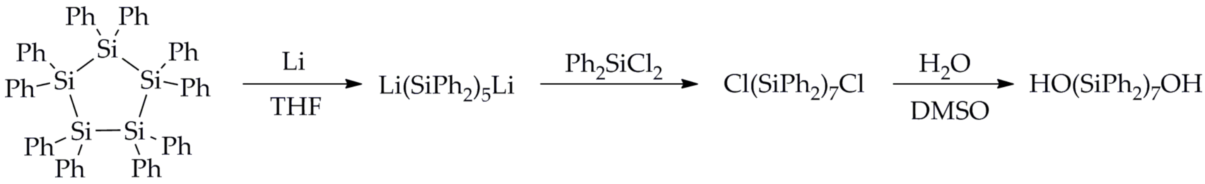

Figure 2.11: Chain elongation reaction with further hydrolysis

Because alkyl and aryl groups only offer small possibilities for reactions on the ring, the exchange against groups with enhanced reactivity was of great interest. The perchloro-substituted cyclopentasilane was obtained by the reaction of Si_5Ph_{10} with $HCl/AlCl_3$ in benzene, which could be applied in further reactions. For example the reaction of hydrochloro-cyclopentasilanes with R_3SnH in toluene led to compounds of the composition $Si_5H_xCl_{10-x}$ with x = 1-3 (Figure 2.12).[30]

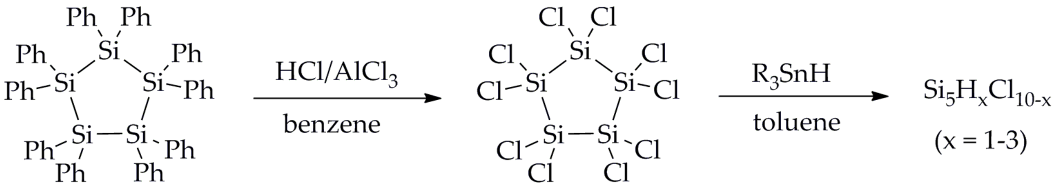

Figure 2.12: Formation of the perchloro-substituted cyclopentasilane

Additional reactions with cyclopentasilanes have been reported and well documented.[31]

Cyclohexasilanes

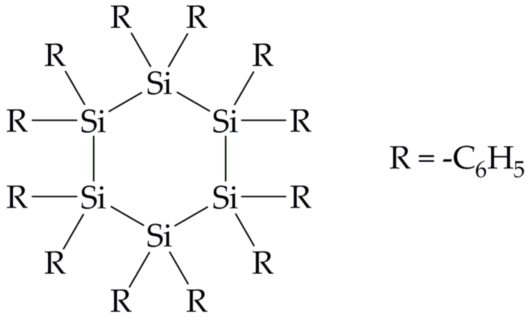

The six-membered perphenylated ring was first synthesized by Kipping[18] in 1921 (Figure 2.13), but the initial proposed structure was incorrect and later assigned correctly by Gilman *et al.*[24]

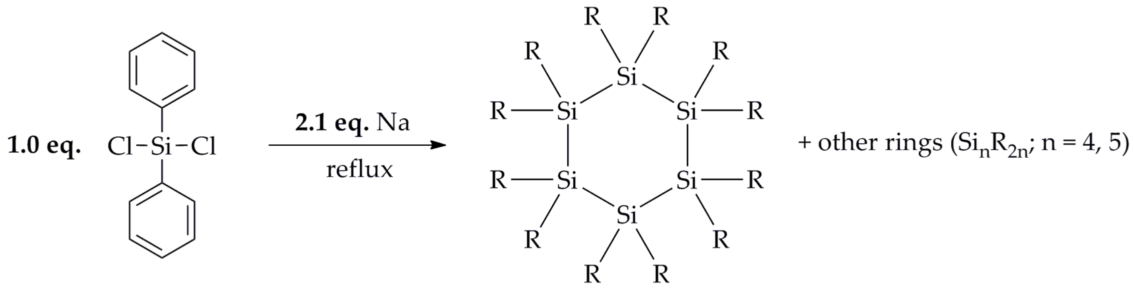

Figure 2.13: Synthesis of dodecaphenylcyclohexasilane

With the intention to synthesize dodecaphenylcyclohexasilane, dichlorodiphenylsilane was treated with 1,5-dilithio-decaphenylpentasilane (formed from decaphenylcyclopentasilane by treatment with lithium).[25] The four- and five-membered rings were isolated and another compound which was apparently the same compound as Kipping's Compound C.

Further chemistry with the six-membered perphenylated ring is similar to that of the four- and five-membered rings. The most common reaction is the dephenylation by for example HX/AlX_3 (X = Cl, Br) or triflic acid.[31]

Another interesting method to open the way for further compounds is to cleave one of the six-ring bonds with Li and THF to get a lithium-terminated open-chain compound. An example for a following conversion is the addition of $(CH_3)_3PO_4$ to the lithiated chain compound to get methyl end groups. An alternative way to obtain final methyl-terminated 4 silicon atoms containing chain is to cleave the six-membered ring with bromide in benzene and treat the bromine-terminated open-chain compound with CH_3Li[32] (Figure 2.14).

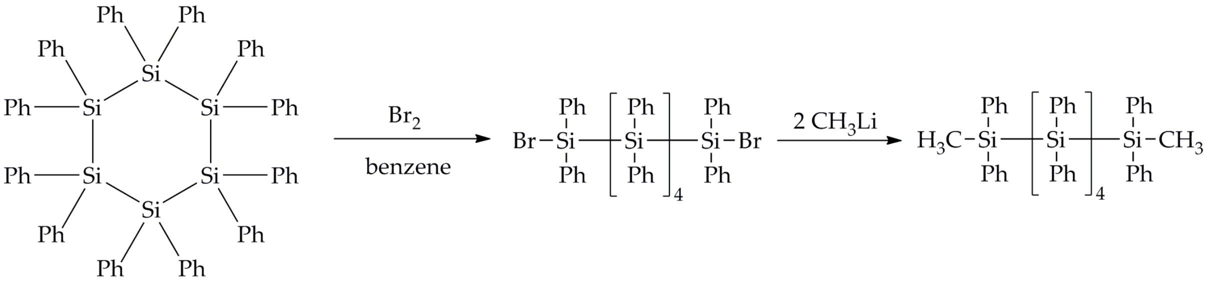

Figure 2.14: Ring cleavage of dodecaphenylcyclohexasilane

2.2.3 Radical Anions of Perphenylcyclopolysilanes

In 1965 Husk *et al.*[6] described the formation of a radical anion of dodecamethylcyclohexasilane. This new knowledge inspired Kira *et al.*[33] to study also the electrochemical behavior of perphenylated rings, published in 1979. They managed to form radical anions of octaphenylcyclotetrasilane and decaphenylcyclopentasilane on reduction with potassium in a mixture of THF and DME (1:1). In the case of the cyclopentasilane, further a radical anion was achieved by a electrolytic reduction using tetra-n-butyl ammonium perchlorate as the providing electrolyte. The anion radicals of the four- and five-membered cyclopolysilanes showed a slight yellow color and were quite stable at low temperatures ($<-65\,°C$). Either a cleavage of perphenylated Si-Si bonds[34] or a further reduction to secondary anion radicals[35] did not go along with the reduction. The observations indicated that an extra electron does not enter the phenyl rings, but is delocalized in the silicon ring.

Because of the insolubility of dodecaphenylcyclohexasilane in most solvents and their mixtures the formation of a radical anion was not successful.

3 Results & Discussion

3.1 Synthesis of Starting Materials

In first steps naphthyl substituted starting materials were synthesized *via* established synthetic routes.

3.1.1 Synthesis of perphenylated cyclosilanes Si_4Ph_8 and Si_5Ph_{10}

The perphenylated 4- and 5-membered rings were isolated and characterized by ^{29}Si-NMR measurements with peaks at -21.8 ppm for Si_4Ph_8 and -34.6 ppm for Si_5Ph_{10}.

The results were confirmed my their melting points:
Si_4Ph_8: 322 °C
Si_5Ph_{10}: 449 °C

3.1.2 Synthesis of di-1-naphthyldichlorosilane (1)

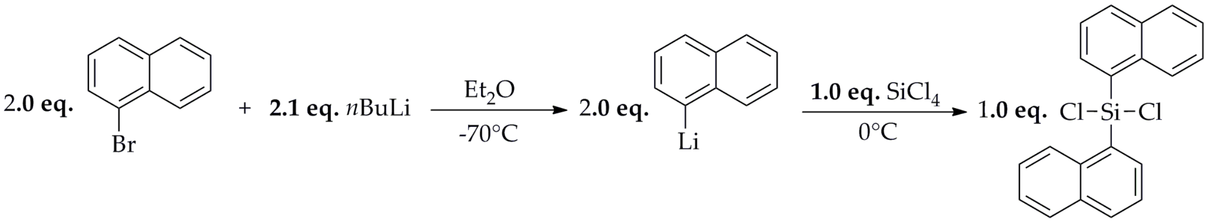

Figure 3.1: Synthesis of dinaphtyldichlorosilane (**1**)

The resulting yellowish solid was investigated *via* ^{29}Si-NMR spectroscopy in C_6D_6. One signal at 7.5 ppm could be found, which was assigned as di-1-naphthyldichlorosilane according to literature.[4] The result was confirmed by the molecular peak (M^+) gained by GC-MS with 352.0 and a melting point of 150 °C.

3.1.3 Synthesis of tri-1-naphthylchlorosilane (2)

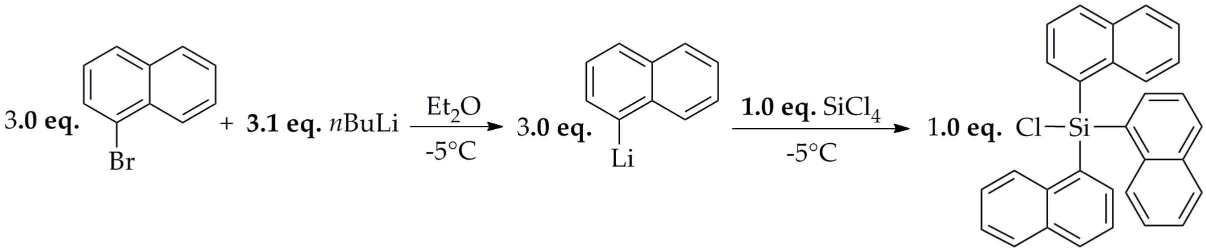

Figure 3.2: Synthesis of trinaphtylchlorosilane (**2**)

The resulting yellowish solid was investigated *via* ^{29}Si-NMR spectroscopy in C_6D_6. A signal at 4.0 ppm could be found, which was assigned as tri-1-naphthylchlorosilane according to literature.[36] The result was confirmed by the molecular peak (M^+) gained by GC-MS with 444.1 and a melting range between 205 – 209 °C.

3.2 Wurtz-coupling reactions with Mg

First magnesium was selected as the reacting metal, required for the reductive elimination of the diaryldichlorosilane to form Si-Si bonds. According to the reactions with Ph_2SiCl_2 it was expected that a series of 4, 5 and 6-membered silicon rings might be formed.

3.2.1 Small-scale serial experiments and the following scale-ups

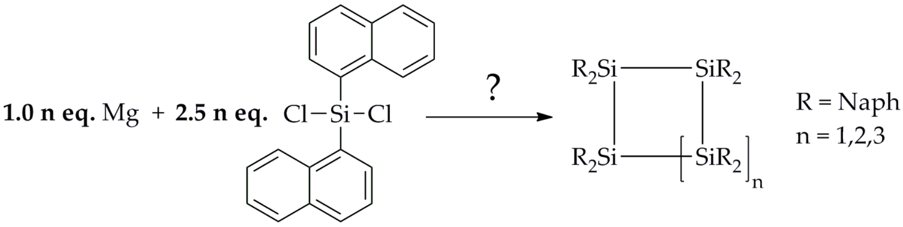

Figure 3.3: Wurtz-coupling reaction using Mg at RT

Regarding the rather passive behavior of the chosen earth alkaline metal magnesium, different methods of metal activation were selected. The different activated magnesium turnings were set up and the diluted di-1-naphthyldichlorosilane (**1**) was added.

Selected methods to activate magnesium:

- iodine crystal
- dibromoethan
- ethereal HCl (Et_2O/HCl)
- rasped

Mg - iodine crystal

The reaction result showed a dark brown solution and a white precipitate. The THF solution was subjected to a ^{29}Si-NMR measurement with a D_2O capillary showing three signals at -6.6 ppm, -21.9 ppm and -43.9 ppm with the corresponding intensities of 80% for -21.9 ppm and 30% for -43.9 ppm of the most intense peak at -6.6 ppm (100 %).

Mg - dibromoethan

Because of undefined results there will be no further discussion.

Mg - ethereal HCl

The reaction showed a dark brown solution and a white precipitate as result. A ^{29}Si-NMR measurement of the THF reaction solution was carried out with a D_2O capillary showing one intense signal at -6.5 ppm. Also small other signals appeared, but in a negligible intensity for this approach. The attempt of crystallization in CH_3Cl led to colorless crystals which were determined as naphthalene by X-Ray analysis.

The result of crystallizing naphthalene implies the cleavage of the Si-C bond between the naphthyl groups and the silicon atom of di-1-naphthyldichlorosilane and the resulting formation of naphthalene (see Figure 3.4). Considering the result of the small-scale experiment of magnesium activated by ethereal HCl, which resulted in one single signal, the reaction was up-scaled and repeated. The result was a totally different one.

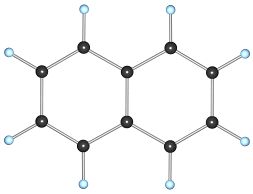

Figure 3.4: Crystal structure of the precipitated naphthalene

The ^{29}Si-NMR measurement showed a single signal at -65.4 ppm and no precipitate appeared (in contrast to the small-scale exp.). No difference in the reaction procedure could be figured out, but a reasonable explanation, or better suggestion for the different result is, that often Wurtz-coupling reactions are uncontrolled and results are hardly reproducible.

Nevertheless, the result showed just one signal of an unknown compound so that it was worth to do the work-up. The THF was replaced by toluene to get precipitate lithium chloride, whereby the reaction solution was heated up. The precipitate was fine dispersed in the toluene solution so that every (in the laboratory available) filter failed in separation. Also the centrifugation did not render the required result.

The toluene solution was taken off with a syringe and subjected to ^{29}Si-NMR measurement. The result was a totally different as the THF solution showed before: in total seven signals. The three signals with the highest and almost same intensity are at -17.1 ppm, -38.3 ppm and -39.8 ppm. The next is the signal at -18.2 ppm with an intensity of 75% of the highest ones. The remaining three signals at 8.1 ppm, -35.5 ppm and -45.8 ppm have the almost same intensity of 50%.

One possible explanation is a temperature sensitive product (meaning signal -65.4 ppm in the THF solution), so that the heating up of the toluene solution induced a cleavage of the compound.

Mg - rasped

The reaction yielded a dark brown solution and a white precipitate. The THF solution was investigated *via* ^{29}Si-NMR measurement with a D_2O capillary revealing three signals at 4.0 ppm, -6.6 ppm and -21.9 ppm with the corresponding intensities of 15% for 4.0 ppm and 50% for -21.9 ppm of the most intense peak at -6.6 ppm. The two signals at -6.6 ppm and -21.9 ppm are identical with two signals of the attempt with iodine activated Mg. In terms of the known preferred migration of naphthyl groups it can be suggested that the signal at 4.0 ppm shows a tri-1-naphthylchlorosilane (compound **2**), where one of the chlorides got cut off by lithium and replaced by a migrating naphthyl-group. Also a MALDI-MS of the precipitate was commissioned, but no suitable result could be achieved. Considering the simpleness of obtaining the rasped activated magnesium the reaction was rerun but due to the unclear statement in respect of the used equivalents in the published work of Gilman,[17] the equivalents were changed to a ratio based on other publications for lithium or rather as the equivalents for the Wurtz-coupling reaction should be chosen.

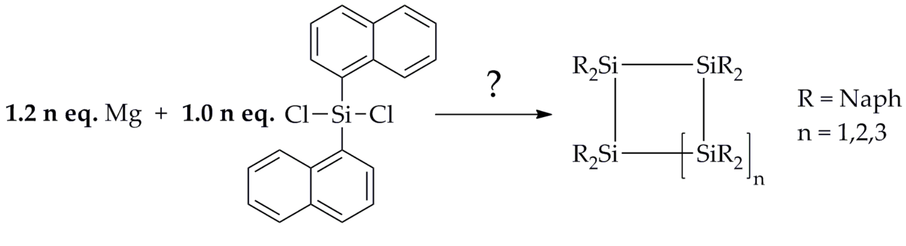

Figure 3.5: Wurtz-coupling reaction using rasped Mg at RT

A red-brown non-transparent reaction mixture with a little Mg residue could be observed. After removing the leftover magnesium a ^{29}Si-NMR measurement was taken which showed seven signals with the most intense at -39.5 ppm. All other signals at -18.1, -22.0, -39.9, -40.6, -41.8 and -46.0 ppm have an almost same intensity of 25% relative to the signal at 39.5 ppm.

The reaction was rerun but a totally different result eventuated. The ^{29}Si-NMR measurement revealed two signals, one at -18.3 ppm and the other at -22.1 ppm, with the almost same intensity.

An ATR-IR spectroscopy measurement of the remaining yellowish solid (shown in Figure 3.6), after removing THF, showed that still naphthyl is contained, so the suggestion of losing all naphthyl groups because of migration by the formation and sublimation of naphthalene can be excluded.

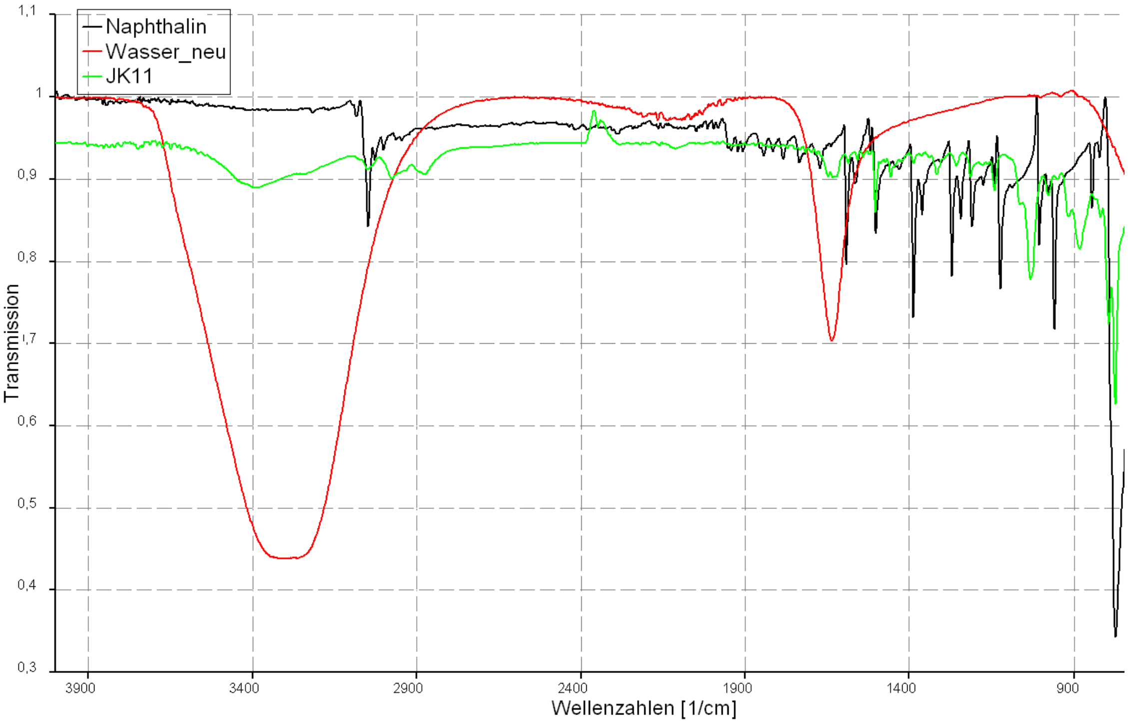

Figure 3.6: ATR-IR spectra

3.2.2 Conclusion for the reactions with Mg

In general can be said, that Wurtz-coupling reactions are often tricky because of the low reproducibility.

In the case of magnesium and di-1-naphthyl dichlorosilane it seems to be difficult to get the same result for the identical reaction two times. Despite the strict control of concentration, temperature and quality of the starting materials the results varied too much.

In regard to the type of magnesium, a dependency of the activation method to the resulting products could be determined.

The reaction with the ethereal activated Mg at the small-scale experiments seemed promising because of the one appearing main product in the ^{29}Si-NMR at -6.5 ppm, but then the unavailable reproducibility upset the plans.

These conclusions led to the change of the used metal from Mg to Li.

3.3 Wurtz-coupling reactions with Li

3.3.1 Wurtz-coupling using lithium band

The reaction procedure of the previous experiments was retained but instead of magnesium, lithium was used. In general lithium should be more reactive than magnesium. The reaction was set up with a lithium band, cut under argon atmosphere and the di-1-naphthyldichlorosilane (**1**) was added. According to the reactions with Ph_2SiCl_2 it was expected that a series of 4, 5 and 6-membered silicon rings might be formed.

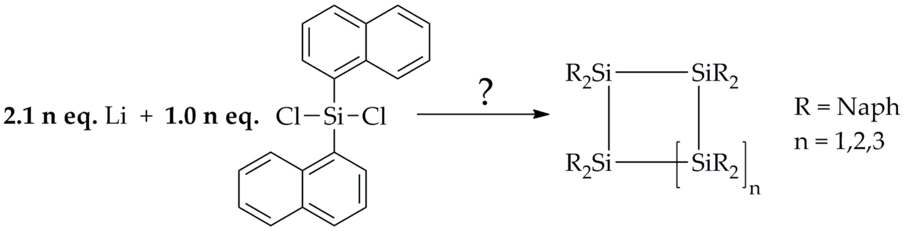

Figure 3.7: Wurtz-coupling reaction using Li at RT

The result was a dark brown solution containing also a residue of Li. After the removal of the leftover lithium a ^{29}Si-NMR measurement was taken which showed two signals as result: -7.4 ppm, with approximately half the intensity of the signal at -57.1 ppm.

Because of the immediate color change from brown to yellow at the moment of air contact the suspicion of possible radicals in the reaction mixture was traced by arranging an EPR measurement (electron paramagnetic resonance). However no radicals could be found in the reaction solution.

According to literature of the synthesis of perphenylated ring systems the reaction mixture was refluxed over 2 days. The still red-brownish reaction solution was again investigated by a ^{29}Si-NMR measurement which resulted in two signals: the one with the highest intensity at -29.0 ppm and the other signal with an intensity of approximately 60% at -24.1 ppm. It was not possible to determine these products so far, since the spectroscopy investigations (NMR, MS) did not give a clear picture.

Conclusively, temperature rise hence refluxing has a great influence on the reaction product. However, it could not be clarified if an existing cyclic compound is cleaved or *vice versa* a cyclic compound is built up from other fragments. Also the migration tendency of the naphthyl groups should be kept in mind.

On the assumption that the result of the room temperature reaction with signals at -7.4 ppm and -57.1 ppm could be an open-chain product, a possible resulting compound containing at least three naphthyl-substituted silicon atoms terminated with lithium (see Figure 3.8) was supposed.

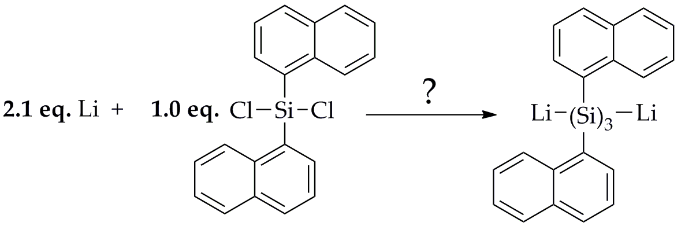

Figure 3.8: Possible lithium terminated open-chain product

The reaction was rerun and a NMR time study was accomplished.

24, 72, 120 and 168 hours after reaction start a ^{29}Si-NMR measurement was taken.

24 hours: -7.2ppm, -39.3 ppm and -57.3 ppm.

72 hours: -7.0 ppm and -57.5 ppm.

120 hours: -7.1 ppm, -39.3 ppm and -57.3 ppm.

168 hours: -7.0 ppm and -57.5 ppm.

With regard to the intensity of the signals it can be said, that at a time of 72 and 168 hours, where just the two already occurred signals show up, the intensity is almost the same. However, when the third signal at -39.3 ppm appears at the other two measurements with an intensity of 50% (relative to the signal at -57.3 ppm), the peak at around -7.0 ppm decreases to an intensity of 50%. This could be a hint for an on-going conversion of various products in the reaction mixture.

In general the result of the previous experiment could be reproduced but another signal at

-39.3 ppm came up at two measurements, which already appeared at two experiments with Mg. However, it has not been possible to determine the nature of the compound/intermediate related to the ^{29}Si-NMR shift at -39.3 ppm so far.

As in every performed experiment one of the huge problems was the work-up, especially the removal of formed LiCl. The result of the first steps of work-up was a beige solid dispersed in a dark brown solution. The main obstacle was the separation of the solid and the toluene solution concerning the chosen filter system:

Every available filter in the laboratory failed because of the fine dispersed particles in the solution. Also the trial to get a separation by centrifugation was not successful. The syringe filter with a pore size of 0.2 μm afforded an isolation of the solution but even if the filter was stored for days in the argon glove box, the solution reacted with the filter.

Due to the suggestion of the previous mentioned lithium terminated open-chain product, the reaction mixture according to figure 3.9 was divided into three parts and quenched either with trimethyl chlorosilane or bromobutane:

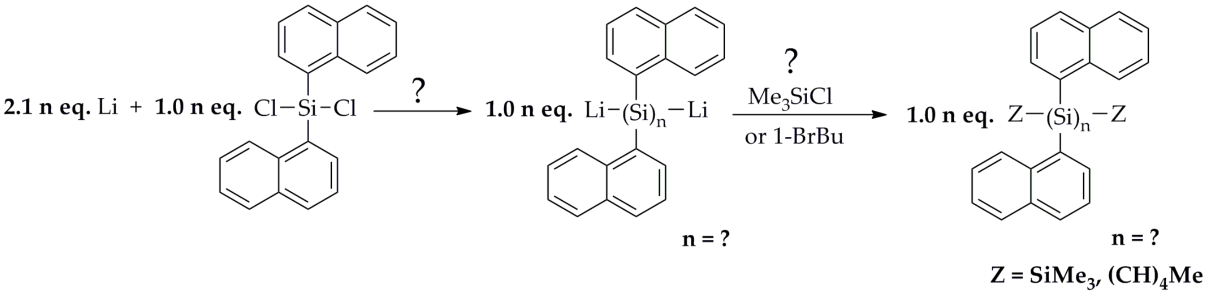

Figure 3.9: Wurtz-coupling reaction followed by the addition of Me_3SiCl respectively 1-BrBu

Addition of 1-bromobutane

In the first flask 1-bromobutane was added. A reddish grey solid precipitated, which was separated with a syringe filter in the dry box. The result was a yellow solution. The ^{29}Si-NMR measurement of the yellow solution exhibited no silicon species.

Even if the reaction mixture reacted with the syringe filter during filtration, no silicon compound is dissolved in the toluene anymore. Hence all the silicon species must be contained in the reddish grey precipitate, but the investigation was limited by the insolubility of the precipitate in organic solvents.

Addition of Me_3SiCl after removing residual of Li

In the second flask the leftover lithium was removed before the addition of freshly distilled Me_3SiCl. A color change to a dark reddish reaction solution with a bit of a black, fine dispersed precipitate could be observed.

The reddish THF solution was investigated by a ^{29}Si-NMR measurement which showed six signals. Three of the signals could be identified easily as the byproducts Me_6Si_2 (-19.7 ppm) and $Me_3Si\text{-}O\text{-}SiMe_3$ (7.2 ppm) as well as the excess of starting material (30.9 ppm).

The remaining three signals at -11.7 ppm, -13.3 ppm and -44.8 ppm (with an intensity of 10% relative to the peak at 30.9 ppm) led to the idea of product shown in Figure 3.10 with the corresponding signals.

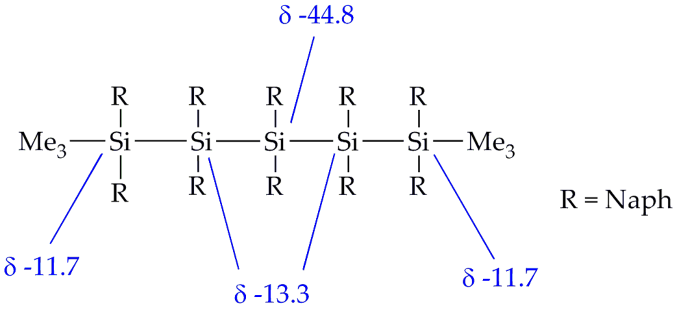

Figure 3.10: Possible lithium terminated open-chain product containing 5 silicon atoms, with corresponding ^{29}Si shifts

Addition of Me_3SiCl

In the third flask freshly distilled Me_3SiCl was added to the unfiltered reaction mixture while stirring at RT. The color of the reaction solution turned from brown to dark red with a bit of a black, fine dispersed solid. A ^{29}Si-NMR measurement of the dark red solution showed a result of eight signals where the most intense at 7.2 ppm was supposed to be Me_3Si-O-$SiMe_3$. The signal at -19.7 ppm (intensity of 50%) is the Me_3Si-$SiMe_3$.

Three signals were already found in the previous reaction ("Addition of Me_3SiCl after removing rest of Li") appearing at -11.9 ppm, -13.3 ppm and -44.9 ppm. However, three additional signals at -16.2 ppm, -37.2 ppm and -39.2 ppm were also detected. All six signals showed an intensity between 40 and 60% relative to the signal at 7.2 ppm.

To confirm the idea of the formation of chain type compounds (see Figure 3.10) DI-EI as well as MALDI-MS were performed. In general the MS showed that an oligomerization of the dinaphthyldichlorosilane occurred. As expected from the ^{29}Si-NMR investigations a number of products could be found. Surprisingly, no chlorine could be detected in the MS investigations as well as only an unusual small number of Me_3Si containing fragments. The latter aspect indicates that Me_3Si-terminated species as indicated in Figure 3.10 are not the main product of the reaction. Nevertheless the MS spectra are displaying $Naph_2Si$ chains of different length. A closer evaluation reveals that not only $Naph_2Si$ fragments could be detected but also fragments of type [$Naph_2Si$ - 2 m/z] indicating the loss of two hydrogens at some of the $Naph_2Si$-units. Comparing these perceptions with the results of the ^{29}Si-NMR investigations the conclusion can be drawn that the obtained oligomers consist not only of $Naph_2Si$ but also of silol-type units (shown in Figure 3.11)

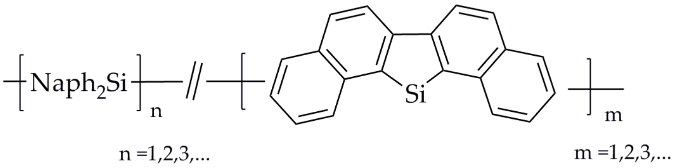

Figure 3.11: Supposed oligomerized chain products

The ^{29}Si-NMR signals at -37.2 ppm, -39.2 ppm and -44.9 ppm are due to [Naph$_2$Si] units while the signals at -11.9 ppm, -13.3 ppm and -16.2 ppm might be due to the silol type silicon. The latte are in a similar range like known silols in literature.[45–47]

Also other fragments, as hexanaphthyl disilane and different chains consisting of [Naph$_2$Si] only, could be found An exact statement about the end groups of the obtained chains was not possible, however there are indications that the main products are terminated by H-atoms only.

3.3.2 Wurtz-coupling using freshly bought lithium band

As shown in the previous chapter the reproducibility of the experiments was rather tricky. To quantify if this was due to the quality of the lithium used, some experiments were repeated by using freshly bought lithium band.

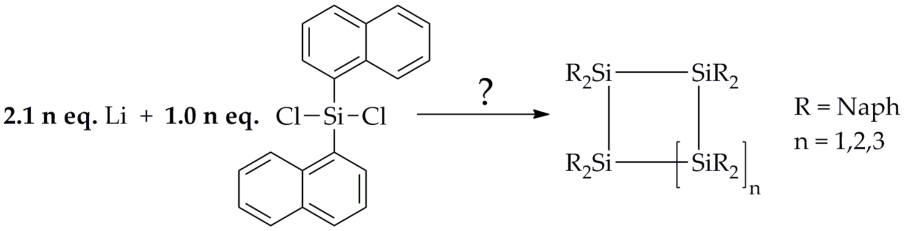

Figure 3.12: Wurtz-coupling reaction using Li (new lithium band) at RT

The reaction showed no brownish color change but turned light yellowish. The yellowish reaction solution without any leftover lithium was investigated with ^{29}Si-NMR which led to one single signal at 7.5 ppm. A spiked sample (addition of educt) was measured and the result was still only the signal at 7.5 ppm, leaving the question what happened with the lithium, if there is just educt in the reaction solution.

Wet THF as source for this reaction behavior could be ruled out since the solvent was checked by a Karl-Fischer titration and gave a content of water less than 4 ppm. Another possibility would be the cleavage of THF by lithium which were not proven so far, however in further investigations the THF should be replaced by another solvent.

Due to the previous result the reaction was rerun but was refluxed from the moment of the addition of the dichlorosilane solution on. A different reaction behavior in contrast to the room temperature experiment was observed.

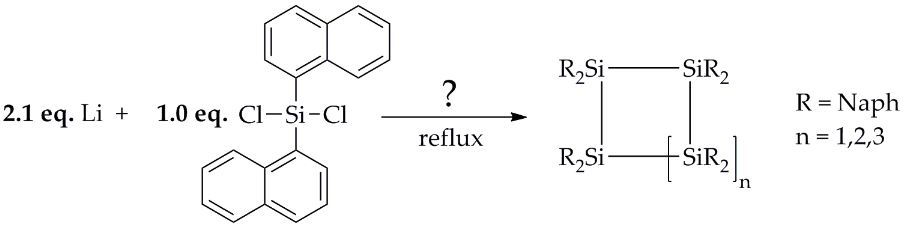

Figure 3.13: Wurtz-coupling reaction using Li supported by refluxing

The reaction resulted in a dark brown solution and little residue of Li. Two main signals at -29.2 ppm and -41.9 ppm appeared in the ^{29}Si-NMR spectra. Other three signals with an intensity of in sum 30 % emerged at -18.3 ppm, -39.4 ppm and -45.9 ppm.

After work-up (THF was removed by turbo molecular pump and replaced by toluene, to get rid of the precipitated LiCl the reaction mixture was filtered by a reverse filter conditioned with celite) a ^{29}Si-NMR measurement was taken and showed two main signals at -29.0 ppm and -39.7 ppm.

Other four signals with an intensity of 40 % of the main peaks showed up at -24.9 ppm, -37.2 ppm, -38.9 ppm and -41.8 ppm. A melting range between 138 and 142 °C was observed.

The product was also investigated by MS measurements which gave results similar to the ones suggested in Figure 3.11 in the previous chapter. Also here other fragments as hexanaphthyl disilane and diverse chains of -Si(Naph$_2$)$_2$- without naphthyl-naphthyl bonds could be found. Nevertheless, by comparing the results of the room temperature reaction with the reaction at the boiling point of THF, the conclusion can be drawn that at higher temperatures freshly cut lithium reacts with the chloro-function first, before undergoing some unexpected side reactions.

3.3.3 Wurtz-coupling of 1-Naph$_3$SiCl with Li

That quality of lithium used, as well as unexpected side reactions are a general effect in the chemistry of chlorosilanes, could be shown also by using Naph$_3$SiCl. The idea of this reaction set-up was to form a pernaphthylated disilane, hexanaphthyl disilane.

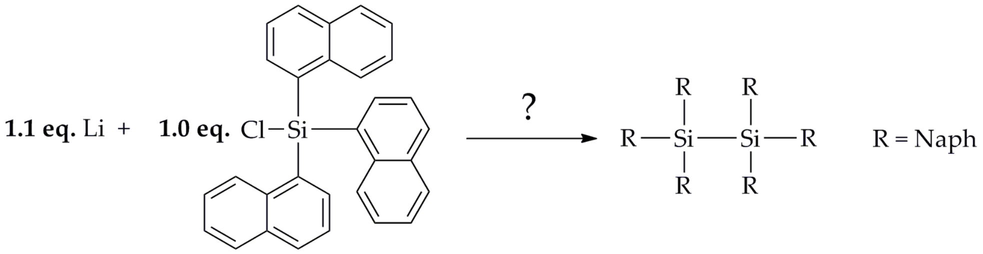

Figure 3.14: Wurtz-coupling reaction of 1-Naph$_3$SiCl using Li

The reaction resulted in a slightly pink white solid. One signal at -28.9 ppm appeared in the ^{29}Si-NMR spectra with a partially melting at 209 °C. With the consideration of the possibility of hydroxy groups on the partially oxidized lithium band, the suggestion of the hydroxy compound Naph$_3$SiOH with a melting point of 210 °C arises. The hydrolysis by moisture could be excluded as possible source by a hydrolysis experiment. A XRD measurement of a crystal obtained from THF approved the suggestion of a hydroxy compound (see Figure 3.15).

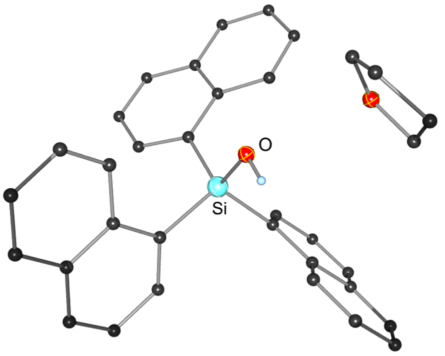

Figure 3.15: Crystal structure of obtained crystal of Naph$_3$SiOH with THF complexed

3.4 First Cyclosilane-based Battery Materials

In a project laboratory[37] in cooperation with Hanzu *et al.*[38] first investigations of the electrochemical behavior of two perphenylated cyclic precursor materials (Si_4Ph_8 and Si_5Ph_{10} see chapter 3.1.1 and 5.7) to silicon nano-composites were carried out.

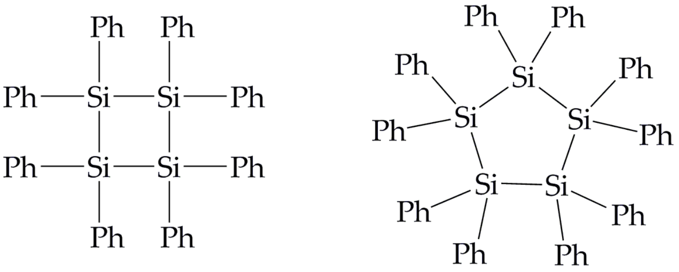

Figure 3.16: Structures of Si_4Ph_8 and Si_5Ph_{10}

Despite the well known properties of state-of-the-art lithium ion batteries[39,40] there is still a highly intensive and competing research going on for the development of novel battery materials meeting the higher energy requirements for advanced applications.

To address such requirements, higher capacity materials are needed. Idota *et al.*[41] found a class of amorphous tin-based composite oxides (TCOs) which could be used as anode active materials that showed 500 – 600 mAh/g reversible capacity. Nanoparticles of transition-metal oxides of the general formula MO with M = Co, Ni, Cu or Fe have been found to deliver capacities up to 700 mAh/g.[42] Further, there is the possibility to increase the capacity of graphite by intercalating another compound into the graphite structure, thus realizing a nano-composite material. Silicon, is a promising negative electrode material having a high theoretical specific capacity. Unfortunately, it also has its drawbacks: if utilized in pure macroscopic elemental form, an anisotropic volume expansion occurs during the electrochemical insertion of lithium leading to cracks, contact loss and electrode destruction.[43] In order to alleviate these issues, silicon nano-composites and nanostructures (e.g. silicon nano-particles (SiNPs) and silicon nano-wires (SiNWs) which have shown reversible capacities of 1700 mAh/g and 900 mAh/g at room temperature[44]) have been proposed and were proven to be a feasible solution for the realization of high-capacity negative electrodes. However, the silicon-based materials are far less developed than carbonaceous (graphitic) materials leaving major opportunities for further research and improvement.

Electrodes containing different amounts of octaphenylcyclotetrasilane respective decaphenylcyclopentasilane and graphite were prepared and tested in electrode SwagelokTM test cells by cyclic voltammetry and galvanostatic cycling.[37] The resulting data shows two reduction peaks in galvanostatic cycling experiments (differential capacity plots) and cyclic voltammetry at 0.5 and 0.7 V that are usually associated with SEI formation.

However, the presence of the cyclic silanes seems to influence this process, as it can be seen in the cyclic voltammetry and differential capacity curves. While the presence of silanes in general is *a priori* expected to degrade the cycling behavior, at least due to their insulating and rather chemically inert nature, this was not found to be true for both perphenylated cyclic silane compounds studied. Indeed, the decaphenylpentasilane actually tends to increase the measured capacity of the system.

4 Conclusion & Outlook

Within the context of this work attempts to synthesize pernaphthylated cyclosilanes as novel battery materials failed so far, but some presumptions about the reactions of naphthyl-substituted chlorosilanes could be gathered.

In general it can be concluded, that Wurtz-coupling reactions with magnesium are tricky and challenging because of the low reproducibility. In regard to the type of magnesium, a dependency of the activation method to the resulting products could be determined. Due to the migration tendency of the naphthyl substituents, also confirmed by the crystallization of naphthalene at the synthesis attempt of di-1-naphthyldichlorosilane and ethereal HCl activated magnesium, the isolation of cyclic products failed.

In respect to the reactions performed with lithium a number of novel assumptions could be made:

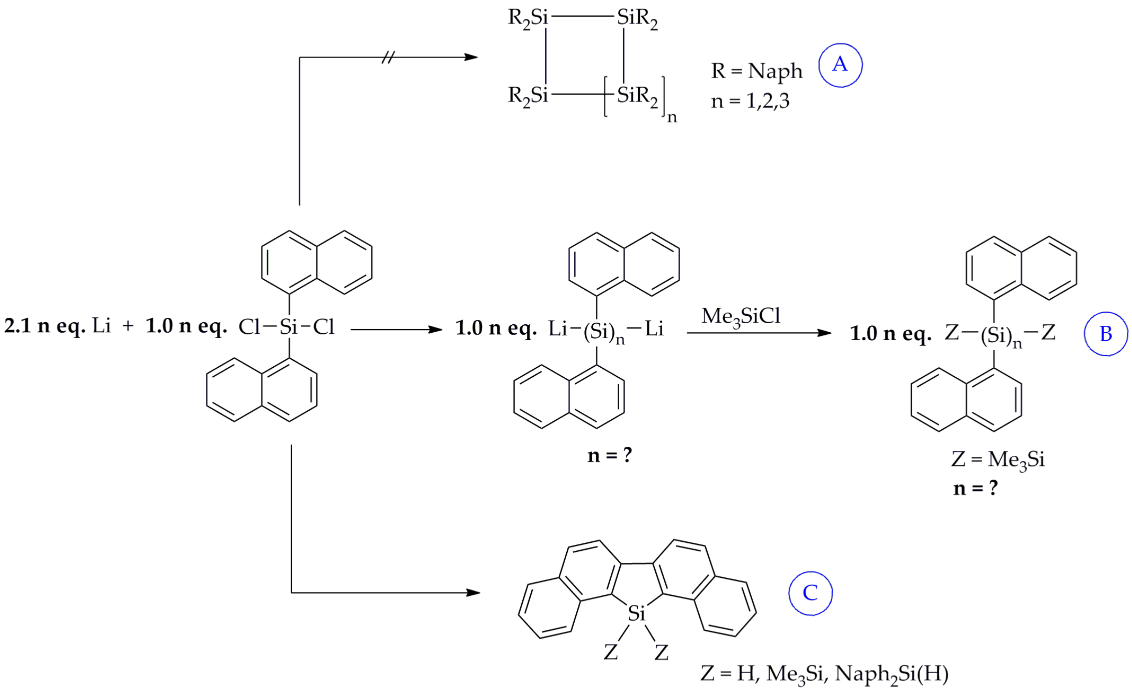

Figure 4.1: Summary of reaction paths and corresponding product types

The reactions carried out using lithium gave the general insight that the formation of rings as shown above as product type A did not take place. No evidence for a Si-ring formation could be found.

According to the received ^{29}Si-NMR shifts and MS data products of the types B and C could be suggested. As found in literature, ^{29}Si-NMR shifts of known compounds as silol derivatives[45–47] similar to the product type C match with the obtained shifts in this work. Finally, it can be said, that an oligomerization of the dinaphthyldichlorosilane occurred, but also a reaction between the naphthyl substituents themselves took place.

Concerning the electrochemical investigation of perphenylated cyclosilanes can be concluded, that an electrochemical process takes place, but the whereabouts of these reactions are still unknown. However, one possibility would be the formation of radical anions, as shown by Kira, Bock and Hengge[33] which could also take place by an electrochemical reaction.

All of the achieved results will need to be confirmed and therefore, the tests will need to be rerun. Besides this rerun experiments due to the sensibility of the results in terms of scientic as well as commercial implications all experimental details are to remain within the Project Laboratory Report[37] and will remain confidential until otherwise decided.

5 Experimental

5.1 General & Analytics

5.1.1 General Procedures and Used Chemicals

All reactions were carried out under inert atmosphere using nitrogen as inert gas. To ensure a dry atmosphere, nitrogen of the house intern line passed a molecular sieve and a glass tube filled with glass wool and phosphorus pentoxide to remove remaining moisture. All dried solvents were obtained from a solvent drying plant (Innovative Technology, inc), whereas THF was additionally stored and distilled over lithium aluminium hydride.

The used chemicals were purchased from commercial sources (see Table 5.1 below) and used without further modification, unless it's mentioned.

Table 5.1: Used chemicals and their commercial sources

chemical compound	**commercial source**
1-bromonaphthalene	Alfa Aeser
nBuLi 2.5 M in hexane	Sigma Aldrich
silicon tetrachloride	Sigma Aldrich
lithium (band)	Sigma Aldrich
lithium aluminium hydride	Sigma Aldrich
trimethyl chlorosilane	Sigma Aldrich
1-bromobutane	Sigma Aldrich
celite 512 medium (calcined)	Sigma Aldrich
syringe filter, 0.2 μm, hydrophobic PTFE	Sigma Aldrich

5.1.2 Analytics

Melting Point Measurements

All melting point measurements were performed by a Stuart Scientific SMP 10 (up to 300 °C) and a threefold determination was carried out.

Elemental Analysis &

All elemental analysis were performed with an Elementar Vario EL using sulfanilic acid as standard.

GC-MS

Compounds were ionized via electron impact (70 eV) ionization. Mass spectra were recorded by a Waters GCT Premier equipped with direct insertion.

NMR spectroscopy

^{1}H-, ^{13}C- and ^{29}Si-NMR spectra were recorded on a Mercury 300 mHz spectrometer from Varian at 25 °C. Chemical shifts are reported in parts per million (ppm) relative to TMS (δ = 0 ppm). Coupling constants (J) are given in Hertz (Hz). The spectra were analyzed in MestRec 4.5.6.0.

MALDI-TOF & EI-DI mass spectroscopy

MALDI-TOF mass spectrometry was performed on a Waters micro MX time-of-flight mass spectrometer. Ions were generated by irradiation just above the threshold laser power (laser: wavelength 337 nm, operated at a frequency of 5 Hz). Positive ion spectra were recorded in reflectron mode and externally calibrated with a suitable mixture of poly(ethyleneglycol)s (PEG). The spectra of 100-150 shots were averaged. Analysis of data was done with MassLynx-Software V4.1 (Micromass/Waters, Manchester, UK). Samples were prepared by mixing a solution of DCTB (c = 10 mg/mL in THF) and a solution of the sample (c = 0.05 mg/mL) in the cap of a microtube in a ratio of 10:1 (v/v). 0.5 L of the resulting mixture were deposited on the sample plate (stainless steel) and allowed to dry under a stream of argon.

Electron impact (EI; 70 eV, source temperature 250 C) mass spectra were recorded on an orthogonal time-of-flight mass spectrometer (Waters GCT Premier) equipped a direct insertion probe (DI). 0.5 L of a solution of the sample (c = 0.1 mg/mL) were placed in the glass cup used for DI, dried under atmospheric pressure using a gentle stream of argon, and transferred into the vacuum. The acquisition of mass spectra (mass range: 50–1300 Da; 1 spectrum/s; resolution: appr. 7500 FWHM) was started immediately. Spectra were continuously acquired while the sample was heated from room temperature to 550 C. Data were processed using MassLynx (version 4.1).

X-Ray Analysis

XRD data collection was performed on a Bruker Apex II diffractometer with use of Mo Kα radiation ($\lambda = 0.71073\ \mathring{A}$) and a CDD area detector. Empirical absorption corrections were applied using SADABS. The structures were solved with use of either direct methods or the Patterson option in SHELXS and refined by the full-matrix least-squares procedures in SHELXL. Non-hydrogen atoms were refined anisotropically. Hydrogen atoms were located in calculated positions corresponding to standard bond lengths and angles.

ATR-IR spectroscopy

A Bruker Alpha-P with a Platinum-ATR-sample module was used for ATR measurements.

Electron Paramagnetic Resonance (EPR)

The EPR spectra was recorded with Miniscope MS300 (Magnettech, Germany) X-Band EPR spectrometer.

5.2 Synthesis of di-1-naphthyldichlorosilane (1)

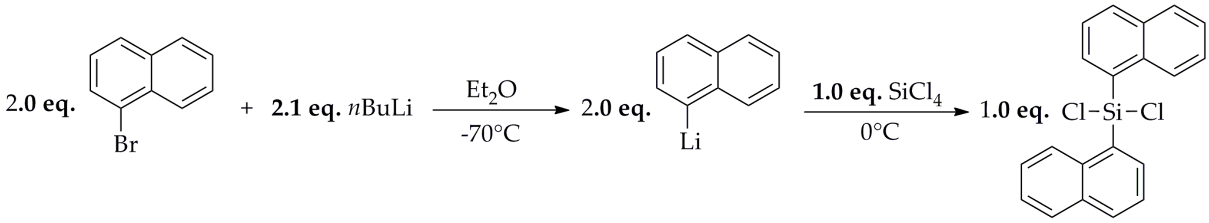

Figure 5.1: Synthesis of dinaphtyldichlorosilane

A flask equipped with a dropping funnel was charged with 11.9 mL (2.0 eq., 84.9 mmol) of 1-NaphBr in 150 mL Et_2O as well as the dropping funnel was loaded with 55.7 mL (2.1 eq., 89.2 mmol) 2.5 M n-BuLi in hexane. The ethereal solution was cooled to $-70\,°C$ using a $EtOH/N_2$-bath. The lithiation reaction was started by slow addition of nBuLi. After completion the cooling bath was removed and the yellowish suspension was stirred and cooled with an ice bath for around 1 hour.
The lithiated reaction suspension was cannulized dropwise to 4.9 mL (1.0 eq., 42.5 mmol) of distilled $SiCl_4$ (in 100 mL of Et_2O) under ice bath cooling. The white suspension was stirred overnight at room temperature.

Et_2O was condensed off and replaced by toluene (∼200 mL). The reaction mixture was heated up to reflux and filtered through celite. The result was a light yellow solution before toluene was removed by distillation with the membrane pump. The received product was a white amorphous solid (with 69% yield).

^{1}H-NMR (300.22 MHz, C_6D_6): δ 8.57-8.48 (dd,2H), 8.12 (d,2H,3J(H2-H3)= 6.9 Hz, 7.59 (d,2H); 3J(H8-H7) = 8.2 Hz, H8), 7.55-7.46 (dd,2H,H7), 7.12-7.01 (m, 6H,H4,H5,H6).
^{13}C-NMR (75.5 MHz, C_6D_6): δ 136.10, 135.57, 133.67, 132.97, 129.66, 129.08, 127.89, 126.89, 126.10, 124.87.
^{29}Si-NMR (59.64 MHz, C_6D_6): δ 7.6.
GC-MS: tR = 23.799; m/z = 352.0.
Melting point: 150 °C

5.3 Synthesis of tri-1-naphthylchlorosilane (2)

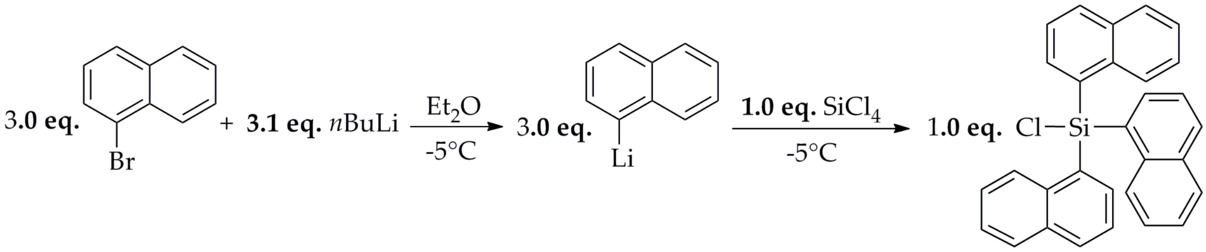

Figure 5.2: Synthesis of trinaphtylchlorosilane

A flask equipped with a dropping funnel was charged with 9.5 mL (3.0 eq., 67.4 mmol) of 1-NaphBr in 100 mL Et_2O as well as the dropping funnel was loaded with 4.4 mL (3.1 eq., 69.7 mmol) 1.6 M *n*-BuLi in hexane. The ethereal solution was cooled to $-5\,^\circ C$ using an ice bath. The lithiation reaction was started by slow addition of *n*BuLi. After complete addition the yellowish suspension was stirred and cooled with an ice bath for around 30 minutes. 2.6 mL (1.0 eq., 22.5 mmol) of freshly distilled $SiCl_4$ (in 200 mL of Et_2O) were added under ice bath cooling. The reaction mixture was stirred for 2 hours before the mixture was poured onto 500 mL of diluted hydrochloric acid. The organic layer was washed well with water. The solvent was dried over Na_2SO_4 filtered off and removed by reduced pressure.
The received product was a white yellowish amorphous solid.

^{1}H-NMR (300.22 MHz, C_6D_6): δ 8.54-8.50 (dd,3H), 8.14-8.11 (d,3H,3J(H2-H3)= 7.0 Hz, 7.61-7.58 (d,3H,3J(H8-H7) = 8.3 Hz, H8), 7.52-7.49 (dd,3H,H7), 7.12-7.07 (m, 9H,H4,H5,H6).
^{13}C-NMR (75.5 MHz, C_6D_6): δ 136.10, 135.57, 133.66, 132.96, 129.65, 129.07, 126.89, 126.10, 124.87, 119.31.
^{29}Si-NMR (59.64 MHz, C_6D_6): δ 4.0.
GC-MS: tR = 37.027; m/z = 444.1.
Melting range: $205 - 209\,^\circ C$

5.4 Wurtz-coupling of 1-Naph$_2$SiCl$_2$ with Mg

5.4.1 Small-scale serial experiment

Some simultaneously started Wurtz-coupling reactions with magnesium as the used metal were set with different methods of Mg-activation:

- rasped Mg
- Mg activated by a iodine crystal
- dibromoethan
- etheral HCl (Et_2O/HCl)

At the first activation mode the Mg was rasped in an argon-drybox from a metal rod. The iodine activated Mg was treated with a iodine crystal, the glass vessel was heated with a heatgun under vacuum until the iodine vapor was completely removed. Dibromoethan was added to the Mg before the Wurtz-coupling reaction was started. Mg turnings were stirred overnight in a 3 molar solution of Et_2O/HCl, MgCl was formed. The turnings and the salt were filtered and washed with distilled THF to remove the salt. Afterwards the turnings were dried under vacuum. According to the work of Gilman *et al.*[17] the used equivalents for the best obtainable yield were Mg : 1-Naph$_2$SiCl$_2$ of 1 : 2.5 eq. The amount of magnesium which was used for each of the reactions was in the range of 0.06 to 0.09 g. A solution of 14.02 g **1** in 160 mL distilled THF was prepared and added volumetrically to the different activated magnesium set up in glass vessels (Table 5.2).

Table 5.2: Weighed portions

Activation method	**Mg [g]**	**Naph$_2$SiCl$_2$ in THF [mL]**
rasped Mg	0.07	24.9
Iodine crystall	0.06	28.9
dibromoethane	0.07	24.9
ethereal HCl	0.09	37.3

The reactions were stirred at room temperature for 4 days.

After reaction start all of the reaction solutions were light brownish and the reaction with dibromoethan was yellowish. After 2 hours stirring the reaction solution with rasped Mg turned brown. After 4 days all reaction mixtures had a brown solution and a white to beige precipitate.

Mg - rasped

^{29}Si-NMR (59.64 MHz, D_2O capillary in THF): δ 4.0, -6.6, -21.9.

MALDI-MS: No results

Mg - iodine crystal

^{29}Si-NMR (59.64 MHz, D_2O capillary in THF): δ -6.6, -21.9, -43.9.

Mg - dibromoethan

^{29}Si-NMR (59.64 MHz, D_2O capillary in THF): δ data loss.

Mg - ethereal HCl

^{29}Si-NMR (59.64 MHz, D_2O capillary in THF): δ -6.5.

MALDI-MS: No results

5.4.2 Magnesium activated by ethereal HCl - Mg : 1-Naph$_2$SiCl$_2$ of 1.0: 2.5 eq.

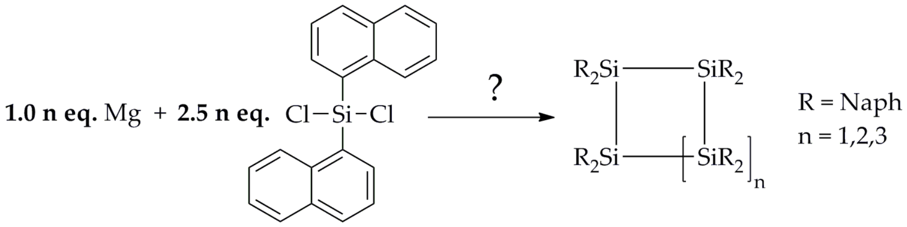

Figure 5.3: Wurtz-coupling reaction using Mg activated by ethereal HCl

As proceeded in the small-scale serial experiment 0.14 g (1.0 eq., 5.8 mmol) Mg were treated with Et$_2$O/HCl and set up. 5.0 g (2.5 eq., 14.4 mmol) of **1** diluted in 30 mL distilled THF was added dropwise with a cannula. The reaction mixture was stirred overnight at RT. The result was a dark red-brown solution, but no precipitate appeared.

^{29}Si-NMR (59.64 MHz, D$_2$O capillary in THF): δ -65.4.

The THF was removed under vacuum and replaced by ~30 mL dry toluene. The reaction solution was refluxed for 10 minutes whereby a white precipitate was formed. The reaction mixture was obtained as a fine dispersion. The trial to separate the solution and the precipitate failed because no filter with an appropriate pore size was available in the laboratory. Also the attempt to get a successful separation by centrifugation failed.

^{29}Si-NMR (59.64 MHz, C$_6$D$_6$) of the toluene solution after work-up: δ 8.1, -17.1, -18.2, -35.5, -38.3, -39.8, -45.8.

GC-MS: tR = 10.123; m/z = 128.1 (79 %, in toluene)

5.4.3 Rasped magnesium - changed ration Mg : 1-Naph$_2$SiCl$_2$ of 1.2 : 1.0 eq.

Because of the unclear statement in respect of the used equivalents in the published work of Gilman,[17] the equivalents were changed to a ratio based on other publications for lithium.

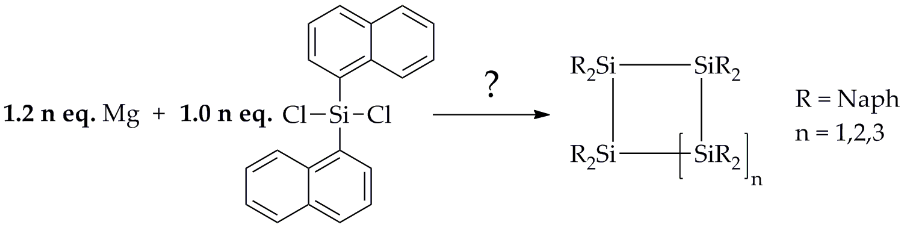

Figure 5.4: Wurtz-coupling reaction using rasped Mg

The magnesium was rasped in the argon-drybox and the reaction was carried out in distilled THF at room temperature. 0.1 g (1.2 eq., 4.1 mmol) of the rasped Mg was set up and 1.2 g (1.0 eq., 3.4 mmol) of **1** was diluted in ~30 mL and added dropwise with a syringe. The reaction mixture was stirred overnight at RT.

The result was a dark red-brown solution and some residual Mg.
The solution was separated from the leftover Mg by a reverse filter and transferred into another dry flask.

^{29}Si-NMR (59.64 MHz, D_2O capillary): δ -18.1, -22.0, -39.5, -39.9, -40.6, -41.8, -46.0.

5.4.4 Rasped magnesium (2. trial) - Mg : 1-Naph$_2$SiCl$_2$ of 1.2 : 1.0 eq

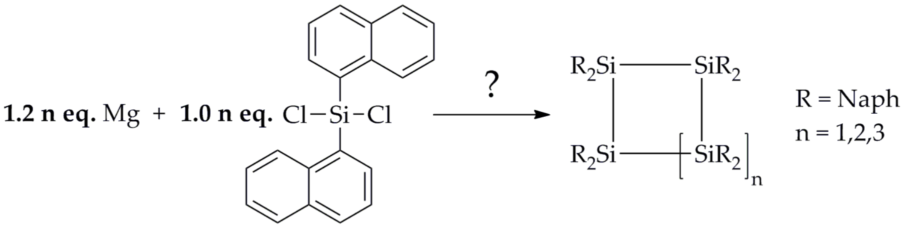

Figure 5.5: Wurtz-coupling reaction using rapsed Mg

The reaction was carried out as 5.4.3.

0.4 g (1.2 eq., 17.3 mmol) of the rasped Mg was set up and 5.1 g (1.0 eq., 14.4 mmol) of **1** was diluted in ∼120 mL and added dropwise with a syringe. The reaction mixture was stirred overnight at RT.

The result was also a dark red-brown solution and some residual Mg.

The solution was separated from the leftover Mg by a reverse filter and transferred into another dry flask. After NMR measurement the THF was removed using the turbo molecular pump (10^{-5} mbar) and the remaining yellowish solid was investigated by an ATR-IR measurement to see if there are any naphthyl groups left anymore.

^{29}Si-NMR (59.64 MHz, D_2O capillary): δ -18.3, -22.1.

ATR-IR: 3600-3400 cm^{-1}, 3050 cm^{-1}, 2950 cm^{-1}, 2900 cm^{-1}, 1600 cm^{-1}, 1500 cm^{-1}, 1150 cm^{-1}, 1050 cm^{-1}, 850 cm^{-1}, 750 cm^{-1}.

5.5 Wurtz-coupling of 1-Naph$_2$SiCl$_2$ with Li

5.5.1 Lithium band - Li : 1-Naph$_2$SiCl$_2$ of 2.1 : 1.0 eq.

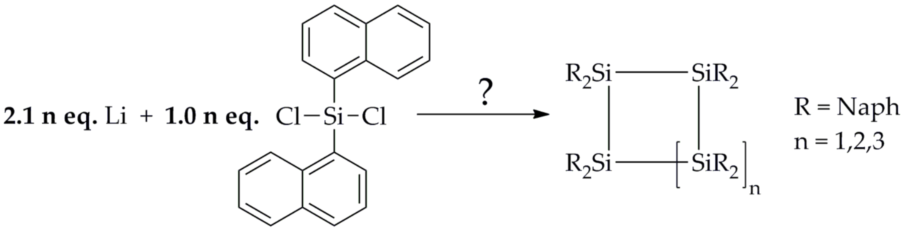

Figure 5.6: Wurtz-coupling reaction using Li (1. trial)

0.083 g (2.1 eq., 11.8 mmol) of the lithium band was cut and prepared in a dry glass vessel under argon atmosphere. 2.0 g (1.0 eq., 5.7 mmol) of **1** diluted in ~30 mL distilled THF was added dropwise by a cannula to the dry lithium pieces.

A few minutes after reaction-start a light temperature rise and a light brownish discoloration could be observed. After stirring overnight the result was a dark brown solution and little residue of Li.
The solution was separated from the leftover Li by a reverse filter and transferred into another dry flask.
After a NMR-measurement the reaction solution was refluxed for 2 days to see what happens if the reaction conditions are carried out based on the literature of the synthesis of the perphenylated ring systems where all reactions are run under reflux conditions.[6] After refluxing another NMR was taken.

EPR: negative, no radicals.

^{29}Si-NMR (59.64 MHz, D_2O capillary in THF) before reflux: δ -7.4, -57.1.

^{29}Si-NMR(59.64 MHz, D_2O capillary in THF) after reflux: δ -24.1, -29.0.

5.5.2 Lithium band (2. trial) - Li : 1-$Naph_2SiCl_2$ of 2.1 : 1.0 eq

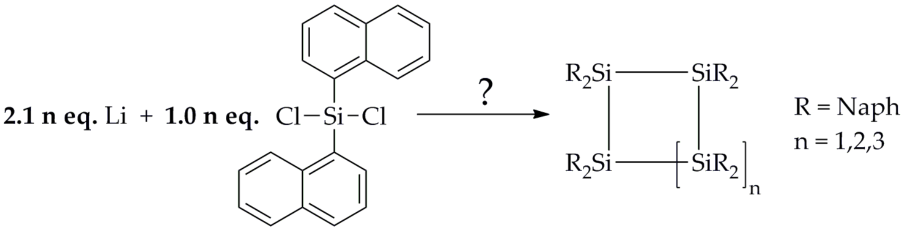

Figure 5.7: Wurtz-coupling reaction using Li (2. trial)

The reaction was carried out as the reaction in 5.5.1.

0.32 g (2.1 eq., 45.3 mmol) of the lithium band was cut and prepared in a dry glass vessel under argon atmosphere. 8.0 g (1.0 eq., 22.1 mmol) of **1** diluted in ~120 mL distilled THF was added dropwise by a cannula to the dry lithium pieces. Also the same observations were made.

NMR study: NMR measurement was taken after 24, 72, 120 and 168 hours.

24 hours: **^{29}Si-NMR** (59.64 MHz, D_2O capillary in THF): δ -7.2, -39.3, -57.3.
72 hours: **^{29}Si-NMR** (59.64 MHz, D_2O capillary in THF): δ -7.0, -57.5.
120 hours: **^{29}Si-NMR** (59.64 MHz, D_2O capillary in THF): δ -7.1, -39.3, -57.3.
168 hours: **^{29}Si-NMR** (59.64 MHz, D_2O capillary in THF): δ -7.0, -57.5.

The solution was separated from the leftover Li by a reverse filter. The result was a brown and clear solution. To get rid of the formed LiCl the THF was removed and replaced by 200 mL of dry toluene. The reaction mixture was stirred overnight, but no precipitate appeared, hence the solution was refluxed for 2 hours. After the 2 hours of reflux a little amount of white solid precipitated so that the outcome was a brown suspension.

The reaction mixture was centrifuged to separate the solid and the solution, but even that left particles in the solution. So the next step was to filter with an syringe filter with a pore size of 0.2 μm. It was not possible to separate the solution because even if the filter was stored under argon atmosphere in the dry box, it reacted with the filter yielding a bright yellow solution.

5.5.3 Lithium band (3. trial) - Li : 1-Naph$_2$SiCl$_2$ of 2.1 : 1.0 eq

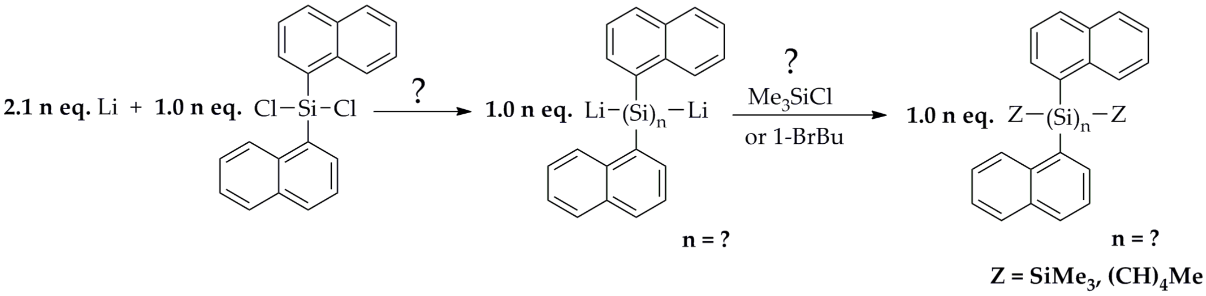

Figure 5.8: Wurtz-coupling reaction using Li (3. trial)

For synthetical details see chapter 5.5.1.

0.17 g (2.1 eq., 23.8 mmol) of the lithium band was cut and prepared in a dry glass vessel under argon atmosphere. 4.0 g (1.0 eq., 11.3 mmol) of **1** diluted in ~60 mL distilled THF was added dropwise by a cannula to the dry lithium pieces.

The reaction showed the same result as in 5.5.1 and 5.5.2, but three further signals with an intensity of ~20 % of the two main signals came up.

168 hours: **^{29}Si-NMR** (59.64 MHz, D$_2$O capillary in THF): δ -7.0, -33.0, -41.8, -51.6, -57.5.

The reaction mixture was divided into three equal parts (with a syringe three volumetrically equal parts of 20 mL were transferred into dry reaction flasks):

Addition of 1-bromobutane

0.5 mL of 1-bromobutane (dried over a molecular sieve) was added to the unfiltered reaction mixture. The THF was removed of the reddish solution and replaced by toluene. A grey reddish solid precipitated and was separated *via* a syringe filter in the dry box. The result was a yellow solution.

^{29}Si-NMR (59.64 MHz, C$_6$D$_6$): no silicon containing.

Addition of Me_3SiCl after removing residual Li

First the extant lithium was removed by a reverse filter followed by the addition of 1.0 mL distilled Me_3SiCl while stirring at RT. The change to a dark reddish reaction solution with a bit of a black, fine dispersed precipitate could be observed.

^{29}Si-NMR (59.64 MHz, D_2O capillary in THF): δ 30.9, 7.2, -11.7, -13.3, -19.7, -44.8.

Addition of Me_3SiCl

Me_3SiCl was distilled and 1.0 mL was added to the untreated reaction mixture while stirring at RT. The reaction solution turned into dark reddish with a bit of a black, fine dispersed precipitate.

^{29}Si-NMR (59.64 MHz, D_2O capillary in THF): δ 7.2, -11.9, -13.3, -16.2, -19.7, -37.2, -39.2, -44.9.

EI-DI: see 6.2

MALDI-MS: see Figure 5.9 at the next page

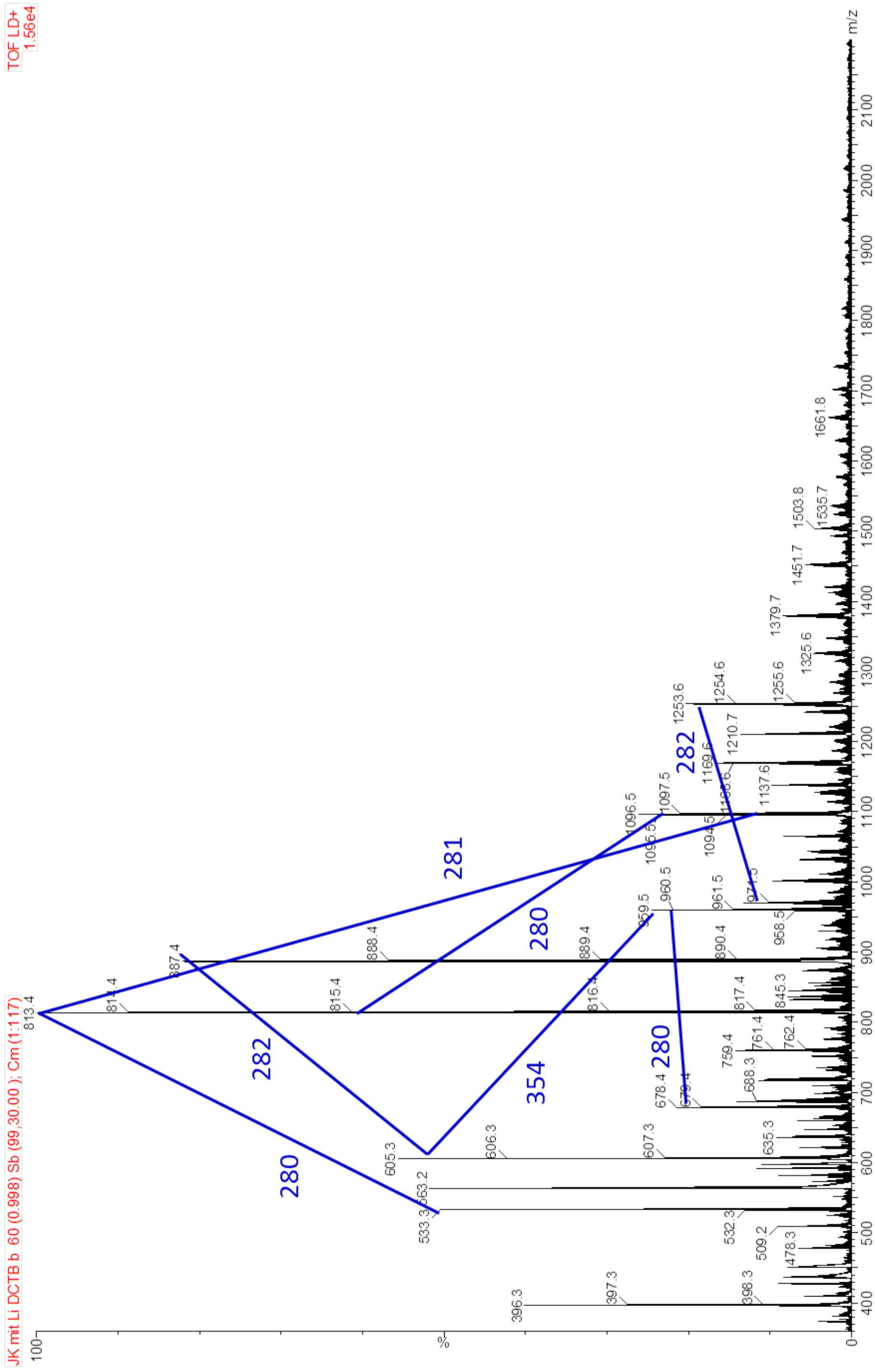

Figure 5.9: MALDI-MS of the sample after addition of Me_3SiCl

5.5.4 New lithium band - Li : 1-Naph$_2$SiCl$_2$ of 2.1 : 1.0 eq

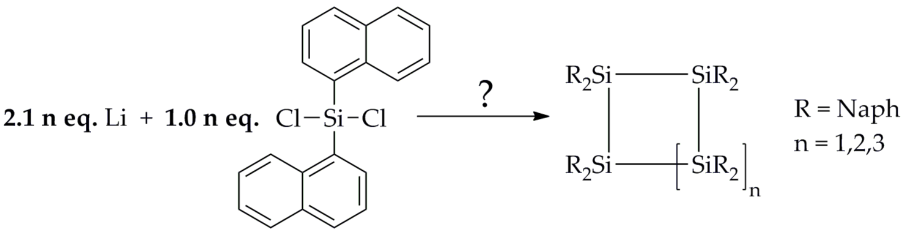

Figure 5.10: Wurtz-coupling reaction using Li - new lithium band

The reaction was carried out as described in 5.5.1, 5.5.2 and 5.5.3, but a freshly bought lithium band was used.

0.08 g (2.1 eq., 11.8 mmol) of the lithium band was cut and prepared in a dry glass vessel under argon atmosphere. 2.0 g (1.0 eq., 5.7 mmol) of **1** diluted in ∼30 mL distilled THF was added dropwise by a cannula to the dry lithium pieces.

A few minutes after reaction start a light temperature rise and a light yellowish discoloration could be observed. After stirring overnight the result was a yellowish solution without any leftover lithium.

^{29}Si-NMR (59.64 MHz, D_2O capillary in THF): 7.5.

Because of the known educt signal at 7.5 ppm a spiked NMR sample (educt was added to the NMR sample) was subjected to a ^{29}Si-NMR measurement, which showed just one signal at 7.5 ppm.

5.5.5 New lithium band (refluxing) - Li : 1-Naph$_2$SiCl$_2$ of 2.1 : 1.0 eq

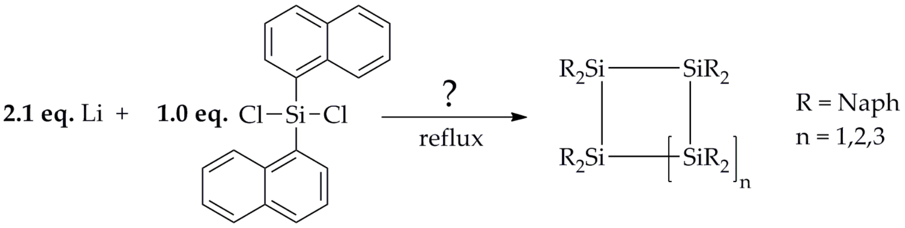

Figure 5.11: Wurtz-coupling reaction using Li supported by refluxing

Regarding the result of 5.5.4 the reaction was repeated: 0.081 g (2.1 eq., 11.8 mmol) of the lithium band was cut under argon atmosphere in the dry box and prepared in a dry glass vessel. 2.0 g (1.0 eq., 5.7 mmol) of **1** diluted in distilled THF was added dropwise by a cannula to the dry lithium pieces. The reaction mixture was refluxed for two days.
Half an hour after start of reflux a brownish discoloration could be observed. After refluxing for 2 days the result was a dark brown solution and little residue of Li.

^{29}Si-NMR (59.64 MHz, D_2O capillary in THF): -18.3, -29.2, -39.4, -41.9, -45.9.

THF was carefully removed, first with the membrane pump and then by a turbo molecular pump (10^{-5} mbar) to ensure that no THF is contained anymore.
Toluene was added to precipitate the formed LiCl. The now brown greenish suspension was filtered by a reverse filter conditioned with celite whereby a yellow clear solution was obtained.

^{29}Si-NMR (59.64 MHz, D_2O capillary in THF): -24.9, -29.0, -37.2, -38.9, -39.7, -41.8.

Toluene was removed first with the membrane pump and then by a turbo molecular pump (10^{-5} mbar) and resulted a yellow and shiny solid.

Melting range: 138 – 142 °C

EI-DI: see 6.3

MALDI-MS: see Figure 5.12 at the next page

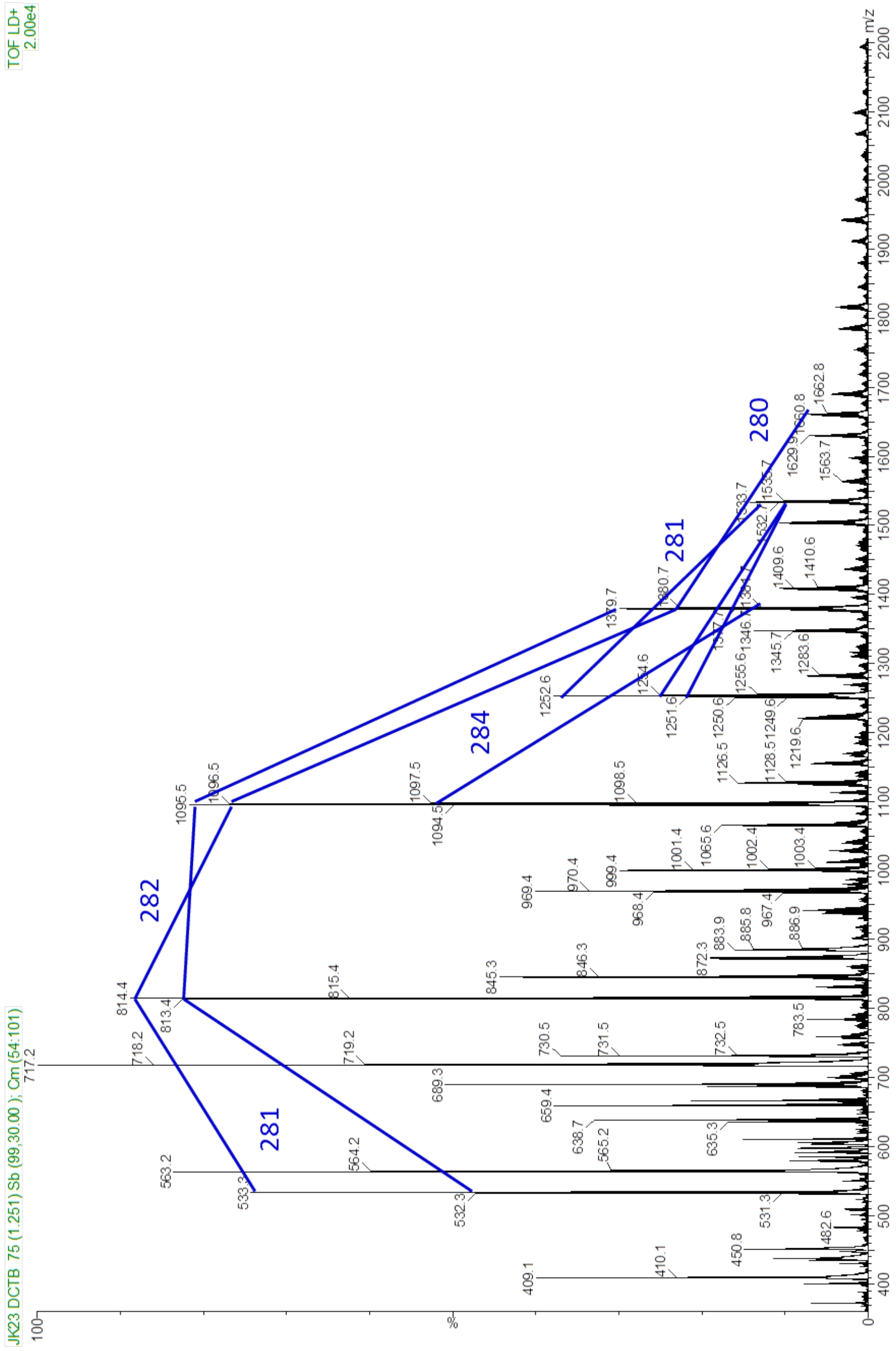

Figure 5.12: MALDI-MS

5.6 Wurtz-coupling of 1-Naph$_3$SiCl with Li - Li : 1-Naph$_3$SiCl of 1.1 : 1.0 eq

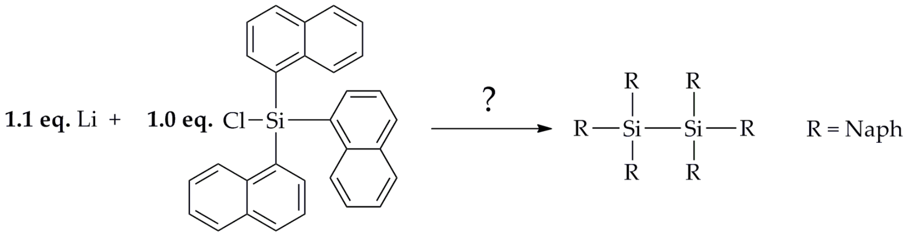

Figure 5.13: Wurtz-coupling reaction of 1-Naph$_3$SiCl using Li

0.041 g (1.1 eq., 4.9 mmol) of the lithium band was cut under argon atmosphere and prepared in a dry glass vessel. 2.0 g (1.0 eq., 4.5 mmol) of **2** diluted in ∼60 mL distilled THF was added dropwise by a cannula to the dry lithium pieces.

Half an hour after reaction-start a white precipitate appeared and led to a fine dispersion. A light purple discoloration could be observed. After stirring for 4 days the result was a red-orange solution and a red grey solid.

^{29}Si-NMR (59.64 MHz, D_2O capillary in THF): -28.9.

THF was removed using the membrane and the turbo molecular pump (10^{-5} mbar) and replaced by 60 ml of toluene. The appeared precipitate was too fine to get a separation by an available filter, so the toluene suspension was filtered by a reverse filter conditioned with celite. The result was a yellowish clear solution where toluene was removed by a membrane and turbo molecular pump leading to a white solid with a slightly pink discoloration.

^{29}Si-NMR (59.64 MHz, D_2O capillary in C_6D_6): -29.0.

Melting point: partially melting at 209 °C

XRD: crystal structure of Naph$_3$SiOH

Hydrolysis experiment of Naph$_3$SiCl:

1.0 g Naph$_3$SiCl was diluted in 10 mL of toluene. 10 mL of H_2O were added and stirred for 24 hours. The organic phase was investigated by a ^{29}Si-NMR measurement (D_2O capillary in toluene) which showed the not reacted Naph$_3$SiCl.

5.7 Synthesis of octaphenylcyclotetrasilane & decaphenylcyclopentasilane

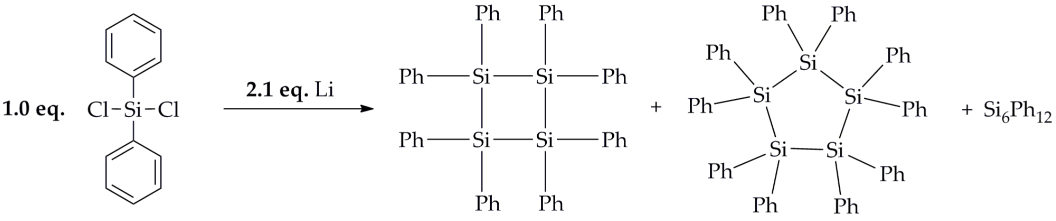

Figure 5.14: Synthesis of Si_5Ph_{10}

The perphenylated cyclosilanes were synthesized according to known literature[25] (see Figure 5.14.

6 Appendix

6.1 Abbreviations & Chemical short names

Table 6.1: Abbreviations

EPR	electron paramagnetic resonance
eq.	equivalent
GC-MS	gas chromatography-mass spectroscopy
LAH	lithium aluminium hydride
NMR	nuclear magnetic resonance
RT	room temperature
THF	tetrahydrofuran

Table 6.2: Chemical Short Names

abbreviation	**fragment name**	**fragment structure**
Me	methyl	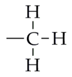 $-CH_3$
n-Bu	n-butyl	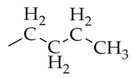
Ph	phenyl	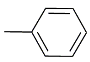
p-Tol	para-tolyl	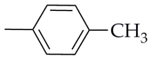
1-naph	1-naphthyl	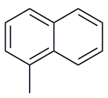

6.2 EI-DI Measurements belonging to 5.5.3

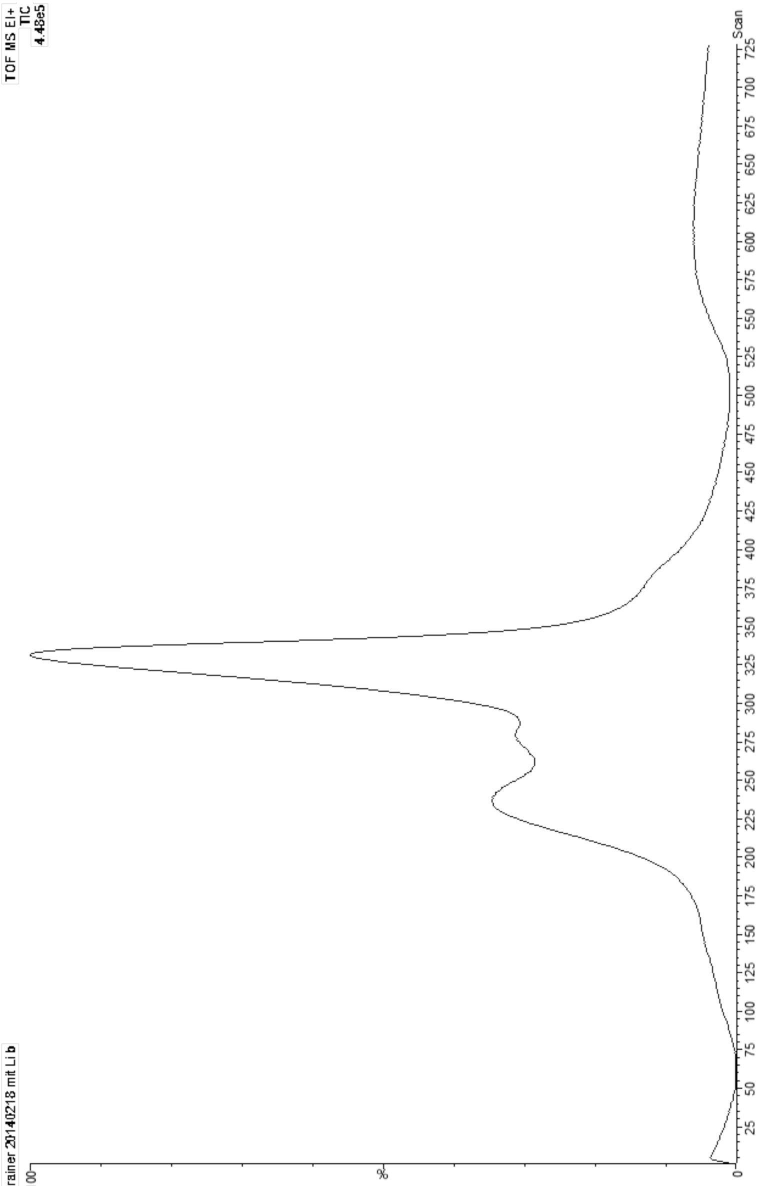

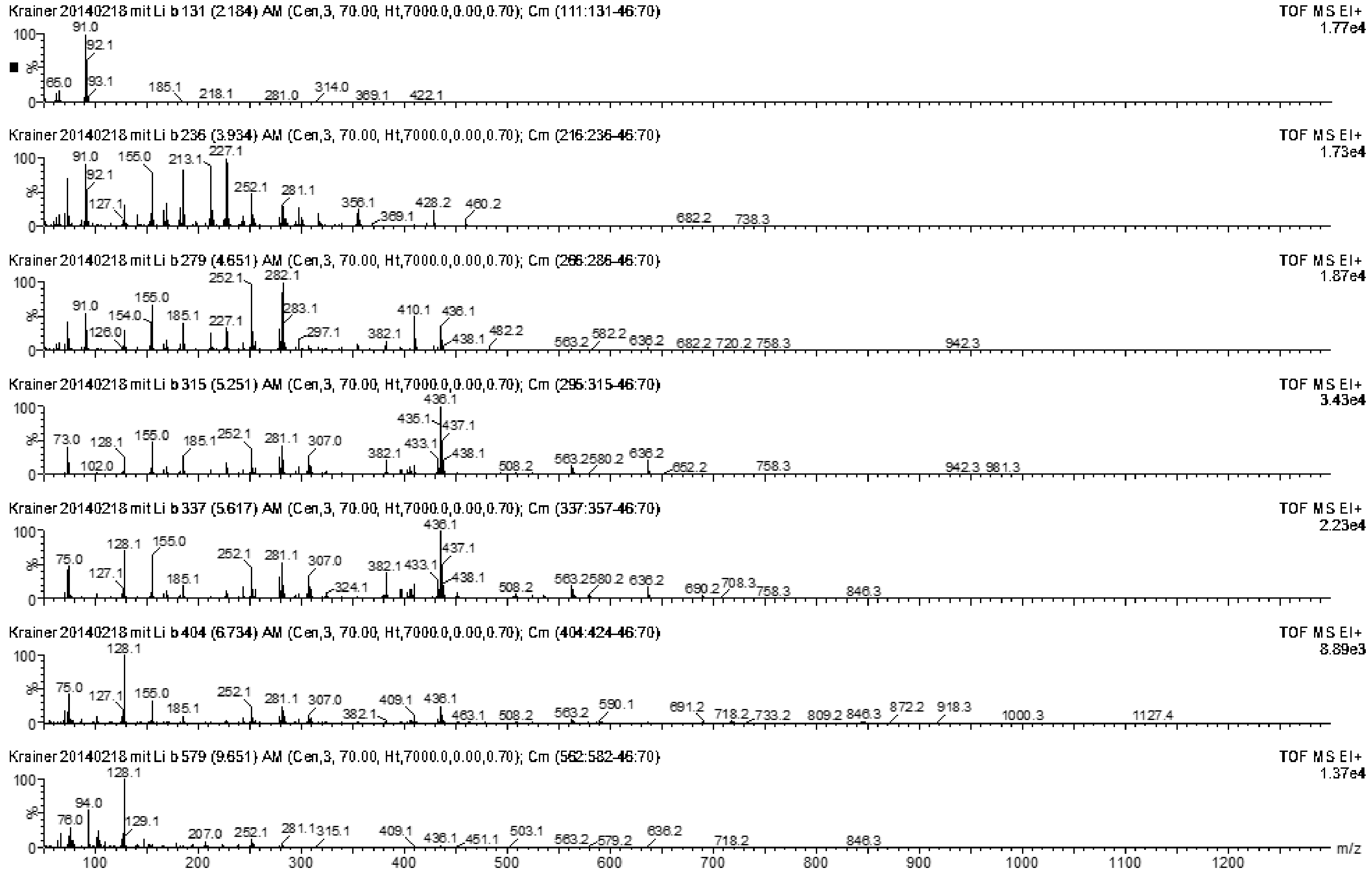
Krainer 20140218 mit Li b 131 (2.184) AM (Cen,3, 70.00, Ht,7000.0,0.00,0.70); Cm (111:131-46:70)
TOF MS EI+
1.77e4
91.0
92.1
65.0
93.1
185.1
218.1
281.0
314.0
369.1
422.1
Krainer 20140218 mit Li b 236 (3.934) AM (Cen,3, 70.00, Ht,7000.0,0.00,0.70); Cm (216:236-46:70)
TOF MS EI+
1.73e4
91.0
92.1
127.1
155.0
213.1
227.1
252.1
281.1
356.1
369.1
428.2
460.2
682.2
738.3
Krainer 20140218 mit Li b 279 (4.651) AM (Cen,3, 70.00, Ht,7000.0,0.00,0.70); Cm (266:286-46:70)
TOF MS EI+
1.87e4
91.0
126.0
154.0
155.0
185.1
227.1
252.1
282.1
283.1
297.1
382.1
410.1
436.1
438.1
482.2
563.2
582.2
636.2
682.2
720.2
758.3
942.3
Krainer 20140218 mit Li b 315 (5.251) AM (Cen,3, 70.00, Ht,7000.0,0.00,0.70); Cm (295:315-46:70)
TOF MS EI+
3.43e4
73.0
102.0
128.1
155.0
185.1
252.1
281.1
307.0
382.1
433.1
435.1
436.1
437.1
438.1
508.2
563.2
580.2
636.2
652.2
758.3
942.3
981.3
Krainer 20140218 mit Li b 337 (5.617) AM (Cen,3, 70.00, Ht,7000.0,0.00,0.70); Cm (337:357-46:70)
TOF MS EI+
2.23e4
75.0
127.1
128.1
155.0
185.1
252.1
281.1
307.0
324.1
382.1
433.1
436.1
437.1
438.1
508.2
563.2
580.2
636.2
690.2
708.3
758.3
846.3
Krainer 20140218 mit Li b 404 (6.734) AM (Cen,3, 70.00, Ht,7000.0,0.00,0.70); Cm (404:424-46:70)
TOF MS EI+
8.89e3
75.0
127.1
128.1
155.0
185.1
252.1
281.1
307.0
382.1
409.1
436.1
463.1
508.2
563.2
590.1
691.2
718.2
733.2
809.2
846.3
872.2
918.3
1000.3
1127.4
Krainer 20140218 mit Li b 579 (9.651) AM (Cen,3, 70.00, Ht,7000.0,0.00,0.70); Cm (562:582-46:70)
TOF MS EI+
1.37e4
76.0
94.0
128.1
129.1
207.0
252.1
281.1
315.1
409.1
436.1
451.1
503.1
563.2
579.2
636.2
718.2
846.3
100
%
0
m/z
100
200
300
400
500
600
700
800
900
1000
1100
1200

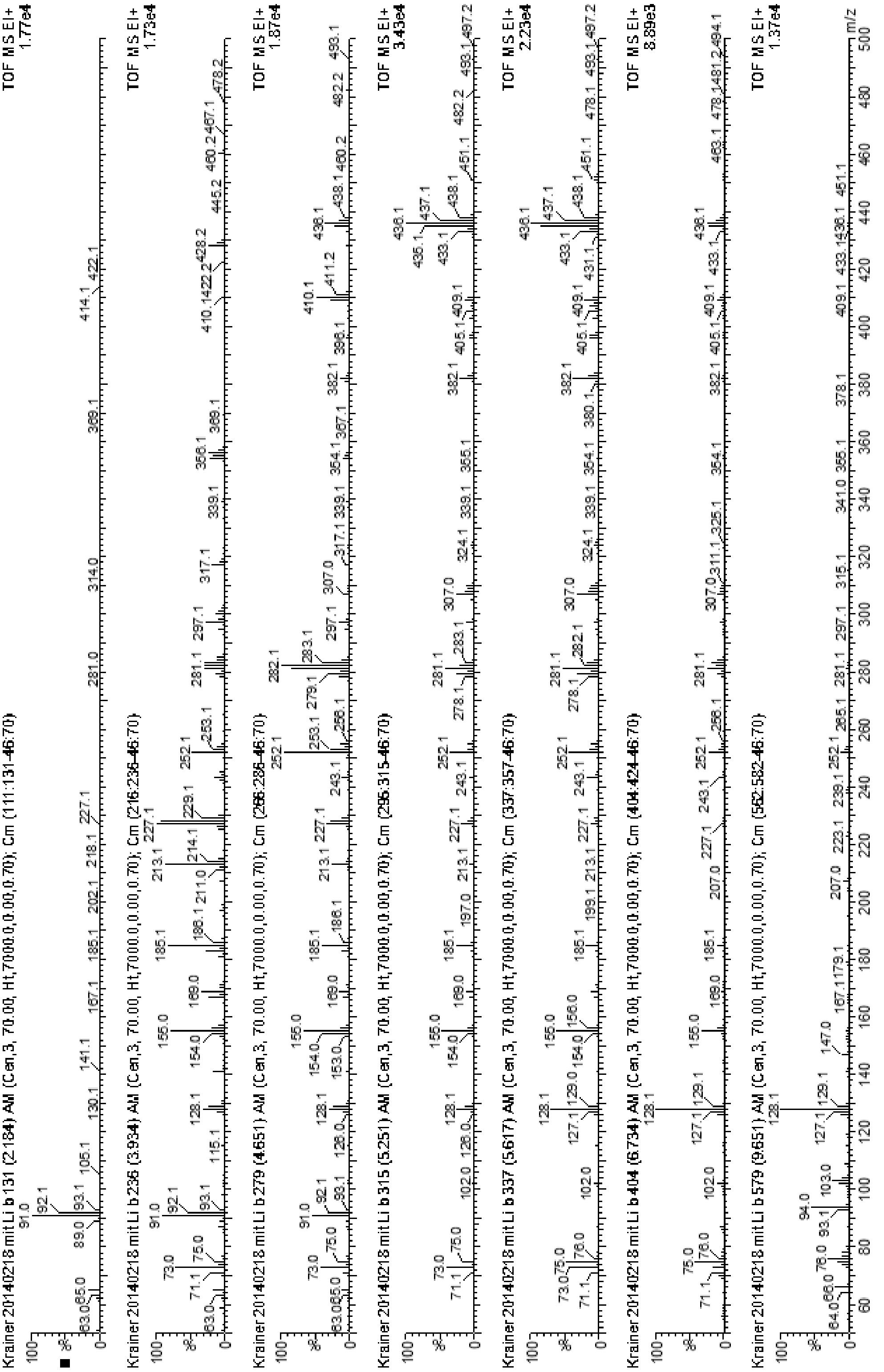
Krainer 20140218 mit Li b 131 (2.184) AM (Cen,3, 70.00, Ht,7000.0,0.00,0.70); Cm (111:131-46:70)
TOF MS EI+ 1.77e4
Krainer 20140218 mit Li b 236 (3.934) AM (Cen,3, 70.00, Ht,7000.0,0.00,0.70); Cm (216:236-46:70)
TOF MS EI+ 1.73e4
Krainer 20140218 mit Li b 279 (4.651) AM (Cen,3, 70.00, Ht,7000.0,0.00,0.70); Cm (266:286-46:70)
TOF MS EI+ 1.87e4
Krainer 20140218 mit Li b 315 (5.251) AM (Cen,3, 70.00, Ht,7000.0,0.00,0.70); Cm (295:315-46:70)
TOF MS EI+ 3.43e4
Krainer 20140218 mit Li b 337 (5.617) AM (Cen,3, 70.00, Ht,7000.0,0.00,0.70); Cm (337:357-46:70)
TOF MS EI+ 2.23e4
Krainer 20140218 mit Li b 404 (6.734) AM (Cen,3, 70.00, Ht,7000.0,0.00,0.70); Cm (404:424-46:70)
TOF MS EI+ 8.89e3
Krainer 20140218 mit Li b 579 (9.651) AM (Cen,3, 70.00, Ht,7000.0,0.00,0.70); Cm (562:582-46:70)
TOF MS EI+ 1.37e4
%
m/z

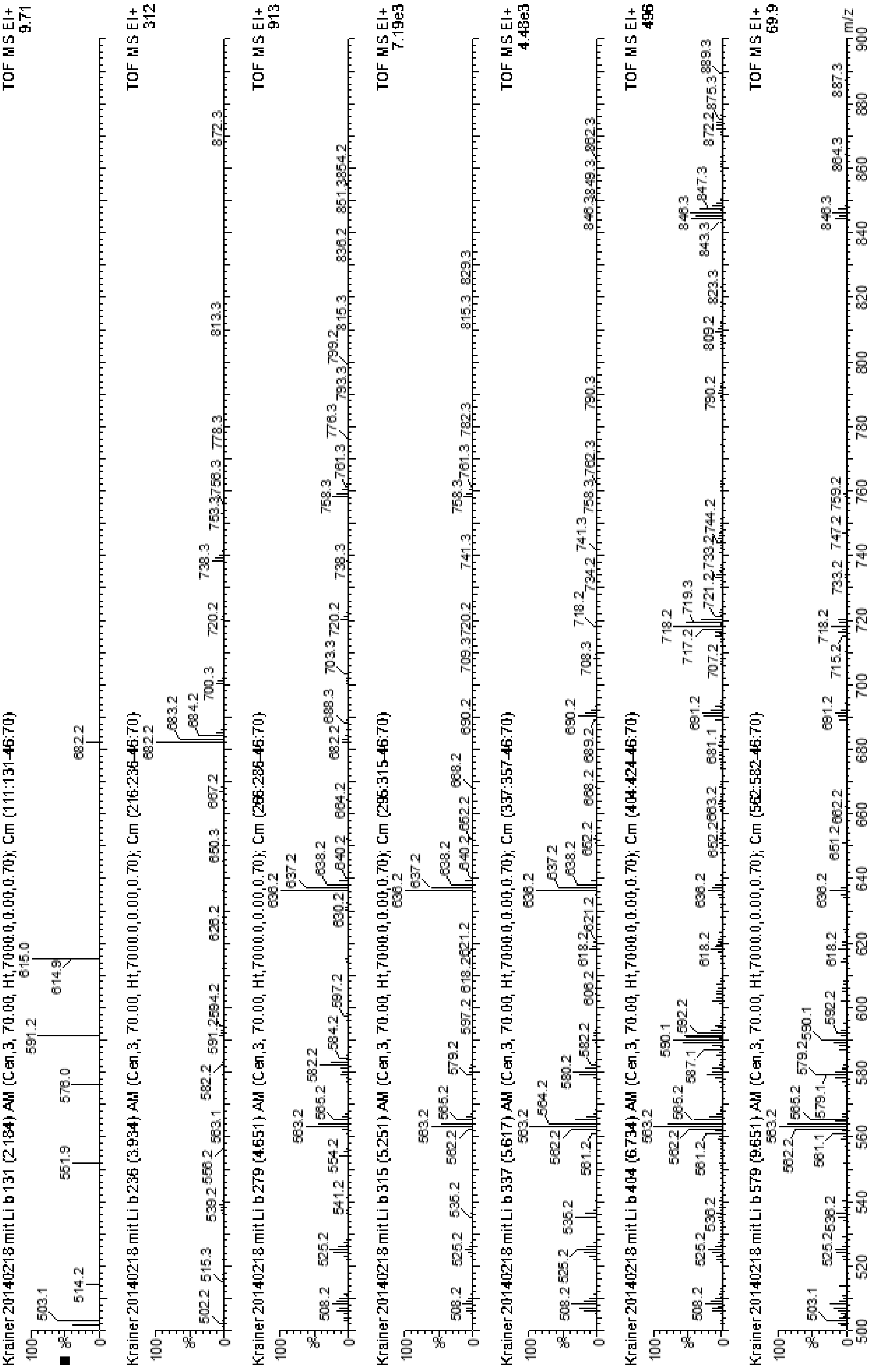
Krainer 20140218 mit Li b 131 (2.184) AM (Cen,3, 70.00, Ht,7000.0,0.00,0.70); Cm (111:131-46:70)
TOF MS EI+
9.71
Krainer 20140218 mit Li b 236 (3.934) AM (Cen,3, 70.00, Ht,7000.0,0.00,0.70); Cm (216:236-46:70)
TOF MS EI+
312
Krainer 20140218 mit Li b 279 (4.651) AM (Cen,3, 70.00, Ht,7000.0,0.00,0.70); Cm (258:285-46:70)
TOF MS EI+
913
Krainer 20140218 mit Li b 315 (5.251) AM (Cen,3, 70.00, Ht,7000.0,0.00,0.70); Cm (295:315-46:70)
TOF MS EI+
7.19e3
Krainer 20140218 mit Li b 337 (5.617) AM (Cen,3, 70.00, Ht,7000.0,0.00,0.70); Cm (337:357-46:70)
TOF MS EI+
4.48e3
Krainer 20140218 mit Li b 404 (6.734) AM (Cen,3, 70.00, Ht,7000.0,0.00,0.70); Cm (404:424-46:70)
TOF MS EI+
496
Krainer 20140218 mit Li b 579 (9.651) AM (Cen,3, 70.00, Ht,7000.0,0.00,0.70); Cm (562:582-46:70)
TOF MS EI+
69.9
%
100
0
500
520
540
560
580
600
620
640
660
680
700
720
740
760
780
800
820
840
860
880
900
m/z

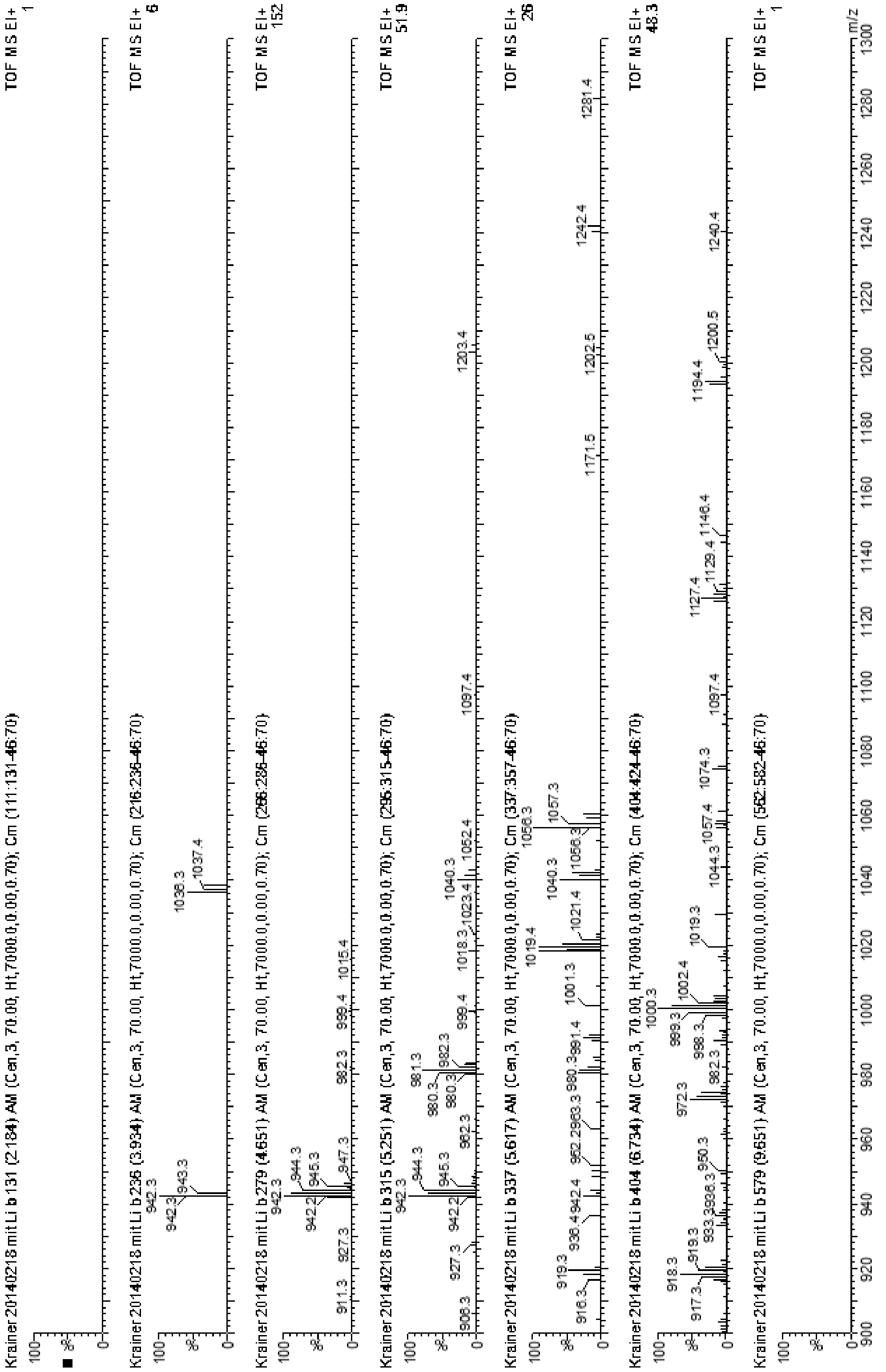
Krainer 20140218 mit Li b 131 (2.184) AM (Cen,3, 70.00, Ht,7000.0,0.00,0.70); Cm (111:131-46:70)
TOF MS EI+
1
Krainer 20140218 mit Li b 236 (3.934) AM (Cen,3, 70.00, Ht,7000.0,0.00,0.70); Cm (216:236-46:70)
TOF MS EI+
6
942.3
942.3
943.3
1036.3
1037.4
Krainer 20140218 mit Li b 279 (4.651) AM (Cen,3, 70.00, Ht,7000.0,0.00,0.70); Cm (266:286-46:70)
TOF MS EI+
152
942.3
944.3
945.3
942.2
947.3
911.3
927.3
982.3
999.4
1015.4
Krainer 20140218 mit Li b 315 (5.251) AM (Cen,3, 70.00, Ht,7000.0,0.00,0.70); Cm (295:315-46:70)
TOF MS EI+
51.9
942.3
944.3
945.3
942.2
981.3
980.3
982.3
980.3
962.3
927.3
906.3
999.4
1018.3
1023.4
1040.3
1052.4
1097.4
1203.4
Krainer 20140218 mit Li b 337 (5.617) AM (Cen,3, 70.00, Ht,7000.0,0.00,0.70); Cm (337:357-46:70)
TOF MS EI+
26
919.3
916.3
936.4
942.4
952.2
963.3
980.3
991.4
1001.3
1019.4
1021.4
1040.3
1056.3
1056.3
1057.3
1171.5
1202.5
1242.4
1281.4
Krainer 20140218 mit Li b 404 (6.734) AM (Cen,3, 70.00, Ht,7000.0,0.00,0.70); Cm (404:424-46:70)
TOF MS EI+
48.3
918.3
917.3
919.3
933.3
936.3
950.3
972.3
982.3
988.3
999.3
1000.3
1002.4
1019.3
1044.3
1057.4
1074.3
1097.4
1127.4
1129.4
1146.4
1194.4
1200.5
1240.4
Krainer 20140218 mit Li b 579 (9.651) AM (Cen,3, 70.00, Ht,7000.0,0.00,0.70); Cm (562:582-46:70)
TOF MS EI+
1
100
%
0
900
920
940
960
980
1000
1020
1040
1060
1080
1100
1120
1140
1160
1180
1200
1220
1240
1260
1280
1300
m/z

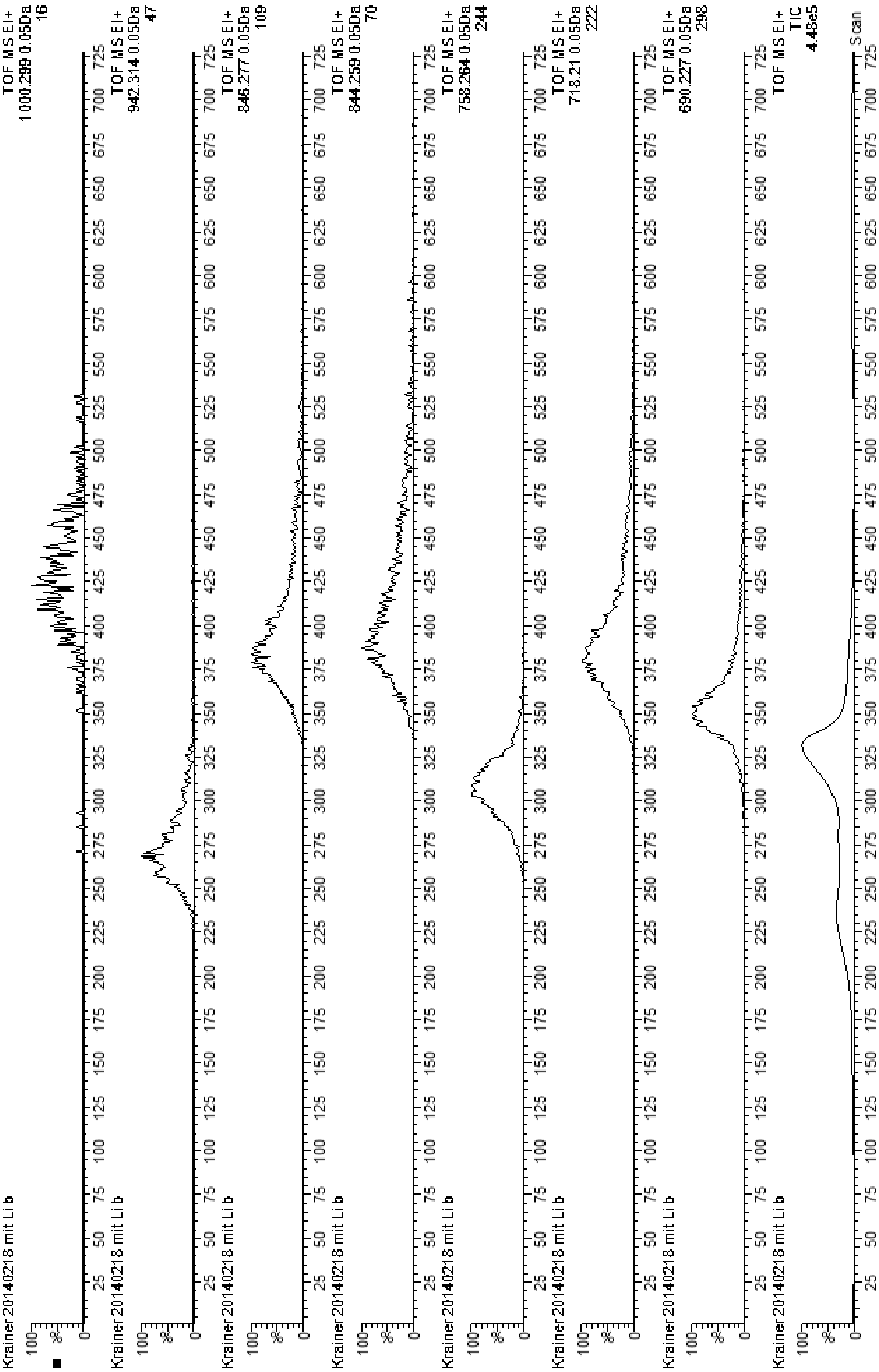
Krainer 20140218 mit Lib
TOF MS EI+
1000.299 0.05Da
16
Krainer 20140218 mit Lib
TOF MS EI+
942.314 0.05Da
47
Krainer 20140218 mit Lib
TOF MS EI+
846.277 0.05Da
109
Krainer 20140218 mit Lib
TOF MS EI+
844.259 0.05Da
70
Krainer 20140218 mit Lib
TOF MS EI+
758.264 0.05Da
244
Krainer 20140218 mit Lib
TOF MS EI+
718.21 0.05Da
222
Krainer 20140218 mit Lib
TOF MS EI+
690.227 0.05Da
298
Krainer 20140218 mit Lib
TOF MS EI+
TIC
4.43e5
100
%
0
25 50 75 100 125 150 175 200 225 250 275 300 325 350 375 400 425 450 475 500 525 550 575 600 625 650 675 700 725
Scan


Krainer 20140218 mit Lib
TOF MS EI+
718.21 0.05Da
222
Krainer 20140218 mit Lib
TOF MS EI+
690.227 0.05Da
298
Krainer 20140218 mit Lib
TOF MS EI+
682.235 0.05Da
68
Krainer 20140218 mit Lib
TOF MS EI+
636.215 0.05Da
4.02e3
Krainer 20140218 mit Lib
TOF MS EI+
590.147 0.05Da
212
Krainer 20140218 mit Lib
TOF MS EI+
582.212 0.05Da
207
Krainer 20140218 mit Lib
TOF MS EI+
563.168 0.05Da
3.05e3
Krainer 20140218 mit Lib
TOF MS EI+
TIC
4.43e5
100
%
0
25
50
75
100
125
150
175
200
225
250
275
300
325
350
375
400
425
450
475
500
525
550
575
600
625
650
675
700
725
Scan

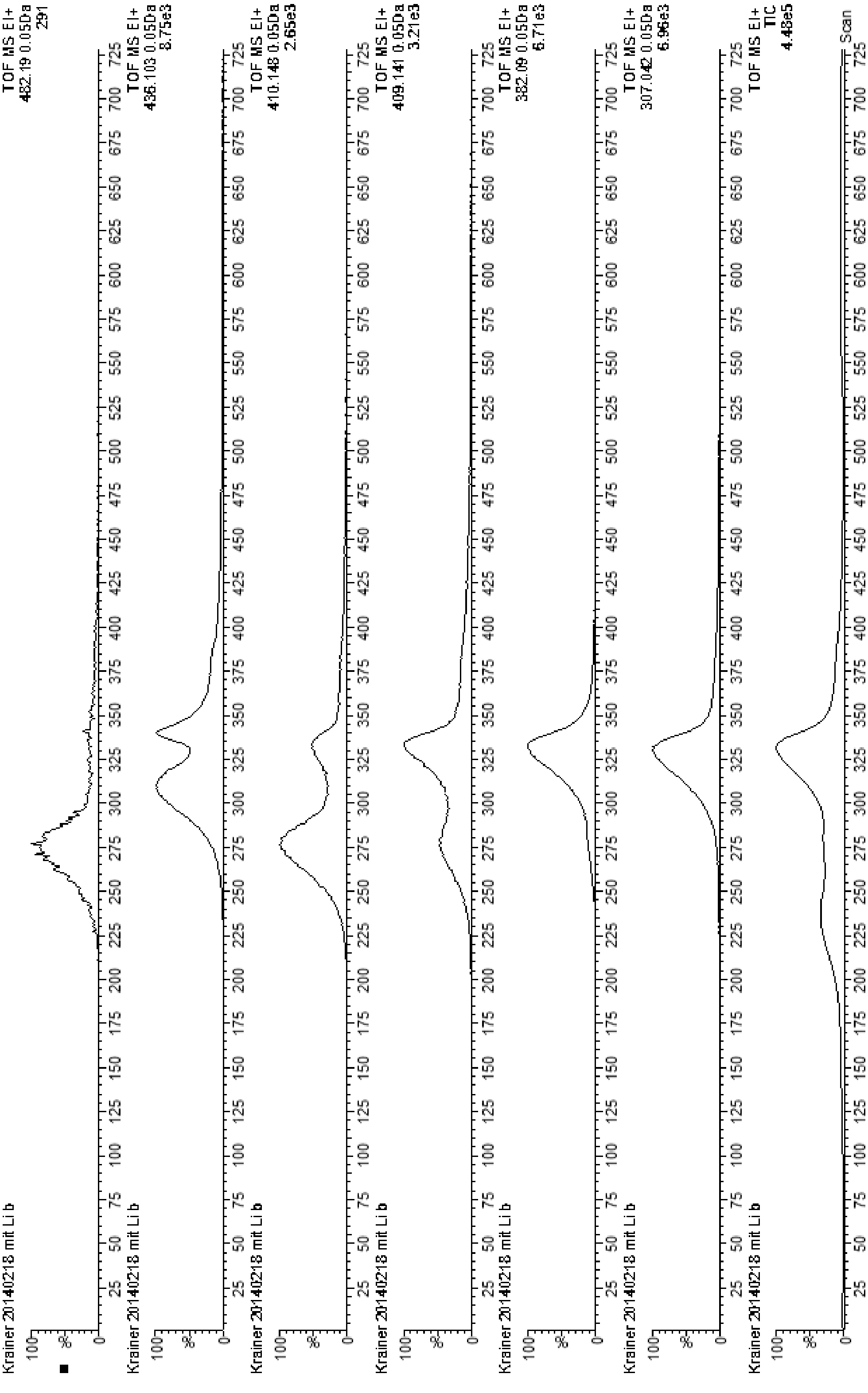
Krainer 20140218 mit Lib
TOF MS EI+
482.19 0.05Da
291
Krainer 20140218 mit Lib
TOF MS EI+
436.103 0.05Da
8.75e3
Krainer 20140218 mit Lib
TOF MS EI+
410.148 0.05Da
2.65e3
Krainer 20140218 mit Lib
TOF MS EI+
409.141 0.05Da
3.21e3
Krainer 20140218 mit Lib
TOF MS EI+
382.09 0.05Da
6.71e3
Krainer 20140218 mit Lib
TOF MS EI+
307.042 0.05Da
6.96e3
Krainer 20140218 mit Lib
TOF MS EI+
TIC
4.48e5
100
%
0
25
50
75
100
125
150
175
200
225
250
275
300
325
350
375
400
425
450
475
500
525
550
575
600
625
650
675
700
725
Scan

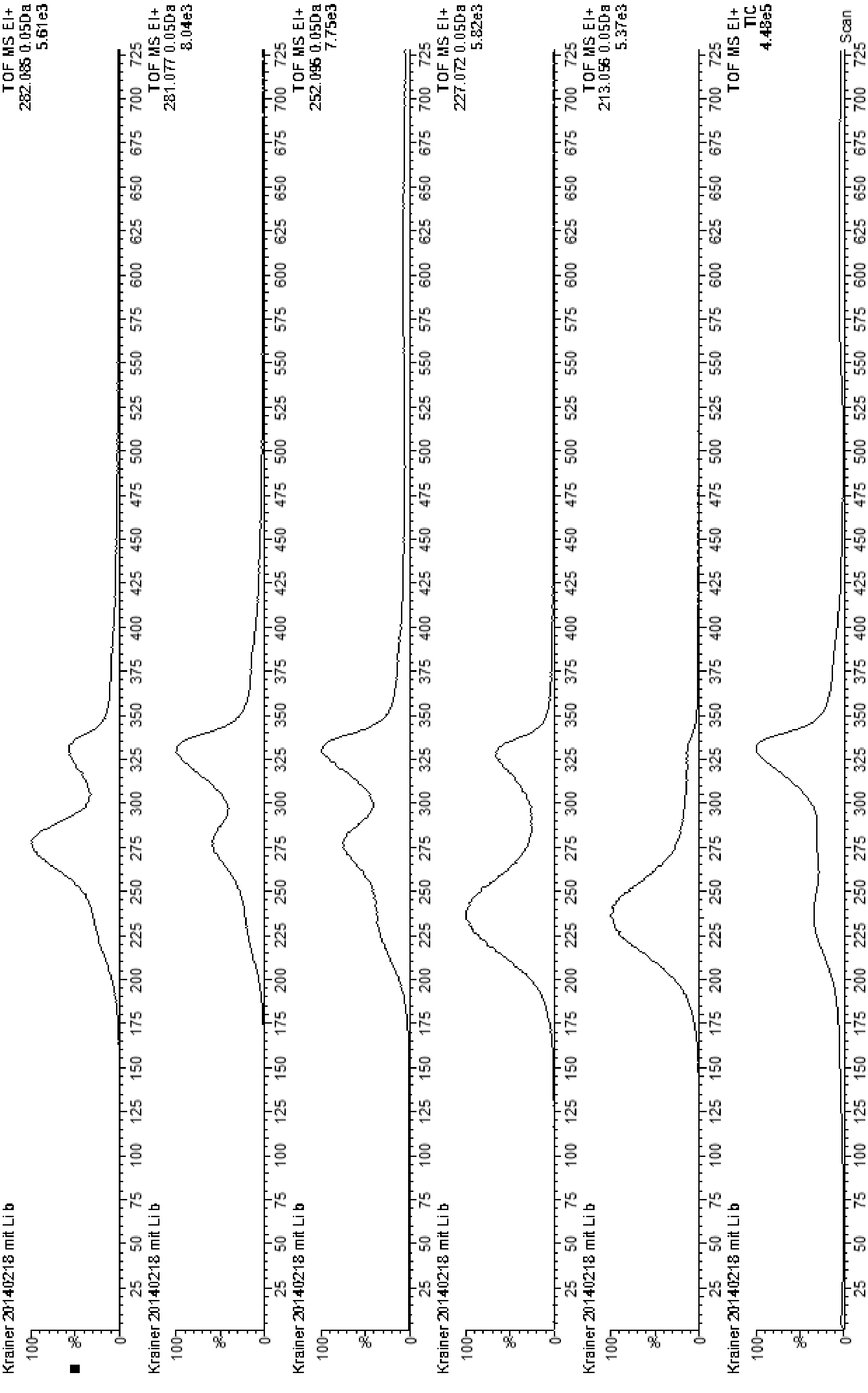
Krainer 20140218 mit Li b
TOF MS EI+
282.085 0.05Da
5.61e3
Krainer 20140218 mit Li b
TOF MS EI+
281.077 0.05Da
8.04e3
Krainer 20140218 mit Li b
TOF MS EI+
252.096 0.05Da
7.75e3
Krainer 20140218 mit Li b
TOF MS EI+
227.072 0.05Da
5.82e3
Krainer 20140218 mit Li b
TOF MS EI+
213.056 0.05Da
5.37e3
Krainer 20140218 mit Li b
TOF MS EI+
TIC
4.48e5
100
%
0
25
50
75
100
125
150
175
200
225
250
275
300
325
350
375
400
425
450
475
500
525
550
575
600
625
650
675
700
725
Scan

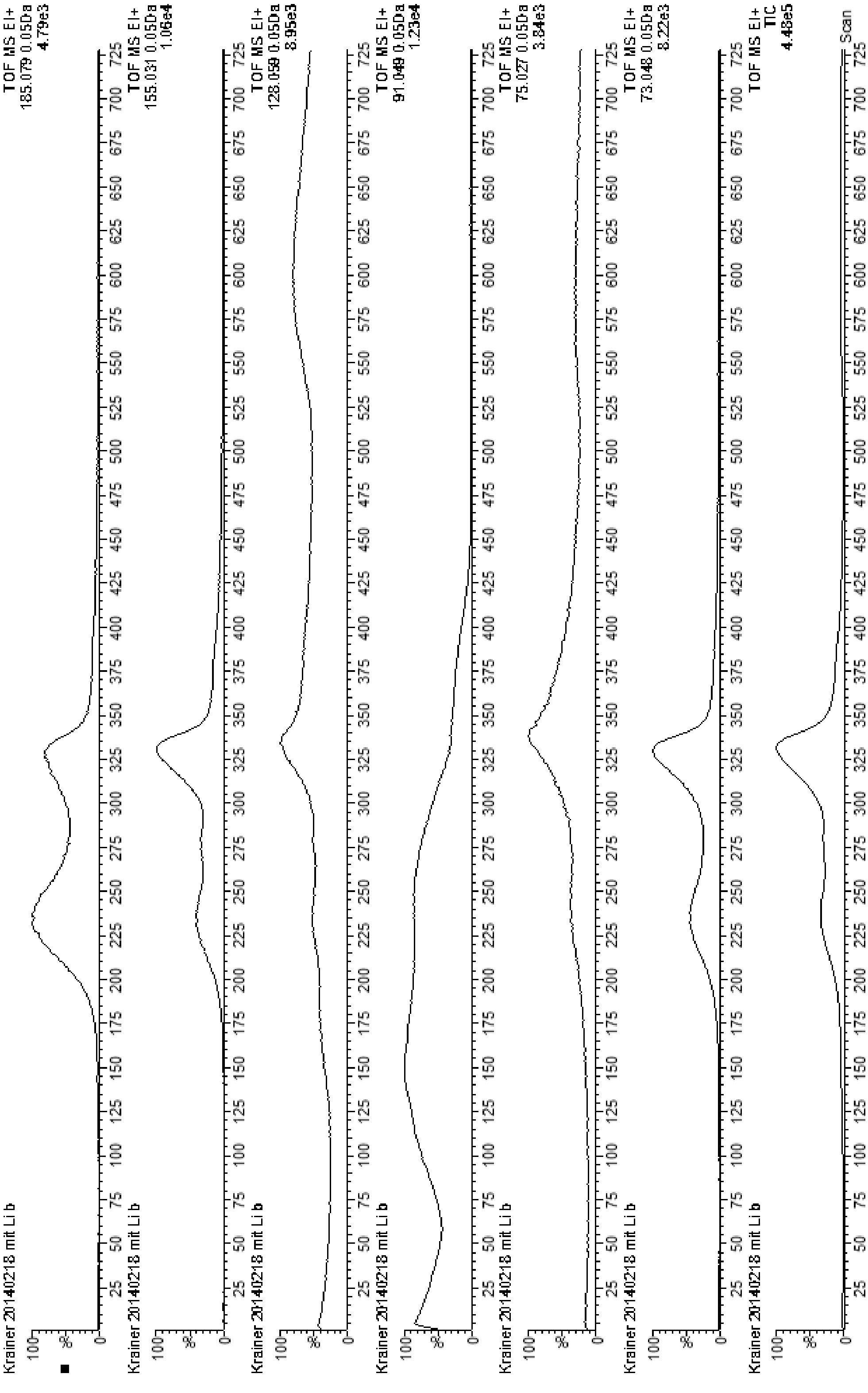
Krainer 20140218 mit Lib
TOF MS EI+
185.079 0.05Da
4.79e3
Krainer 20140218 mit Lib
TOF MS EI+
155.031 0.05Da
1.06e4
Krainer 20140218 mit Lib
TOF MS EI+
128.059 0.05Da
8.95e3
Krainer 20140218 mit Lib
TOF MS EI+
91.049 0.05Da
1.23e4
Krainer 20140218 mit Lib
TOF MS EI+
75.027 0.05Da
3.84e3
Krainer 20140218 mit Lib
TOF MS EI+
73.048 0.05Da
8.22e3
Krainer 20140218 mit Lib
TOF MS EI+
TIC
4.48e5
100
%
0
25 50 75 100 125 150 175 200 225 250 275 300 325 350 375 400 425 450 475 500 525 550 575 600 625 650 675 700 725
Scan

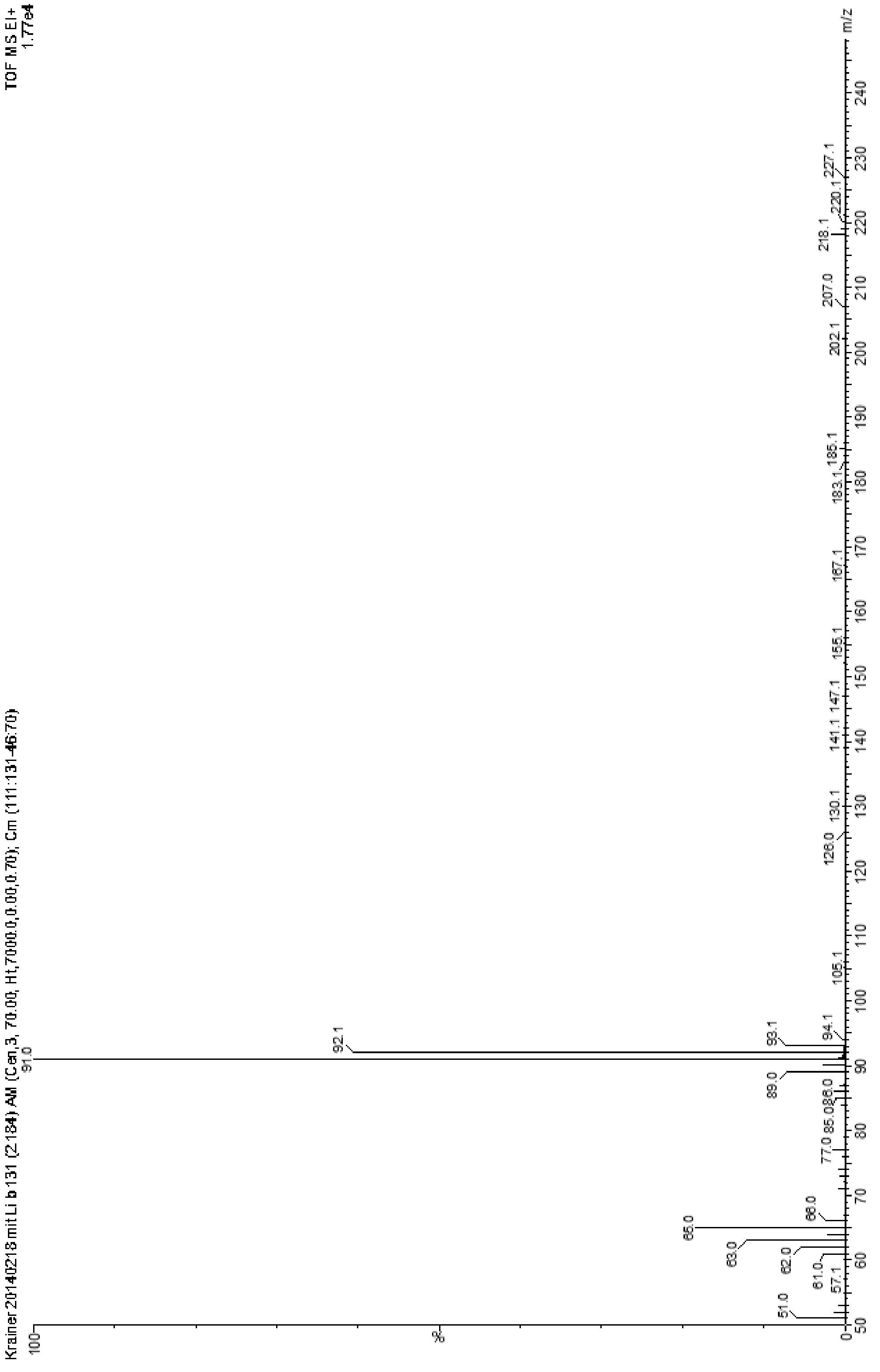
Krainer 20140218 mit Li b 131 (2.184) AM (Cen,3, 70.00, Ht,7000.0,0.00,0.70); Cm (111:131-46:70)
TOF MS EI+
1.77e4
100
%
0
91.0
92.1
93.1
94.1
89.0
85.086.0
77.0
66.0
65.0
63.0
62.0
61.0
57.1
51.0
105.1
128.0
130.1
141.1
147.1
155.1
167.1
183.1
185.1
202.1
207.0
218.1
220.1
227.1
50
60
70
80
90
100
110
120
130
140
150
160
170
180
190
200
210
220
230
240
m/z

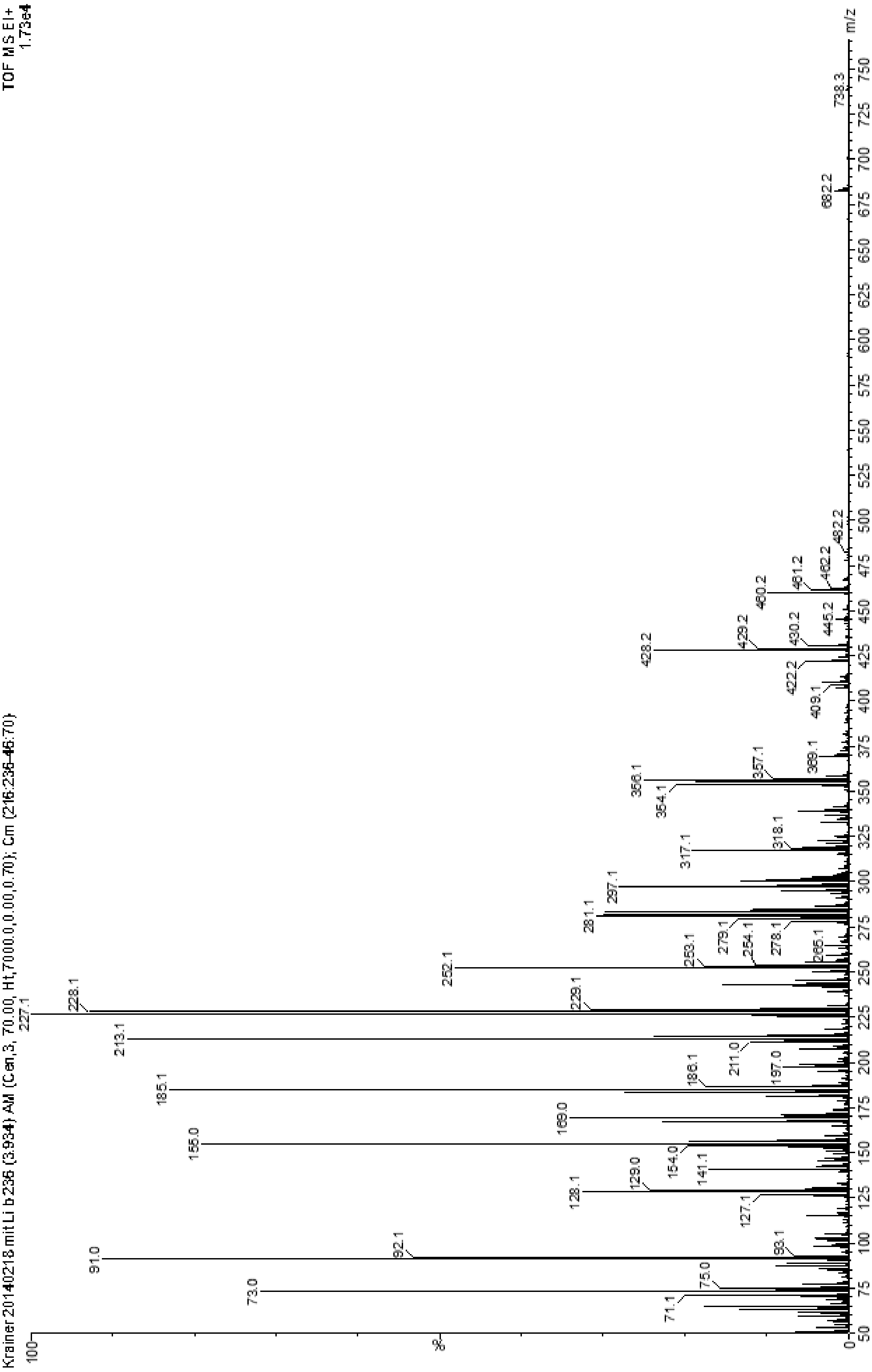
Krainer 20140218 mit Li b236 (3.934) AM (Cen,3, 70.00, Ht,7000.0,0.00,0.70); Cm (216:236-46:70)
TOF MS EI+
1.73e4
100
%
0
m/z
50
75
100
125
150
175
200
225
250
275
300
325
350
375
400
425
450
475
500
525
550
575
600
625
650
675
700
725
750
71.1
73.0
75.0
91.0
92.1
93.1
127.1
128.1
129.0
141.1
154.0
155.0
169.0
185.1
186.1
197.0
211.0
213.1
227.1
228.1
229.1
252.1
253.1
254.1
265.1
278.1
279.1
281.1
297.1
317.1
318.1
354.1
356.1
357.1
369.1
409.1
422.2
428.2
429.2
430.2
445.2
460.2
461.2
462.2
482.2
682.2
738.3

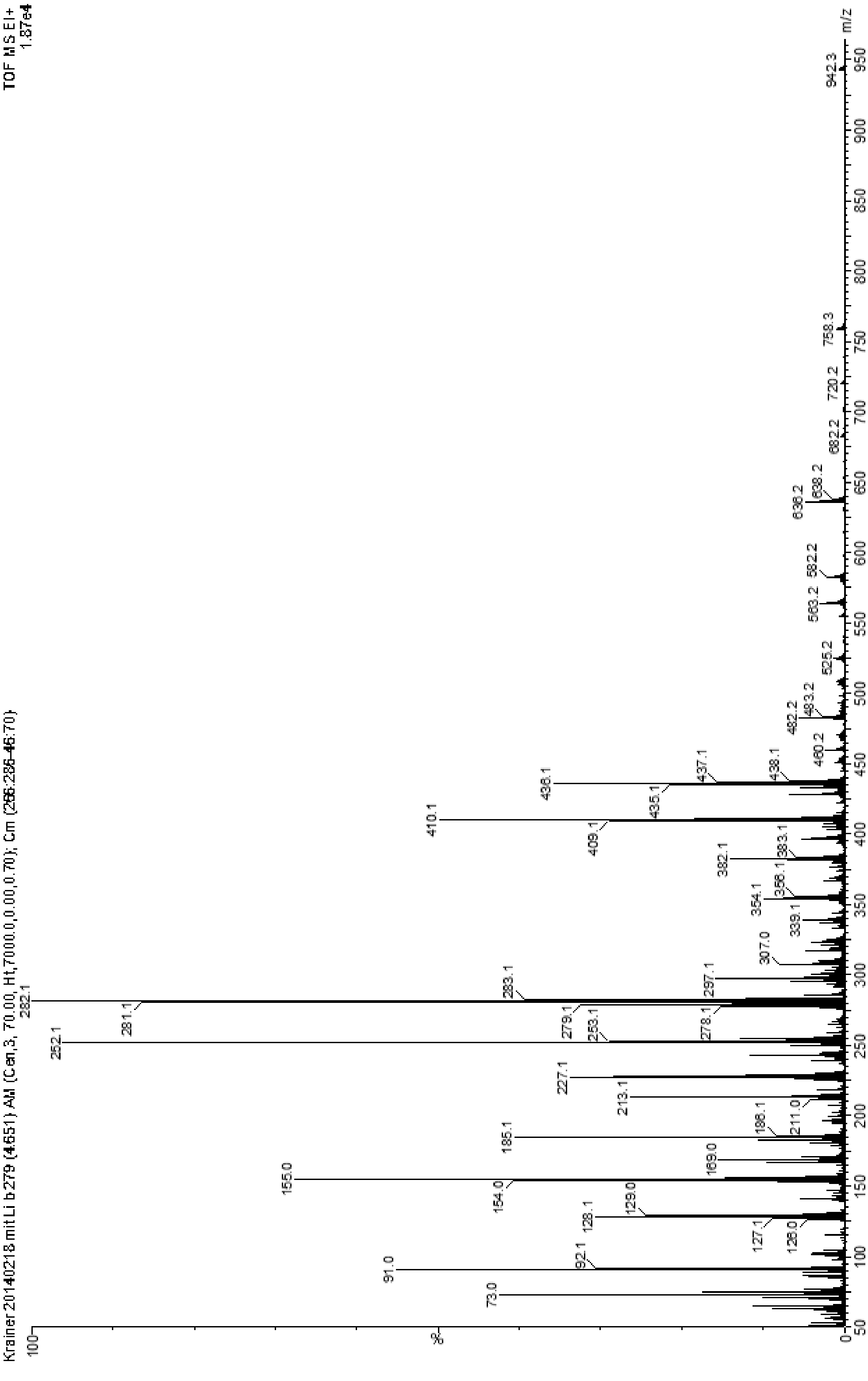
Krainer 20140218 mit Li b279 (4.651) AM (Cen,3, 70.00, Ht,7000.0,0.00,0.70); Cm (256:286-46:70)
TOF MS EI+
1.87e4
100
%
0
m/z
50
100
150
200
250
300
350
400
450
500
550
600
650
700
750
800
850
900
950
73.0
91.0
92.1
127.1
126.0
128.1
129.0
154.0
155.0
169.0
185.1
188.1
211.0
213.1
227.1
252.1
253.1
278.1
279.1
281.1
282.1
283.1
297.1
307.0
339.1
354.1
356.1
382.1
383.1
409.1
410.1
435.1
436.1
437.1
438.1
460.2
482.2
483.2
525.2
563.2
582.2
636.2
638.2
682.2
720.2
758.3
942.3

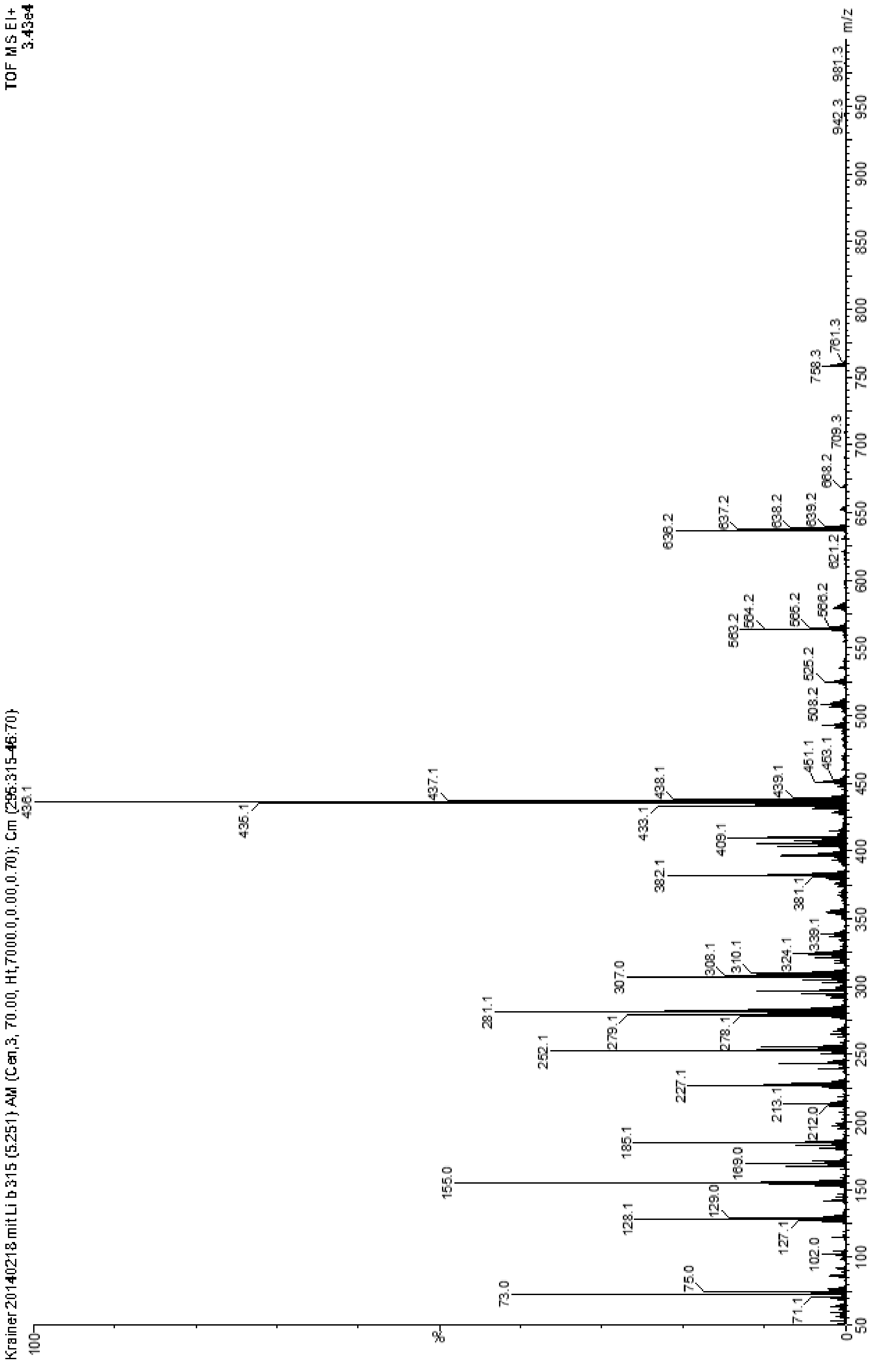
Krainer 20140218 mit Li b 315 (5.251) AM (Cen,3, 70.00, Ht,7000.0,0.00,0.70); Cm (295:315-46:70)
TOF MS EI+
3.43e4
100
%
0
m/z
50
100
150
200
250
300
350
400
450
500
550
600
650
700
750
800
850
900
950
436.1
435.1
437.1
438.1
433.1
439.1
73.0
71.1
75.0
102.0
127.1
128.1
129.0
155.0
169.0
185.1
212.0
213.1
227.1
252.1
278.1
279.1
281.1
307.0
308.1
310.1
324.1
339.1
381.1
382.1
409.1
451.1
453.1
508.2
525.2
563.2
564.2
565.2
568.2
621.2
636.2
637.2
638.2
639.2
668.2
709.3
758.3
761.3
942.3
981.3

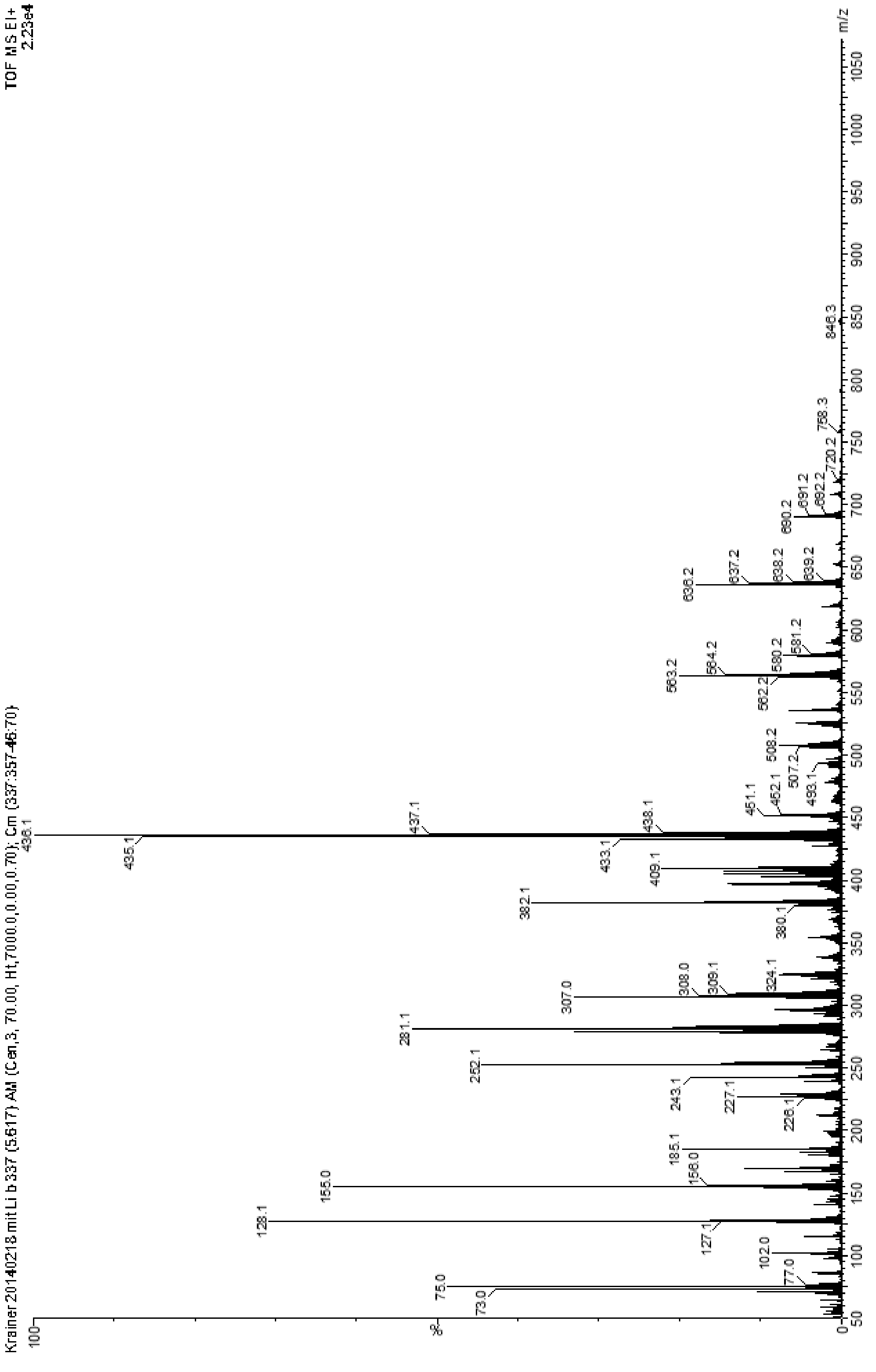
Krainer 20140218 mit Li b 337 (5.617) AM (Cen,3, 70.00, Ht,7000.0,0.00,0.70); Cm (337:357-46:70)
TOF MS EI+
2.23e4
100
%
0
436.1
435.1
437.1
438.1
433.1
409.1
382.1
380.1
307.0
308.0
309.1
324.1
281.1
252.1
243.1
227.1
226.1
185.1
156.0
155.0
128.1
127.1
102.0
77.0
75.0
73.0
451.1
452.1
493.1
507.2
508.2
563.2
564.2
562.2
580.2
581.2
636.2
637.2
638.2
639.2
690.2
691.2
692.2
720.2
758.3
846.3
m/z
50
100
150
200
250
300
350
400
450
500
550
600
650
700
750
800
850
900
950
1000
1050

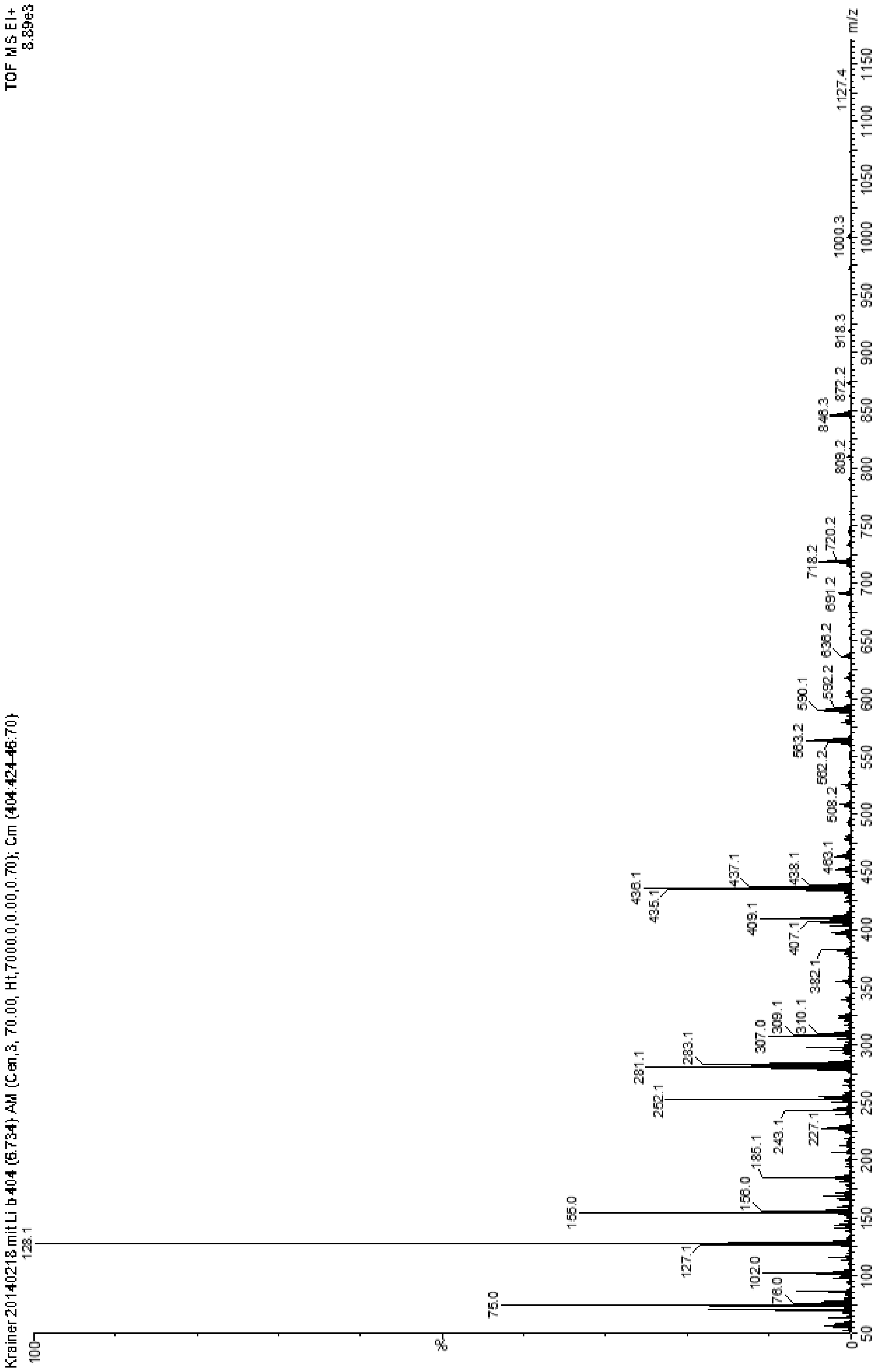
Krainer 20140218 mit Li b 404 (6.734) AM (Cen,3, 70.00, Ht,7000.0,0.00,0.70); Cm (404:424-46:70)
TOF MS EI+
3.39e3
100
%
0
75.0
76.0
102.0
127.1
128.1
155.0
156.0
185.1
227.1
243.1
252.1
281.1
283.1
307.0
309.1
310.1
382.1
407.1
409.1
435.1
436.1
437.1
438.1
463.1
508.2
562.2
563.2
590.1
592.2
638.2
691.2
718.2
720.2
809.2
846.3
872.2
918.3
1000.3
1127.4
50
100
150
200
250
300
350
400
450
500
550
600
650
700
750
800
850
900
950
1000
1050
1100
1150
m/z

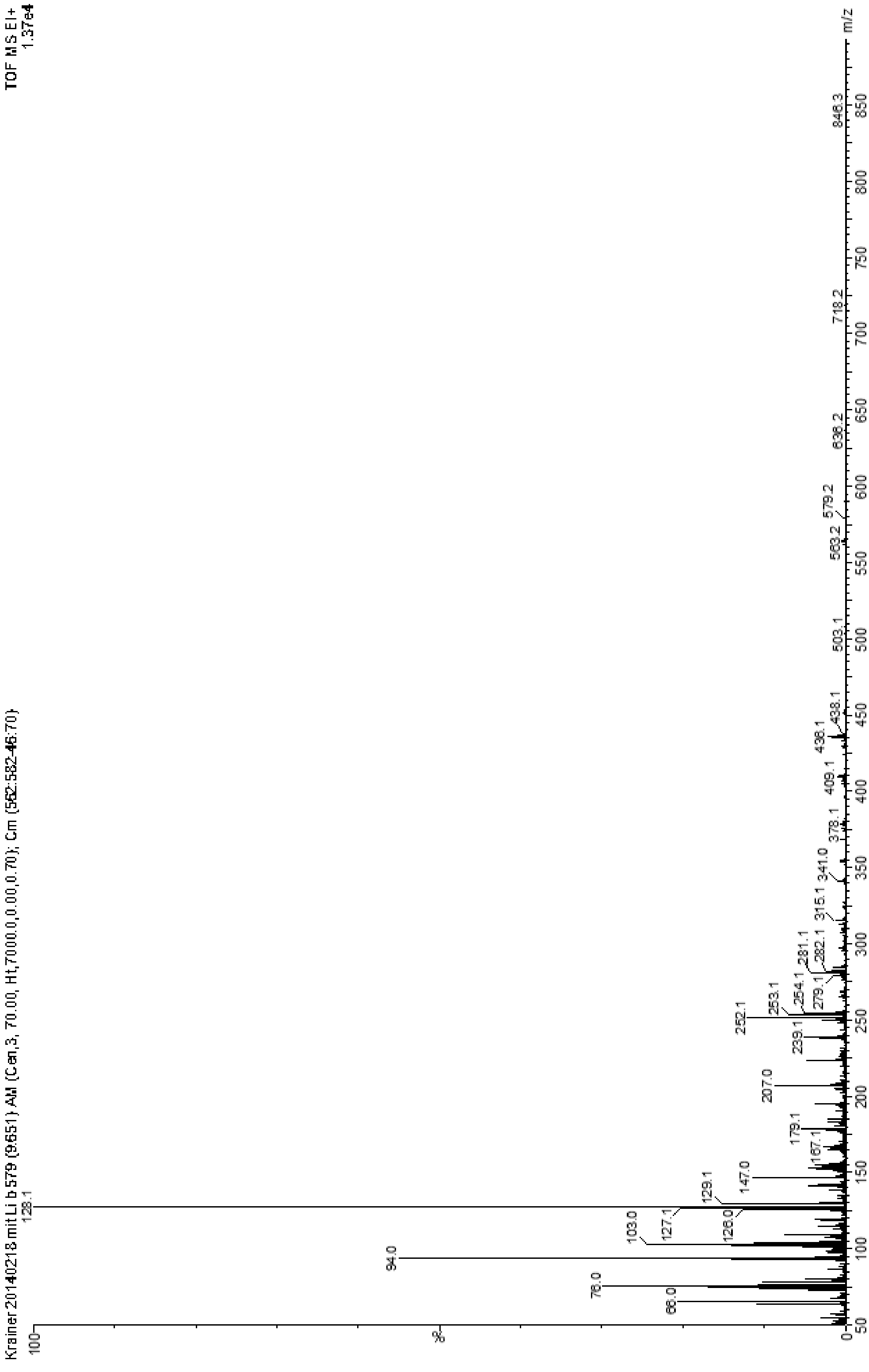
Krainer 20140218 mit Li b 579 (9.651) AM (Cen,3, 70.00, Ht,7000.0,0.00,0.70); Cm (562:582-46:70)
TOF MS EI+
1.37e4
100
%
0
128.1
94.0
78.0
66.0
103.0
127.1
129.1
126.0
147.0
179.1
167.1
207.0
252.1
253.1
239.1
254.1
279.1
281.1
282.1
315.1
341.0
378.1
409.1
436.1
438.1
503.1
563.2
579.2
636.2
718.2
846.3
50
100
150
200
250
300
350
400
450
500
550
600
650
700
750
800
850
m/z

6.3 EI-DI Measurements belonging to 5.5.5

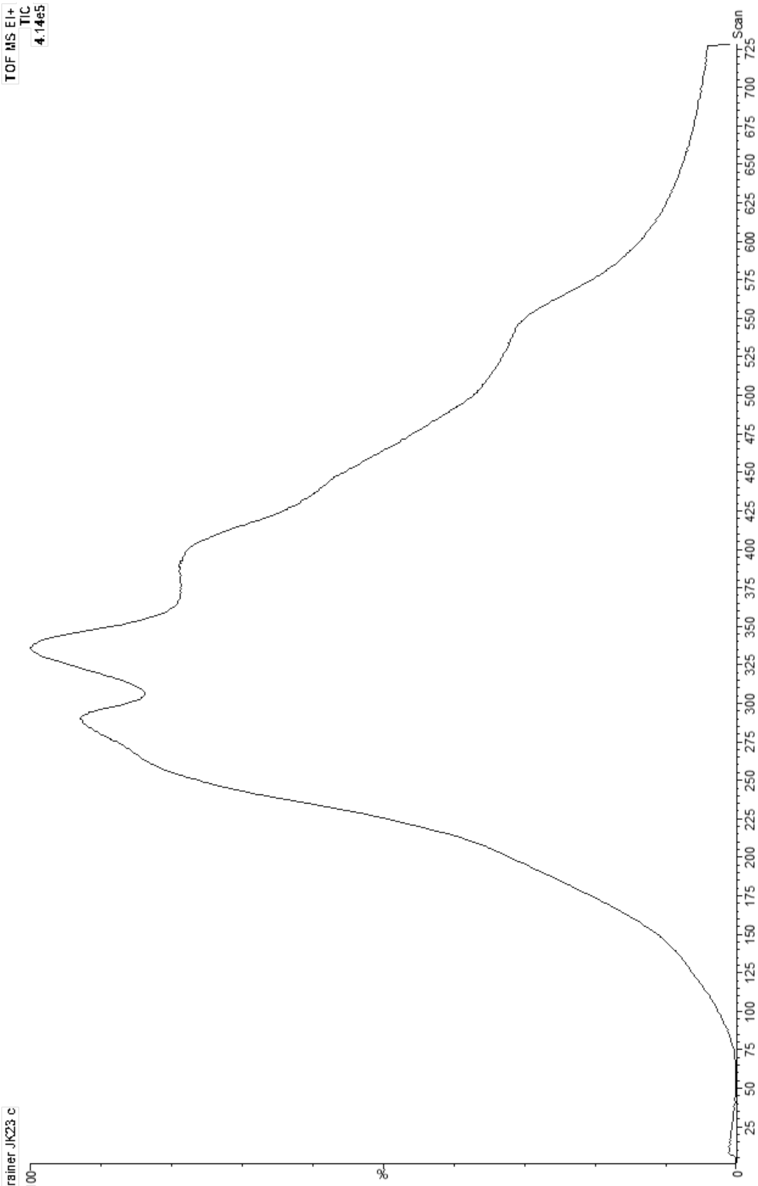

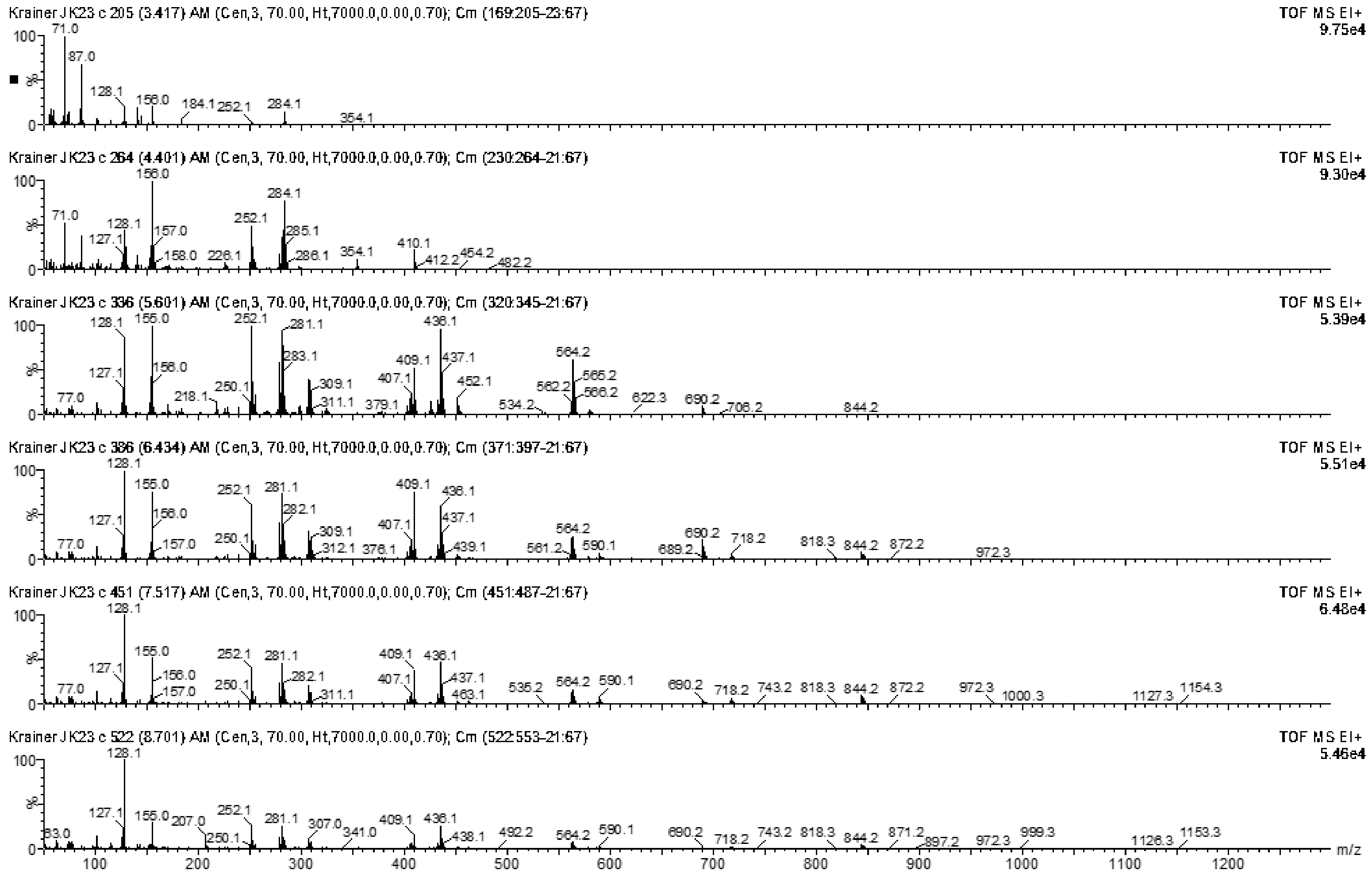
Krainer JK23 c 205 (3.417) AM (Cen,3, 70.00, Ht,7000.0,0.00,0.70); Cm (169:205-23:67)
TOF MS EI+
9.75e4
100
%
0
71.0
87.0
128.1
156.0
184.1
252.1
284.1
354.1
Krainer JK23 c 264 (4.401) AM (Cen,3, 70.00, Ht,7000.0,0.00,0.70); Cm (230:264-21:67)
TOF MS EI+
9.30e4
156.0
71.0
128.1
127.1
157.0
158.0
226.1
252.1
284.1
285.1
286.1
354.1
410.1
412.2
454.2
482.2
Krainer JK23 c 336 (5.601) AM (Cen,3, 70.00, Ht,7000.0,0.00,0.70); Cm (320:345-21:67)
TOF MS EI+
5.39e4
77.0
128.1
127.1
155.0
156.0
218.1
250.1
252.1
281.1
283.1
309.1
311.1
379.1
407.1
409.1
436.1
437.1
452.1
534.2
562.2
564.2
565.2
566.2
622.3
690.2
706.2
844.2
Krainer JK23 c 386 (6.434) AM (Cen,3, 70.00, Ht,7000.0,0.00,0.70); Cm (371:397-21:67)
TOF MS EI+
5.51e4
77.0
127.1
128.1
155.0
156.0
157.0
250.1
252.1
281.1
282.1
309.1
312.1
376.1
407.1
409.1
436.1
437.1
439.1
561.2
564.2
590.1
689.2
690.2
718.2
818.3
844.2
872.2
972.3
Krainer JK23 c 451 (7.517) AM (Cen,3, 70.00, Ht,7000.0,0.00,0.70); Cm (451:487-21:67)
TOF MS EI+
6.48e4
77.0
127.1
128.1
155.0
156.0
157.0
250.1
252.1
281.1
282.1
311.1
407.1
409.1
436.1
437.1
463.1
535.2
564.2
590.1
690.2
718.2
743.2
818.3
844.2
872.2
972.3
1000.3
1127.3
1154.3
Krainer JK23 c 522 (8.701) AM (Cen,3, 70.00, Ht,7000.0,0.00,0.70); Cm (522:553-21:67)
TOF MS EI+
5.46e4
53.0
127.1
128.1
155.0
207.0
250.1
252.1
281.1
307.0
341.0
409.1
436.1
438.1
492.2
564.2
590.1
690.2
718.2
743.2
818.3
844.2
871.2
897.2
972.3
999.3
1126.3
1153.3
m/z
100
200
300
400
500
600
700
800
900
1000
1100
1200

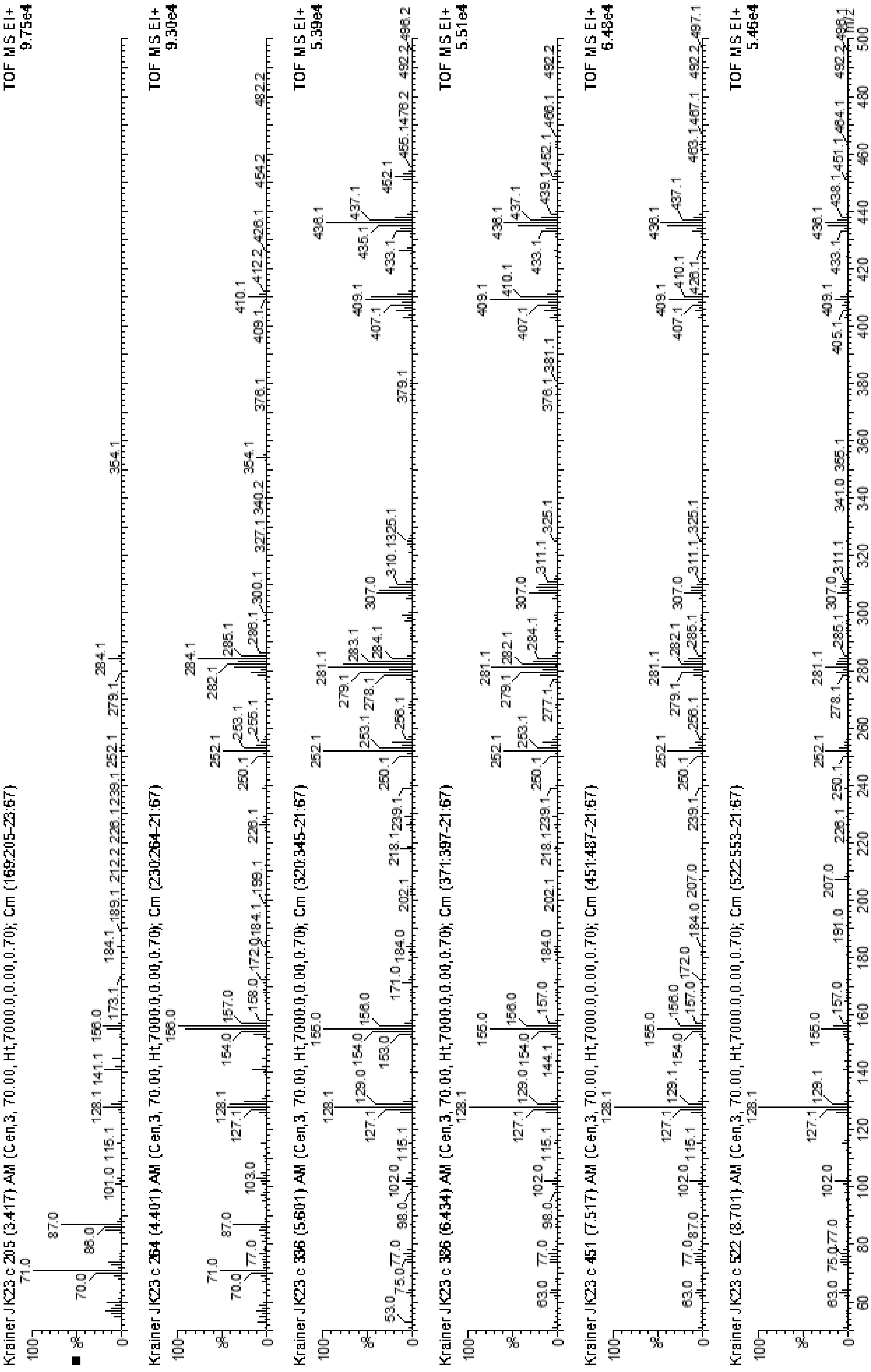
Krainer JK23 c 205 (3.417) AM (Cen,3, 70.00, Ht,7000.0,0.00,0.70); Cm (169:205-23:67)
TOF MS EI+
9.75e4
Krainer JK23 c 264 (4.401) AM (Cen,3, 70.00, Ht,7000.0,0.00,0.70); Cm (230:264-21:67)
TOF MS EI+
9.30e4
Krainer JK23 c 336 (5.601) AM (Cen,3, 70.00, Ht,7000.0,0.00,0.70); Cm (320:345-21:67)
TOF MS EI+
5.39e4
Krainer JK23 c 386 (6.434) AM (Cen,3, 70.00, Ht,7000.0,0.00,0.70); Cm (371:397-21:67)
TOF MS EI+
5.51e4
Krainer JK23 c 451 (7.517) AM (Cen,3, 70.00, Ht,7000.0,0.00,0.70); Cm (451:487-21:67)
TOF MS EI+
6.48e4
Krainer JK23 c 522 (8.701) AM (Cen,3, 70.00, Ht,7000.0,0.00,0.70); Cm (522:553-21:67)
TOF MS EI+
5.46e4
100
%
0
60
80
100
120
140
160
180
200
220
240
260
280
300
320
340
360
380
400
420
440
460
480
500
m/z

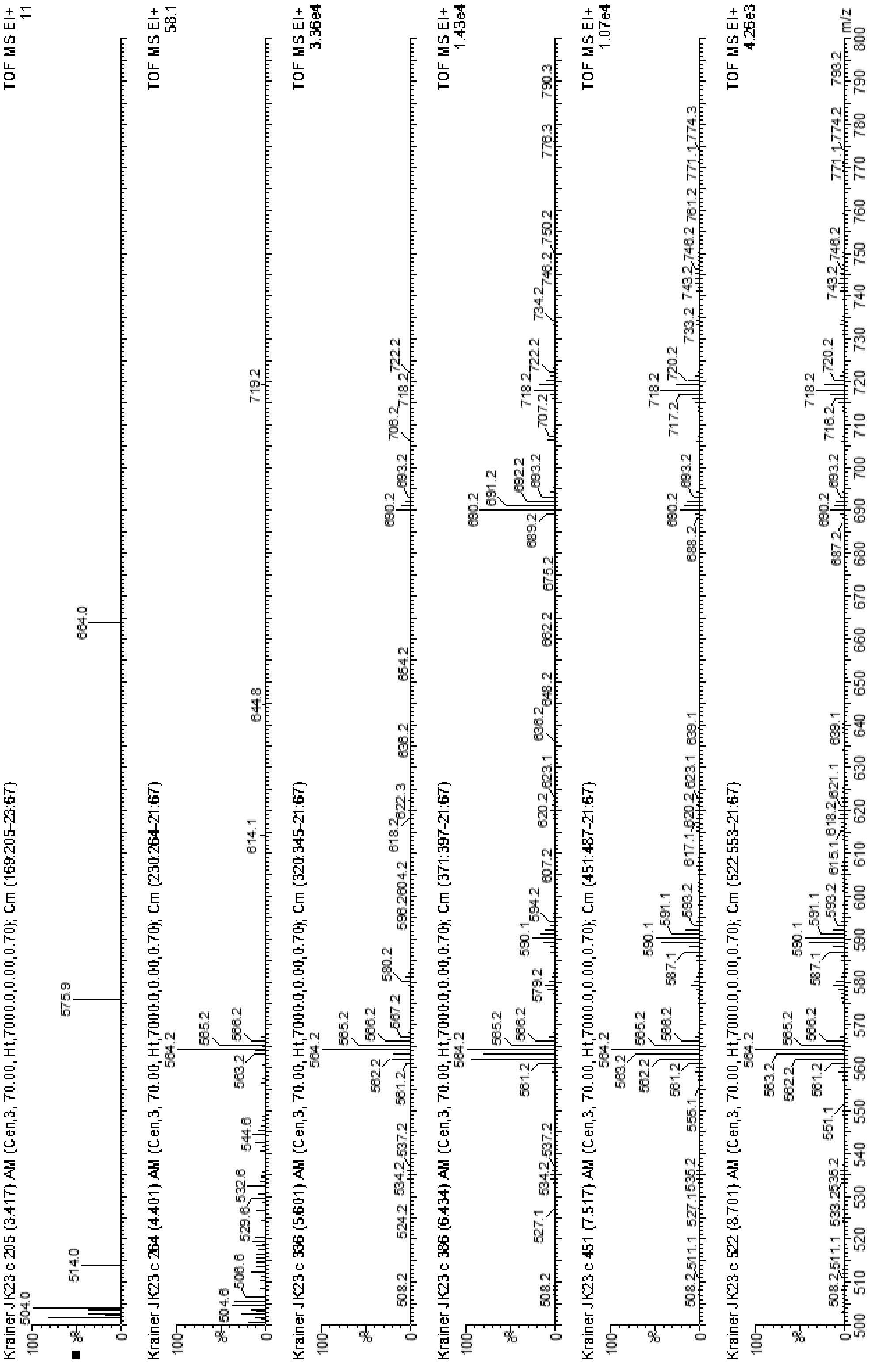
Krainer JK23 c 205 (3.417) AM (Cen,3, 70.00, Ht,7000.0,0.00,0.70); Cm (169:205-23:67)
TOF MS EI+
11
Krainer JK23 c 264 (4.401) AM (Cen,3, 70.00, Ht,7000.0,0.00,0.70); Cm (230:264-21:67)
TOF MS EI+
58.1
Krainer JK23 c 336 (5.601) AM (Cen,3, 70.00, Ht,7000.0,0.00,0.70); Cm (320:345-21:67)
TOF MS EI+
3.36e4
Krainer JK23 c 386 (6.434) AM (Cen,3, 70.00, Ht,7000.0,0.00,0.70); Cm (371:397-21:67)
TOF MS EI+
1.43e4
Krainer JK23 c 451 (7.517) AM (Cen,3, 70.00, Ht,7000.0,0.00,0.70); Cm (451:487-21:67)
TOF MS EI+
1.07e4
Krainer JK23 c 522 (8.701) AM (Cen,3, 70.00, Ht,7000.0,0.00,0.70); Cm (522:553-21:67)
TOF MS EI+
4.26e3
%
m/z
500
510
520
530
540
550
560
570
580
590
600
610
620
630
640
650
660
670
680
690
700
710
720
730
740
750
760
770
780
790
800

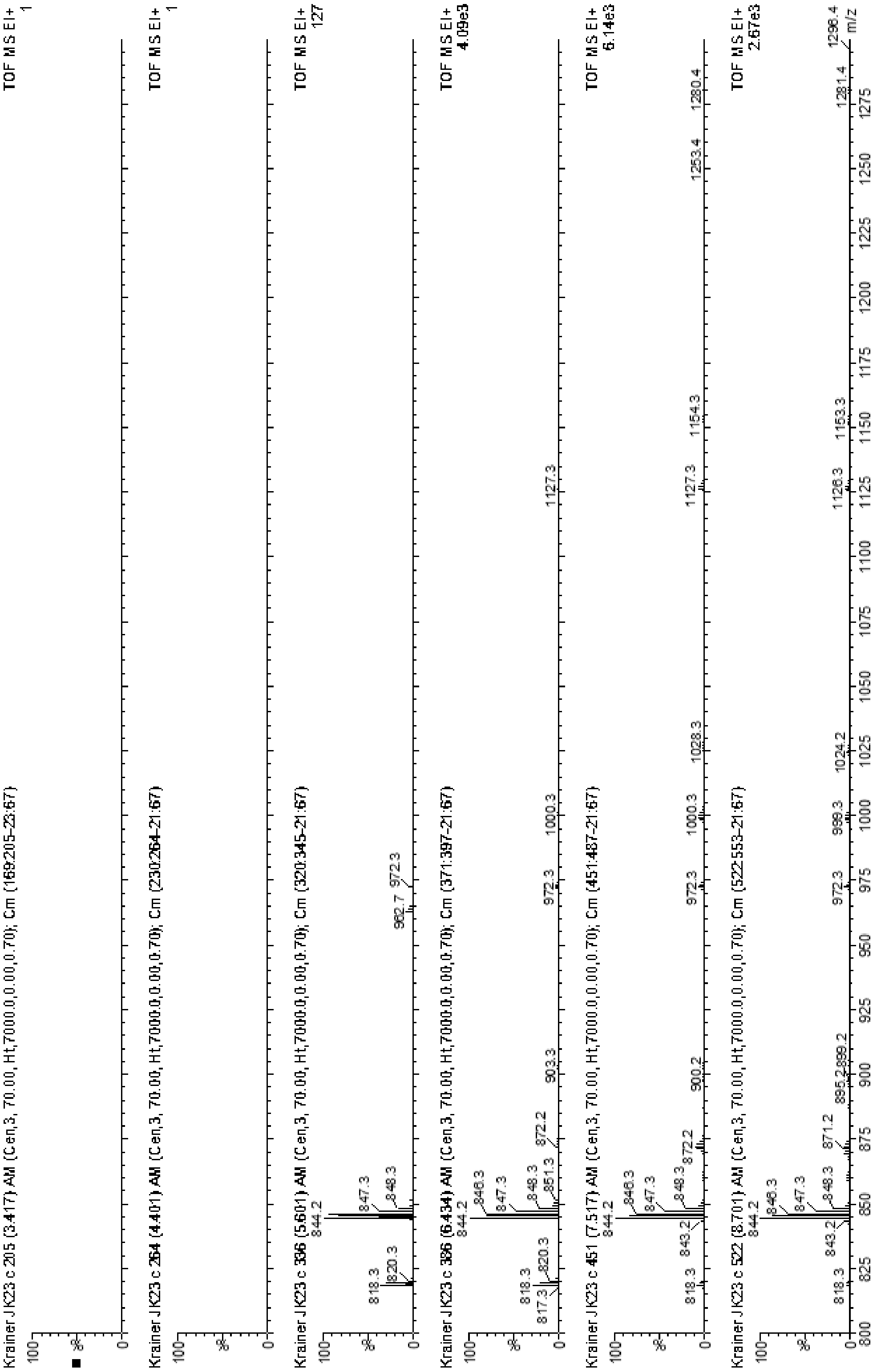
Krainer JK23 c 205 (3.417) AM (Cen,3, 70.00, Ht,7000.0,0.00,0.70); Cm (169:205-23:67)
TOF MS EI+
1
Krainer JK23 c 264 (4.401) AM (Cen,3, 70.00, Ht,7000.0,0.00,0.70); Cm (230:264-21:67)
TOF MS EI+
1
Krainer JK23 c 336 (5.601) AM (Cen,3, 70.00, Ht,7000.0,0.00,0.70); Cm (320:345-21:67)
TOF MS EI+
127
818.3
820.3
844.2
847.3
848.3
962.7
972.3
Krainer JK23 c 386 (6.434) AM (Cen,3, 70.00, Ht,7000.0,0.00,0.70); Cm (371:397-21:67)
TOF MS EI+
4.09e3
817.3
818.3
820.3
844.2
846.3
847.3
848.3
851.3
872.2
903.3
972.3
1000.3
1127.3
Krainer JK23 c 451 (7.517) AM (Cen,3, 70.00, Ht,7000.0,0.00,0.70); Cm (451:487-21:67)
TOF MS EI+
6.14e3
818.3
843.2
844.2
846.3
847.3
848.3
872.2
900.2
972.3
1000.3
1028.3
1127.3
1154.3
1253.4
1280.4
Krainer JK23 c 522 (8.701) AM (Cen,3, 70.00, Ht,7000.0,0.00,0.70); Cm (522:553-21:67)
TOF MS EI+
2.67e3
818.3
843.2
844.2
846.3
847.3
848.3
871.2
895.2
899.2
972.3
999.3
1024.2
1126.3
1153.3
1281.4
1296.4
100
%
0
800
825
850
875
900
925
950
975
1000
1025
1050
1075
1100
1125
1150
1175
1200
1225
1250
1275
m/z

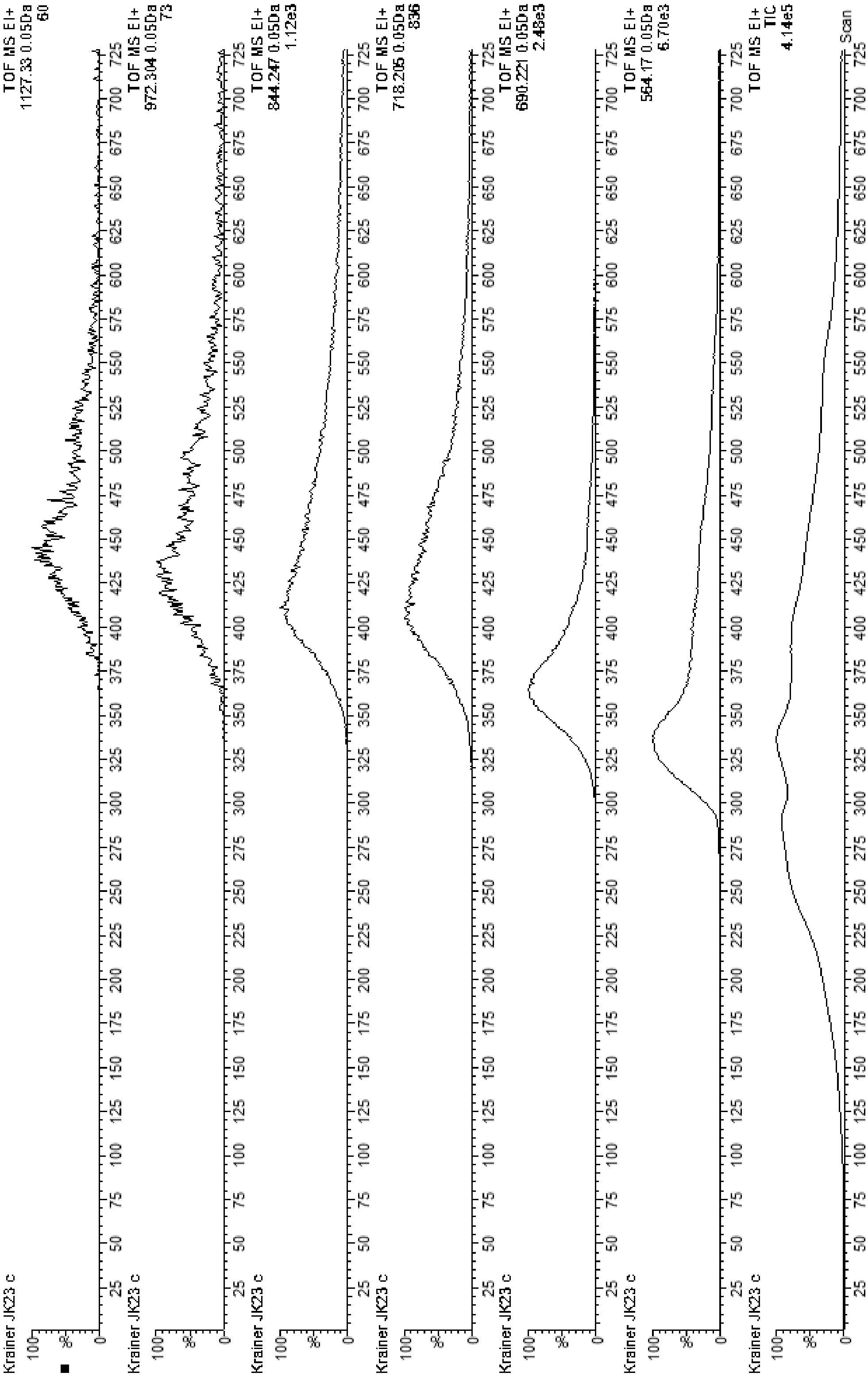
Krainer JK23 c
TOF MS EI+
1127.33 0.05Da
60
Krainer JK23 c
TOF MS EI+
972.304 0.05Da
73
Krainer JK23 c
TOF MS EI+
844.247 0.05Da
1.12e3
Krainer JK23 c
TOF MS EI+
718.205 0.05Da
836
Krainer JK23 c
TOF MS EI+
690.221 0.05Da
2.48e3
Krainer JK23 c
TOF MS EI+
564.17 0.05Da
6.70e3
Krainer JK23 c
TOF MS EI+
TIC
4.14e5
100
%
0
25
50
75
100
125
150
175
200
225
250
275
300
325
350
375
400
425
450
475
500
525
550
575
600
625
650
675
700
725
Scan

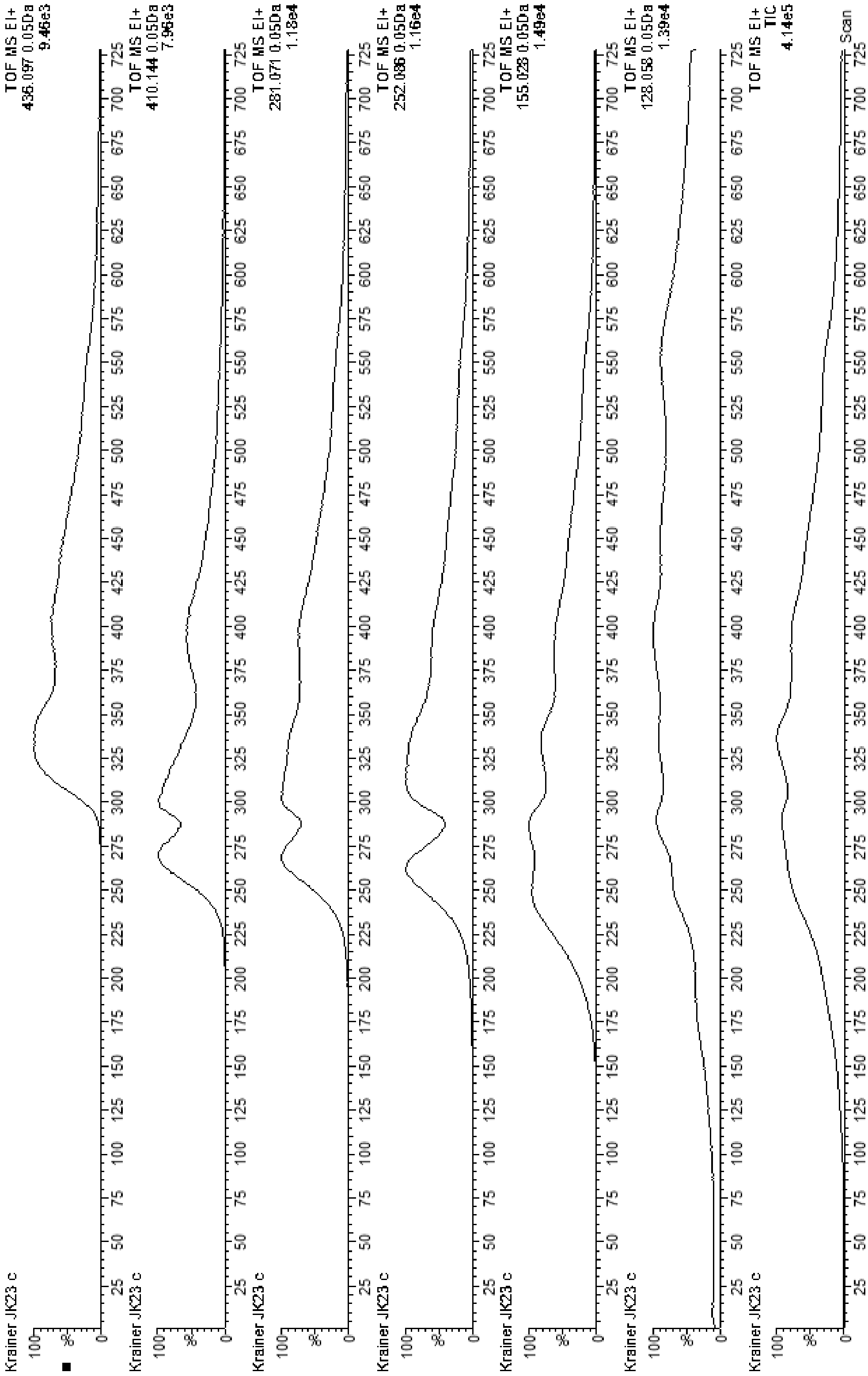
Krainer JK23 c
TOF MS EI+
436.097 0.05Da
9.46e3
Krainer JK23 c
TOF MS EI+
410.144 0.05Da
7.96e3
Krainer JK23 c
TOF MS EI+
281.071 0.05Da
1.18e4
Krainer JK23 c
TOF MS EI+
252.086 0.05Da
1.16e4
Krainer JK23 c
TOF MS EI+
155.029 0.05Da
1.49e4
Krainer JK23 c
TOF MS EI+
128.058 0.05Da
1.39e4
Krainer JK23 c
TOF MS EI+
TIC
4.14e5
100
%
0
25
50
75
100
125
150
175
200
225
250
275
300
325
350
375
400
425
450
475
500
525
550
575
600
625
650
675
700
725
Scan

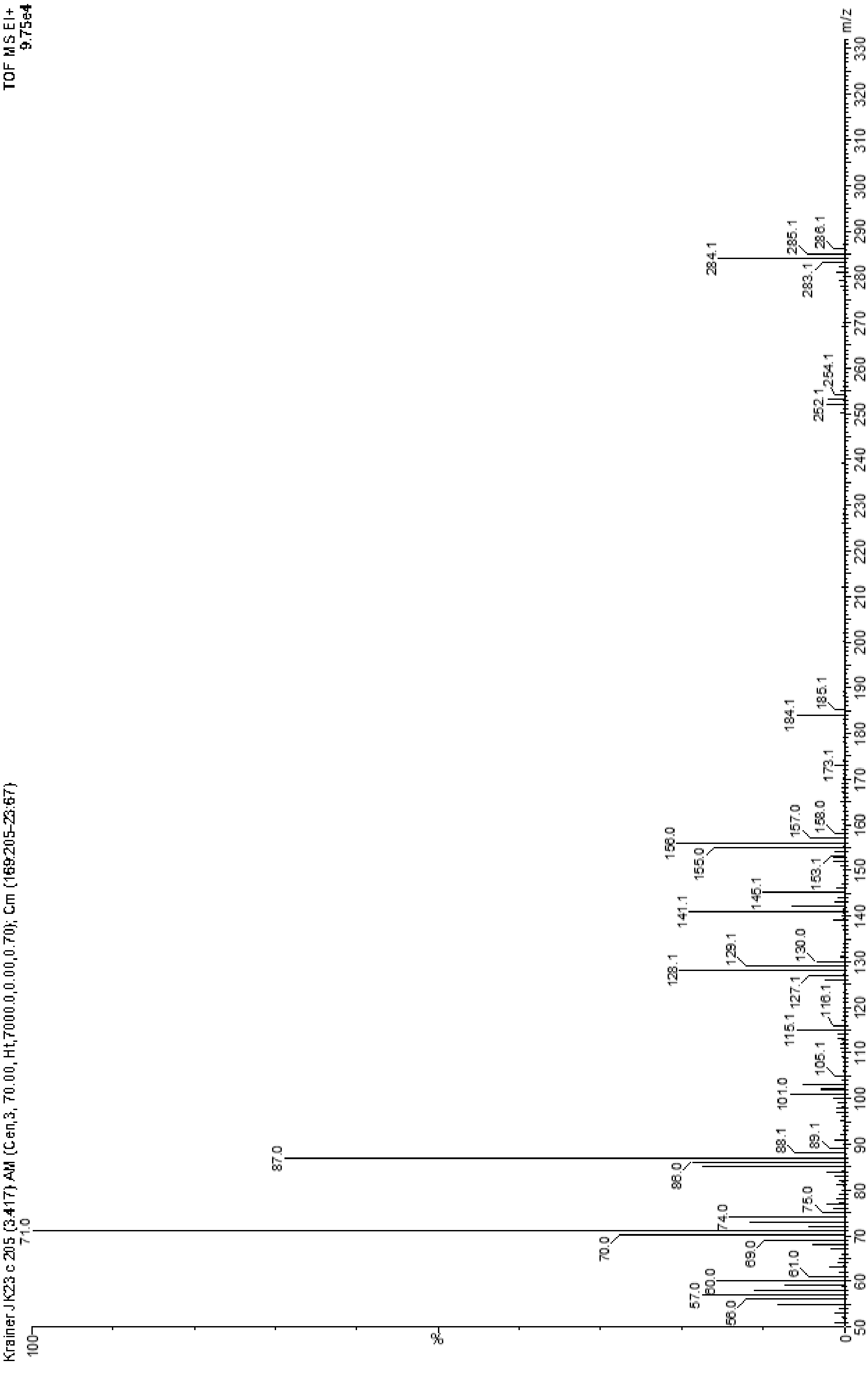
Krainer JK23 c 205 (3.417) AM (Cen,3, 70.00, Ht,7000.0,0.00,0.70); Cm (169:205-23:67)
TOF MS EI+
9.75e4
100
%
0
m/z
50
60
70
80
90
100
110
120
130
140
150
160
170
180
190
200
210
220
230
240
250
260
270
280
290
300
310
320
330
56.0
57.0
60.0
61.0
69.0
70.0
71.0
74.0
75.0
86.0
87.0
88.1
89.1
101.0
105.1
115.1
116.1
127.1
128.1
129.1
130.0
141.1
145.1
153.1
155.0
156.0
157.0
158.0
173.1
184.1
185.1
252.1
254.1
283.1
284.1
285.1
286.1

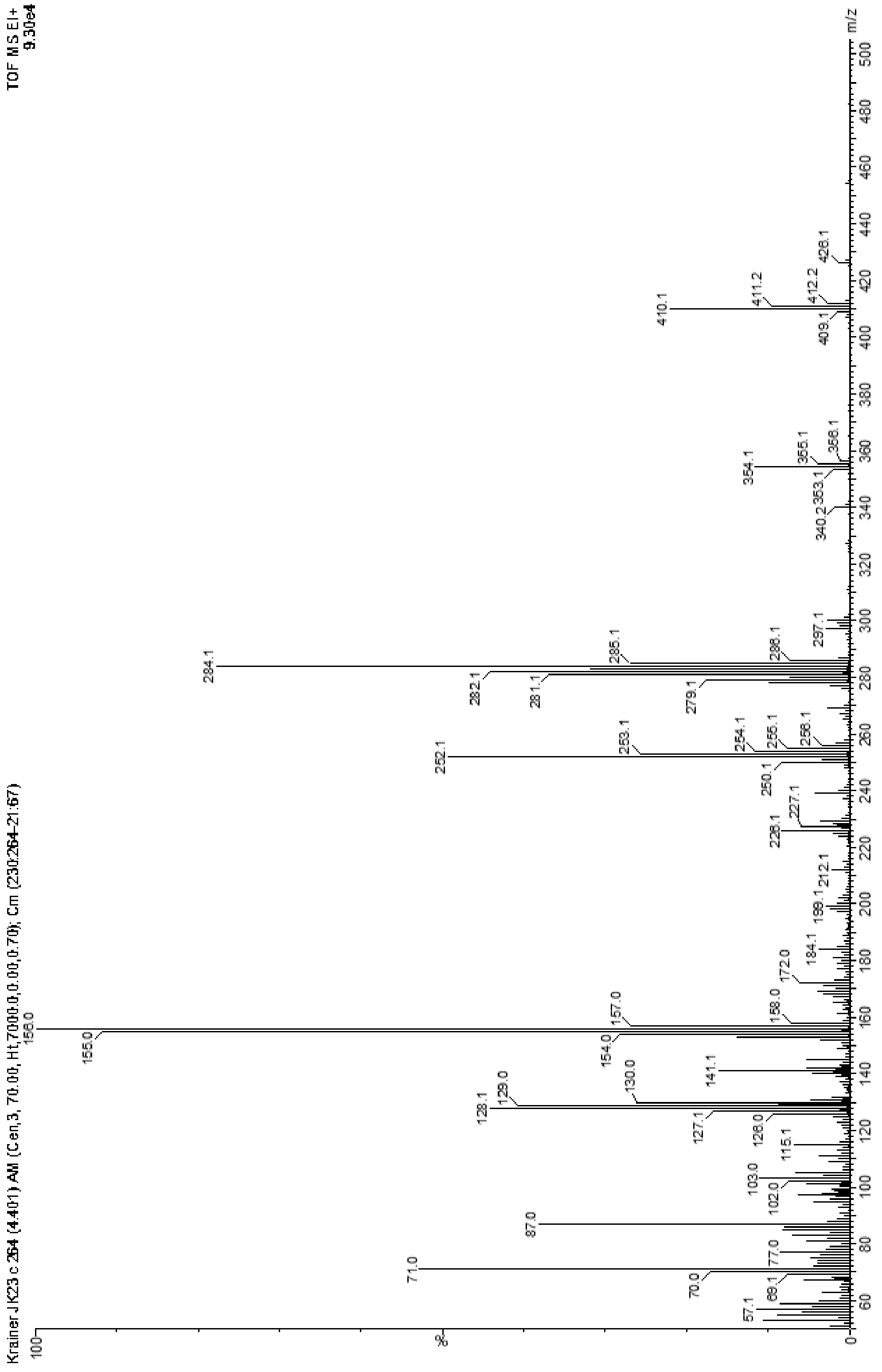
Krainer JK23 c 264 (4.401) AM (Cen,3, 70.00, Ht,7000.0,0.00,0.70); Cm (230:264-21:67)
TOF MS EI+
9.30e4
100
%
0
m/z
60
80
100
120
140
160
180
200
220
240
260
280
300
320
340
360
380
400
420
440
460
480
500
57.1
69.1
70.0
71.0
77.0
87.0
102.0
103.0
115.1
126.0
127.1
128.1
129.0
130.0
141.1
154.0
155.0
156.0
157.0
158.0
172.0
184.1
199.1
212.1
226.1
227.1
250.1
252.1
253.1
254.1
255.1
256.1
279.1
281.1
282.1
284.1
285.1
286.1
297.1
340.2
353.1
354.1
355.1
356.1
409.1
410.1
411.2
412.2
426.1

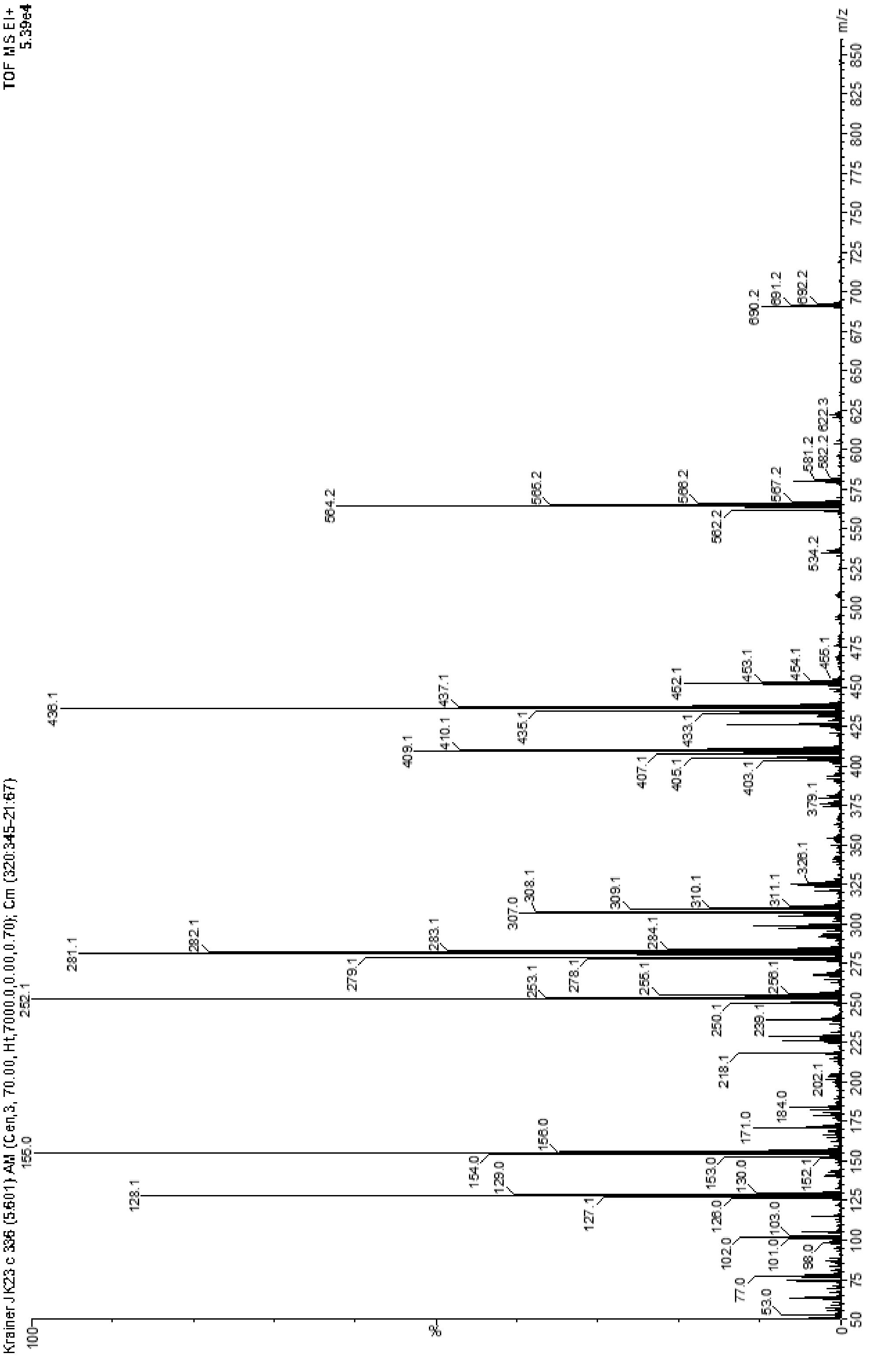
Krainer JK23 c 336 (5.601) AM (Cen,3, 70.00, Ht,7000.0,0.00,0.70); Cm (320:345-21:67)
TOF MS EI+
5.39e4
100
%
0
m/z
50
75
100
125
150
175
200
225
250
275
300
325
350
375
400
425
450
475
500
525
550
575
600
625
650
675
700
725
750
775
800
825
850
53.0
77.0
98.0
101.0
102.0
103.0
126.0
127.1
128.1
129.0
130.0
152.1
153.0
154.0
155.0
156.0
171.0
184.0
202.1
218.1
239.1
250.1
252.1
253.1
255.1
256.1
278.1
279.1
281.1
282.1
283.1
284.1
307.0
308.1
309.1
310.1
311.1
326.1
379.1
403.1
405.1
407.1
409.1
410.1
433.1
435.1
436.1
437.1
452.1
453.1
454.1
455.1
534.2
562.2
564.2
565.2
566.2
567.2
581.2
582.2
622.3
690.2
691.2
692.2

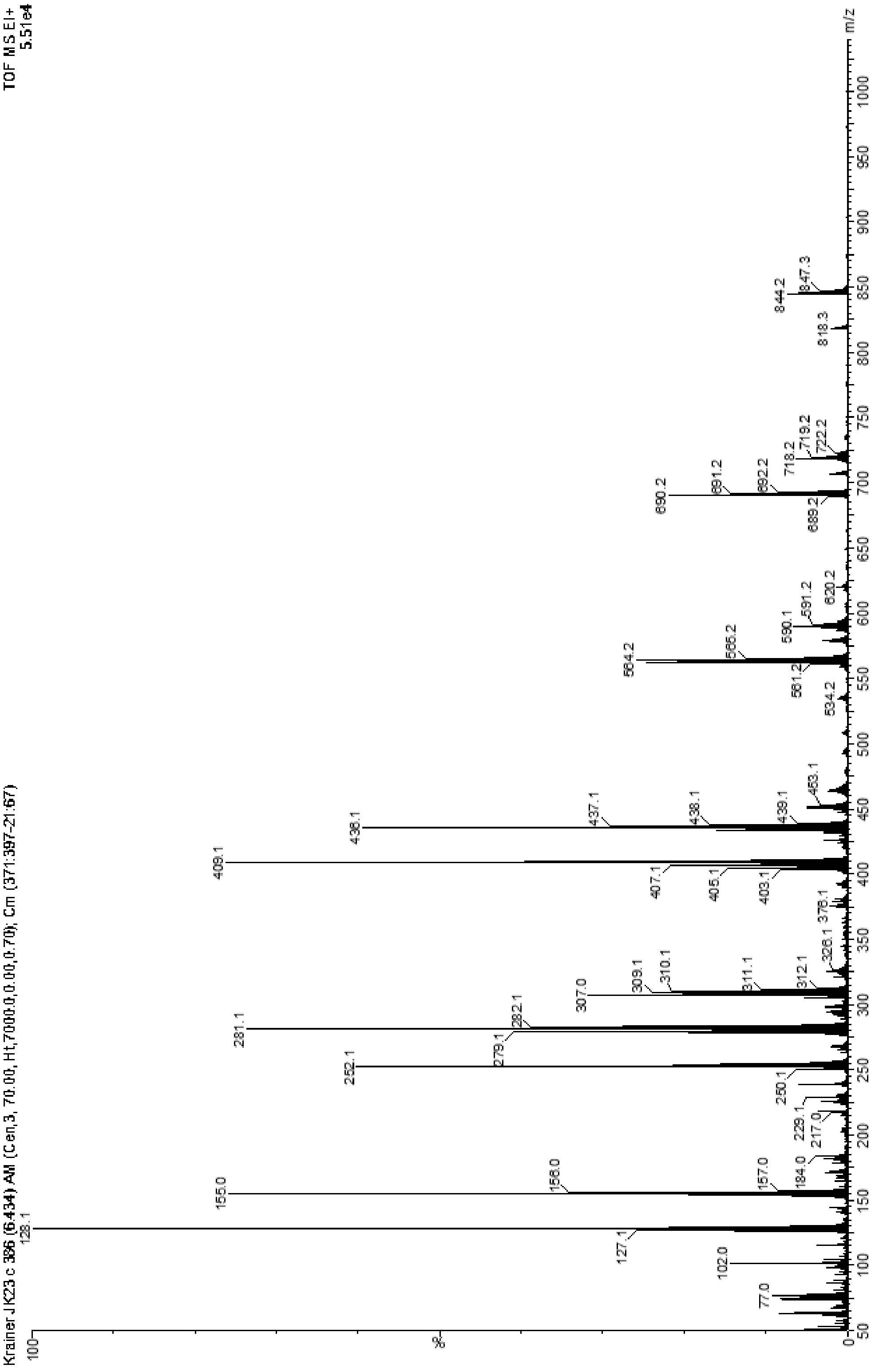
Krainer JK23 c 386 (6.434) AM (Cen,3, 70.00, Ht,7000.0,0.00,0.70); Cm (371:397-21:67)
TOF MS EI+
5.51e4
100
%
0
77.0
102.0
127.1
128.1
155.0
156.0
157.0
184.0
217.0
229.1
250.1
252.1
279.1
281.1
282.1
307.0
309.1
310.1
311.1
312.1
326.1
378.1
403.1
405.1
407.1
409.1
436.1
437.1
438.1
439.1
453.1
534.2
561.2
564.2
565.2
590.1
591.2
620.2
689.2
690.2
691.2
692.2
718.2
719.2
722.2
818.3
844.2
847.3
50
100
150
200
250
300
350
400
450
500
550
600
650
700
750
800
850
900
950
1000
m/z

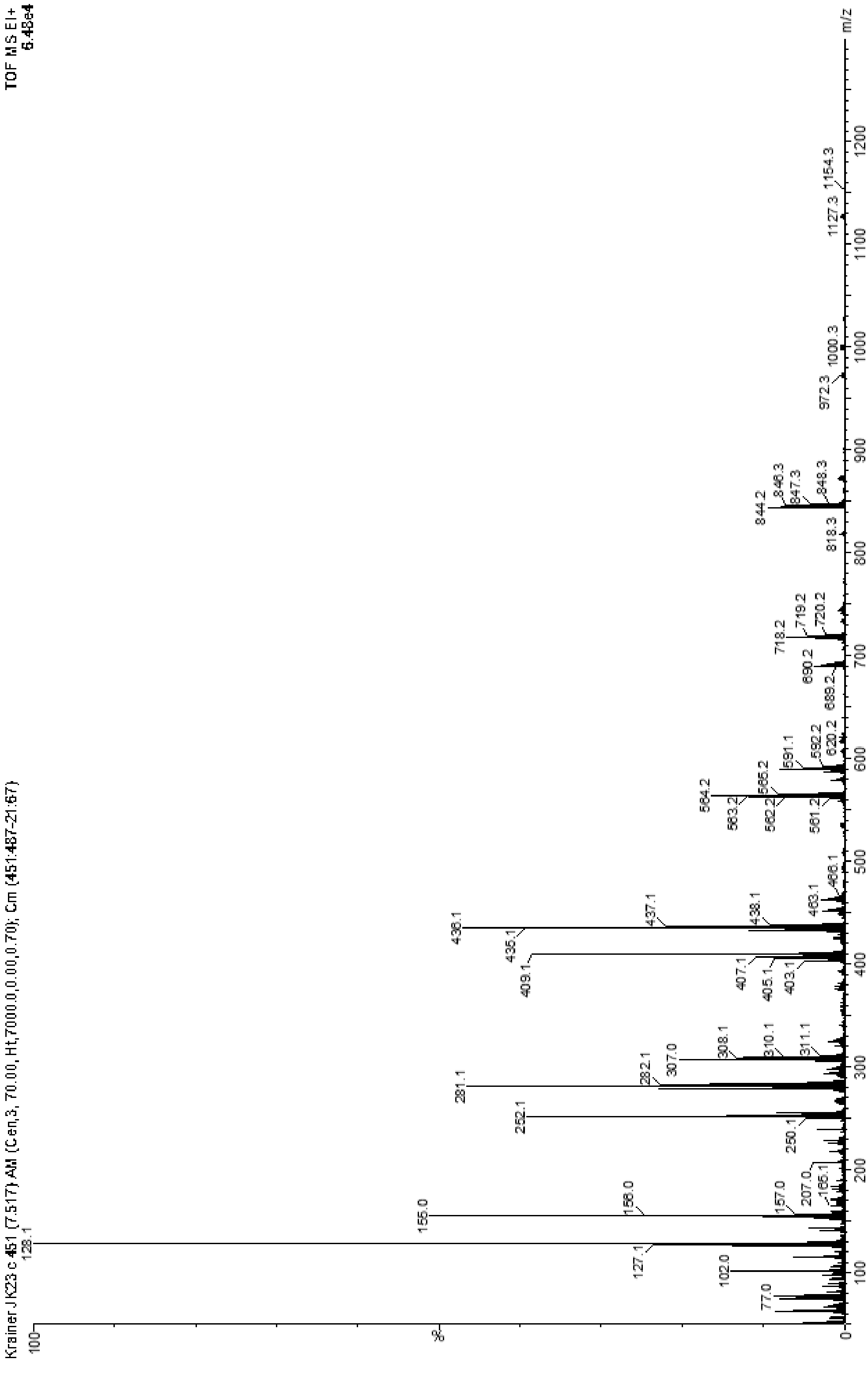
Krainer JK23 c 451 (7.517) AM (Cen,3, 70.00, Ht,7000.0,0.00,0.70); Cm (451:487-21:67)
TOF MS EI+
6.48e4
100
%
0
m/z
100
200
300
400
500
600
700
800
900
1000
1100
1200
77.0
102.0
127.1
128.1
155.0
156.0
157.0
207.0
165.1
250.1
252.1
281.1
282.1
307.0
308.1
310.1
311.1
409.1
435.1
407.1
405.1
403.1
436.1
437.1
438.1
463.1
466.1
561.2
562.2
563.2
564.2
565.2
591.1
592.2
620.2
689.2
690.2
718.2
719.2
720.2
818.3
844.2
846.3
847.3
848.3
972.3
1000.3
1127.3
1154.3

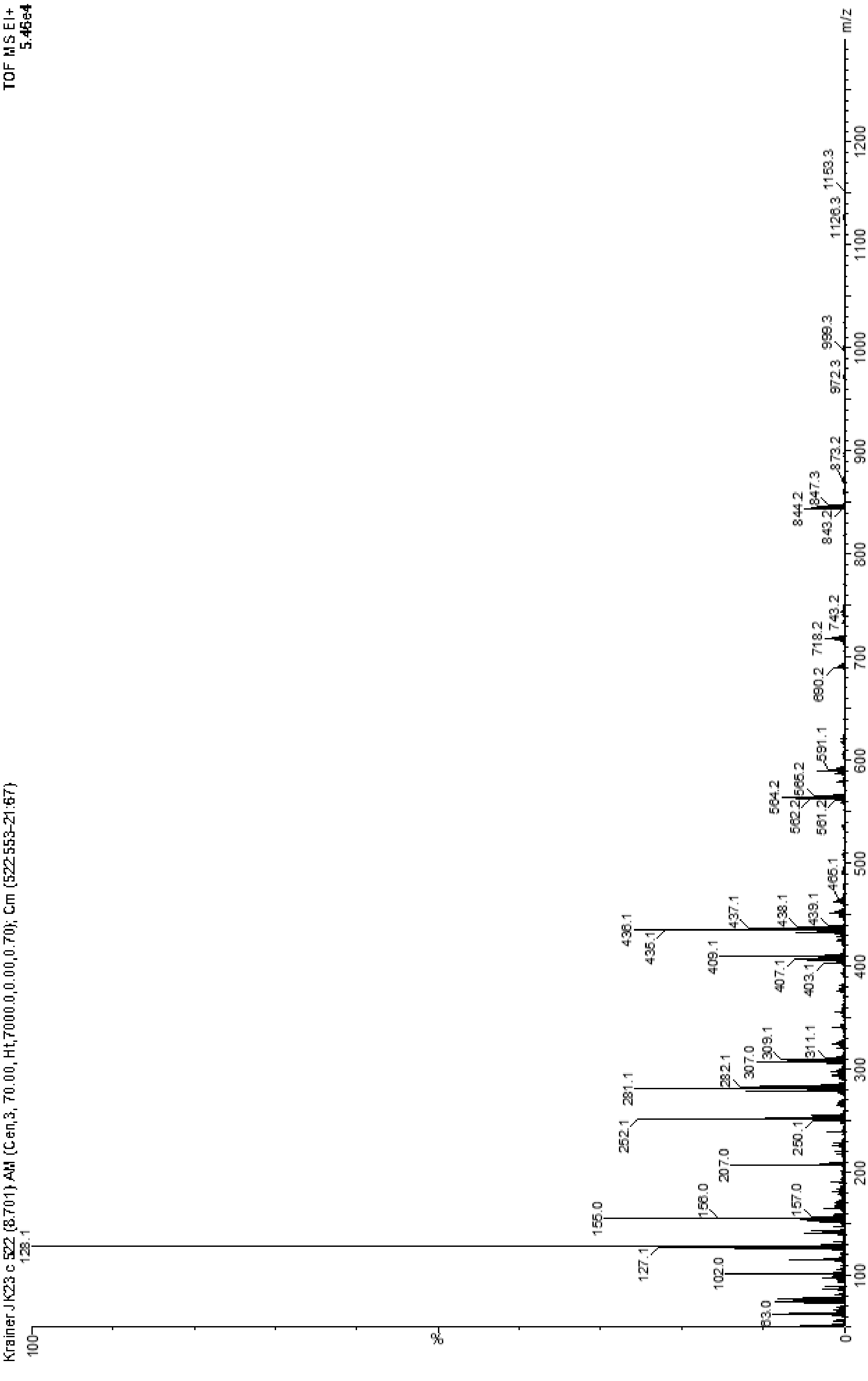
Krainer JK23 c 522 (8.701) AM (Cen,3, 70.00, Ht,7000.0,0.00,0.70); Cm (522:553-21:67)
TOF MS EI+
5.46e4
100
%
0
m/z
100
200
300
400
500
600
700
800
900
1000
1100
1200
83.0
102.0
127.1
128.1
155.0
156.0
157.0
207.0
250.1
252.1
281.1
282.1
307.0
309.1
311.1
403.1
407.1
409.1
435.1
436.1
437.1
438.1
439.1
465.1
561.2
562.2
564.2
565.2
591.1
690.2
718.2
743.2
843.2
844.2
847.3
873.2
972.3
999.3
1126.3
1153.3

7 References

[1] Gilman, H., Smart, G.N.R. *J. Org. Chem.* **1950**, *15*, 720

[2] Pink, H. S., Kipping, F. S. *J. Chem. Soc.* **1923**, *123*, 2830

[3] Yamaguchi, S., Akiyama, S., Tamao, K. *Organomet.* **1998**, *17*, 4347

[4] PhD thesis Kristina Schrempf, Anorganic Institute of Chemistry, TU Graz, 2014

[5] West, R. *Pure Appl. Chem.* **1982**, *54*, 1041

[6] Husk, G. R., West, R. *J. Am. Chem. Soc.* **1965**, *87*, 3993

[7] Hengge, E., Janokschek, R. *Chem. Rev.* **1995**, *95*, 1495

[8] Shafiee, F., West, R. *Silicon, Germanium, Tin Lead Compd.* **1986**, *9*, 1

[9] Watanabe, H., Yoshizumi, K., Muraoka, T., Kato, M., Nagai, Y., Sato, T. *Chem. Lett.* **1985**, 1683

[10] Brough, L. F., West, R. *J. Am. Chem. Soc.* **1981**, *103*, 3049

[11] Cartledge, F. K. *Organomet.* **1983**, *2*, 425

[12] Masamune, S., Hanzawa, Y., Murakami, S., Bally, T., Blount, J. F. *J. Am. Chem. Soc.* **1982**, *104*, 1150

[13] Masamune, S., Murakami, S., Snow, J. T., Tobita, H., Williams, D. *Organomet.* **1984**, *3*, 333

[14] Probst, R., Leis, C., Gamper, S., Herdtweck, E., Auner, N., Zybill, C. *Angew. Chem.* **1991**, *103*, 1155

[15] Weidenbruch, M. *Chem. Rev.* **1995**, *95*, 1479

[16] Kipping, F. S., Sands, J. E. *J. Chem. Soc.* **1921**, *119*, 830

[17] Gilman, H., Peterson, D. J. *J. Organomet. Chem.* **1965**, *4*, 163

[18] Kipping, F. S., Sands, J. E. *J. Chem. Soc.* **1921**, *119*, 830

[19] Gilman, H., Peterson, D. J., Jarvie, A. W., Winkler, H. J. S. *J. Am. Chem. Soc.* **1960**, *82*, 2076

[20] Steele, A. R., Kipping, J. S. *J. Chem. Soc. 1929*, 2545

[21] Hengge, E., Firgo, H. *J. Organomet. Chem.* **1981**, *212*, 155

[22] Hassler, K., Kovar, D., Söllradl, H. Hengge, E. *Z. Anorg. Allg. Chem.* **1982**, *488*, 27

[23] Becker, G., Hartmann, H.-M., Hengge, E., Schrank, F. *Z. Anorg. Allg. Chem.* **1989**, *572*, 63

[24] Gilman, H., Peterson, D. J., Jarvie, A. W., Winkler, H. J. S. *Tetrahedron Lett.* **1960**, *23*, 5

[25] Gilman, H., Schwebke, G. L. *J. Am. Chem. Soc.* **1964**, *86*, 2693

[26] Lemanski, M. F., Schram, E. P. *Inorg. Chem.* **1976**, *10(15)*, 2515

[27] Parkanyi, L., Sasvari, K., Declercq, J. P., Germain, G. *Acta Crystallogr.* **1978**, *B34*, 3678

[28] Hengge, E., Stüger, H. *Monatsh. Chem.* **1980**, *111*, 1043

[29] Ovchinnikov, Y. E., Shklover, V. E., Struchkov, Y. T., Dement'ev, V. V., Frunze, T. M. Antipova, B. A. *J. Organomet. Chem.* **1987**, *335*, 157

[30] Hengge, E., Pätzold, U. *unpublished results*

[31] Hengge, E., Janoschek, R. *Chem. Rev.* **1995**, *95*, 1495

[32] Winkler, H. J. S., Jarvie, A. W. P., Peterson, D. J., Gilman, H. *J. Am. Chem. Soc.* **1961**, *83*, 4089

[33] Kira, M., Bock, H., Hengge, E. *J. Organomet. Chem.* **1979**, *164(3)*, 277

[34] Gilman, H., Schwebke, G. L. *Advanc. Organomet.* **1964**, *1*, 89

[35] Wan, T. P., O'Brien, D. H., Smentowski, F. J. *J. Am. Chem. Soc.* **1972**, *94*, 7680

[36] Gilman, H., Brannen, C. G. *Am. Chem. Soc.* **1951**, *73*, 4640

[37] Biedermann, J. *Project Laboratory Report*, Graz University of Technology 2014

[38] Hanzu, I. *Institute for Chemistry and Technology of Materials*, Graz University of Technology

[39] Yazami, R., Touzain, Ph. *Journal of Power Sources* **1983**, *9*, 365

[40] Aurbach, D., Ein-Eli, Y., Markovsky, B., Zaban, A. *J. Electrochem. Soc.* **1995**, *142*, 2882

[41] Idota, Y., Kubota, T., Matsufuji, A., Maekawa, Y., Miyasaka. T. *Science* **1997**, *267*, 1395

[42] Poizot, P., Laruelle, S., Grugeon, S., Dupont, L., Tarascon, J-M. *Nature* **2000**, *407*, 496

[43] Jung, S. C., Choi, J. W., Han, Y-K. *Nano Lett.* **2012**, *12*, 5342

[44] Li, H., Wang, Z., Chen, L., Huang, X. *Adv. Mater.* **2009**, *21*, 4593

[45] Freeman, W. P., Tilley, T. D., Yap, G. P. A., Rheingold, A.L. *Angew. Chem.* **1996**, *35*, 882

[46] Hong, J.-H., Boudjouk, P., Castellino, S. *Organomet.* **1994**, *13*, 3387

[47] Liu, Y., Stringfellow, T. C., Ballweg, D., Guzei, I. A., West, R. *J. Am. Chem. Soc.* **2001**, *124*, 49

8 List of Figures